



**UNIVERSITÀ  
DEGLI STUDI  
DI TRIESTE**

## **UNIVERSITÀ DEGLI STUDI DI TRIESTE**

### **XXXV CICLO DEL DOTTORATO DI RICERCA IN SCIENZE DELLA RIPRODUZIONE E DELLO SVILUPPO**

FINANZIATORE DELLA BORSA  
" PO FRIULI VENEZIA GIULIA - FONDO SOCIALE EUROPEO 2014/2020"

### **PRECISION THERAPY FOR KINASE-MEDIATED AUTOIMMUNE DISEASES: DEVELOPMENT OF AN *IN VITRO* SYSTEM FOR DIAGNOSIS AND CLINICAL MONITORING**

Settore scientifico-disciplinare: **BIO/14**

DOTTORANDA

**STEFANIA BRAIDOTTI**

COORDINATORE

**PROF. PAOLO GASPARINI**

SUPERVISORE DI TESI

**DOTT. RAFFAELLA FRANCA**

CO-SUPERVISORE DI TESI

**PROF. GABRIELE STOCCO**

**ANNO ACCADEMICO 2021/2022**

# INDEX

<b>ABSTRACT</b> .....	<b>1</b>
<b>RIASSUNTO</b> .....	<b>3</b>
<b>1 - INTRODUCTION</b> .....	<b>5</b>
1.1    JAK TYROSINE KINASES .....	6
1.2    JAK/STAT PATHWAY Deregulation .....	10
1.3    JAK INHIBITORS (JAKi) .....	12
1.3.1    JAKi REPURPOSING .....	15
1.3.2    JAKi SIDE EFFECTS .....	16
1.4    TYPE I INTERFERONOPATHIES .....	17
1.4.1    AICARDI-GOUTIÈRES SYNDROME (AGS) .....	17
1.4.2    AGS THERAPY .....	20
1.5    PRECISION MEDICINE .....	24
1.5.1    iPSC TECHNOLOGY .....	24
1.5.2    PATIENT-SPECIFIC iPSCs AS A MODEL FOR PRIMARY IMMUNODEFICIENCIES .....	26
1.5.3    KINASE ACTIVITY MONITORING .....	27
1.5.3.1    PEPTIDE BIOSENSORS .....	27
<b>2 - AIM</b> .....	<b>29</b>
<b>3 - MATERIALS AND METHODS</b> .....	<b>31</b>
3.1    DRUG AND CHEMICALS .....	32
3.2    AGS PATIENTS .....	32
3.3    CELL CULTURES .....	32
3.3.1    AGS PATIENT DERIVED CELLS .....	32
3.3.1.1    iPSCs REPROGRAMMING AND CULTURE .....	32
3.3.1.2    NSCs INDUCTION AND CULTURE .....	33
3.3.2    IMMORTALIZED HEMATOPOIETIC CELL LINES .....	34
3.3.3    MYCOPLASMA DETECTION .....	35
3.4    CELL VIABILITY ASSAYS .....	35
3.4.1    MTT ASSAY .....	35
3.4.1    PROLIFERATION ASSAYS .....	37
3.4.1.1    [3H] THYMIDINE .....	37
3.4.1.2    CFSE .....	37
3.5    CELL CYCLE ANALYSIS .....	37
3.6    TOTAL RNA ISOLATION AND REVERSE TRANSCRIPTION .....	38

3.7	QUANTITATIVE REAL-TIME PCR.....	38
3.8	CELL LYSATES PREPARATION FROM HEMATOPOIETIC CELL LINES	40
3.9	IMMUNOPRECIPITATION .....	40
3.10	WESTERN BLOT .....	40
3.11	<i>IN VITRO</i> ASSAY WITH PEPTIDE BIOSENSORS .....	41
3.11.1	PEPTIDE BIOSENSORS.....	41
3.11.2	PEPTIDE BIOSENSORS-BASED ELISA ASSAY ON WHOLE PROTEIN CELL LYSATES .	41
3.11.3	PEPTIDE BIOSENSORS-BASED ELISA ASSAY ON IMMUNOPRECIPITATED JAK2 PROTEIN.....	42
3.12	STATISTICAL ANALYSIS .....	43
<b>4</b>	<b>RESULTS – PART I .....</b>	<b>44</b>
4.1	iPSCs AND NSCs CHARACTERIZATION .....	45
4.1.1	STEMNESS .....	45
4.1.2	iPSCs PROLIFERATION BY [3H]-THYMIDINE INCORPORATION ASSAY .....	46
4.1.3	iPSCs CELL CYCLE ANALYSIS.....	46
4.1.4	NSCs PROLIFERATION BY CFSE STAINING.....	47
4.1.5	NSCs VIABILITY BY MTT ASSAY .....	48
4.2	iPSCs AND NSCs CYTOTOXICITY ASSAYS.....	49
4.2.1	CYTOTOXIC EFFECT OF JAK INHIBITORS .....	49
4.2.2	CYTOTOXIC EFFECT OF ANTIRETROVIRALS.....	52
4.2.3	CYTOTOXICITY OF cGAMP .....	54
4.3	ANALYSIS OF <i>STING</i> EXPRESSION .....	55
<b>5</b>	<b>RESULTS – PART II .....</b>	<b>57</b>
5.1	CELL LINES CHARACTERIZATION .....	58
5.1.1	JAK2, STAT5 AND CRLF2 PROTEIN EXPRESSION IN HEMATOPOIETIC CELL LINES	58
5.1.2	<i>IN VITRO</i> SENSITIVITY TO JAK INHIBITORS OF HEMATOPOIETIC CELL LINES.....	60
5.2	PEPTIDE BIOSENSORS <i>IN VITRO</i> FUNCTIONAL ANALYSIS .....	61
5.2.1	PEPTIDE-BASED ELISA ASSAY ON WHOLE PROTEIN LYSATES .....	61
5.2.2	PEPTIDE-BASED ELISA ASSAY ON IMMUNOPRECIPITATED PROTEIN .....	62
5.2.3	PEPTIDE-BASED ELISA ASSAY OPTIMIZATION ON WHOLE LYSATES AND P <sub>JAK-L</sub> ....	64
<b>6</b>	<b>DISCUSSION.....</b>	<b>66</b>
<b>7</b>	<b>CONCLUSION.....</b>	<b>75</b>
<b>8</b>	<b>REFERENCES .....</b>	<b>77</b>

# ABSTRACT

---

This thesis is part of a broader project for the development of molecular strategies for precision medicine, and focuses on the Janus tyrosine kinases, JAK. The study consists of two parts, both with the aim to develop *in vitro* systems for improving diagnosis, clinical monitoring, and precision therapy of kinase-mediated diseases. The first part is related to set up patient-specific models of rare Aicardi-Goutières syndrome (AGS) by differentiation of patient's induced pluripotent stem cells (iPSC) into derived neurons to investigate the safety and efficacy of JAK inhibitors (JAKi) in this pathogenetic context. The second part aims to develop a point-of-care device for diagnosis and clinical monitoring of aberrant JAK enzymatic activity in patients affected by JAK kinases related diseases.

AGS are rare genetic diseases classified among type I interferonopathies and characterized by neuro-inflammation and autoimmune phenotype. To date, pharmacological treatment of AGS is symptomatic and mainly supportive; recently JAKi and antiretrovirals (RTIs: abacavir, lamivudine, zidovudine) have been proposed as novel therapies for AGS in clinics. Patient-specific induced pluripotent stem cells (iPSCs) were generated by reprogramming fibroblasts of 3 AGS patients with different disease mutations (AGS1, AGS2, AGS7), and differentiated into neural stem cells (NSC); the commercial BJ fibroblasts from a healthy donor was used as control. Characterization of iPSC and NSCs was assessed evaluating the expression of gene markers (i.e., *OCT4*, *SOX1*, *SOX2*, *Nestin* and *PAX6*), confirming the different grade of stemness. Cytotoxic effects of JAKi (ruxolitinib, baricitinib, tofacitinib and pacritinib) and RTI were investigated on patients'-derived iPSCs and NSCs. With the exception of pacritinib, JAKi did not compromise iPSC and NSC viability, as measured by MTT assay. In contrast, a 3-day exposure to high concentration of ruxolitinib (2.5  $\mu\text{M}$ ) increased cell viability in AGS2-iPSC compared to controls BJ-iPSC ( $P < 0.05$ ); a similar result was observed for AGS7-iPSC and ruxolitinib ( $P < 0.05$ ) and for AGS7-iPSC and baricitinib at concentration higher than 2.5  $\mu\text{M}$  ( $P < 0.05$ ). The exposure to high concentrations of ruxolitinib, baricitinib and tofacitinib increased cell viability in AGS7-NSC compared to BJ-NSC ( $P < 0.05$ ); a similar result was observed for AGS2-NSC and baricitinib at 0.6  $\mu\text{M}$  and 2.5  $\mu\text{M}$  ( $P < 0.001$ ) or tofacitinib at 2.5 ( $P < 0.05$ ) and also for AGS1-NSC treated with tofacitinib at 10  $\mu\text{M}$  ( $P < 0.05$ ). Pacritinib was cytotoxic to all iPSC (range  $\text{IC}_{50} \pm \text{SE}$ , from  $0.29 \pm 0.13 \mu\text{M}$  to  $0.61 \pm 0.03 \mu\text{M}$ ) and NSC (range  $\text{IC}_{50} \pm \text{SE}$  from  $0.63 \pm 0.13 \mu\text{M}$  to  $1.05 \pm 0.34 \mu\text{M}$ ); AGS2-NSC were less sensitive than BJ-NSC at 0.06  $\mu\text{M}$  ( $P < 0.05$ ) and 0.56  $\mu\text{M}$ , ( $P < 0.0001$ ). Expression of genes involved in JAKi pharmacodynamics (i.e., *JAK1/STAT1* *TYK2/STAT2*) were comparable between iPSC and the derived-NSC of each cell line (except for *STAT2* in AGS7, iPSC *versus* NSC,  $p < 0.05$ , t-test analysis) and among all iPSC and all NSC. RTIs did not show cytotoxicity activity, except for AGS2-iPSCs compared to control BJ-iPSC after zidovudine exposure ( $> 2.5 \mu\text{M}$ ,  $P < 0.001$ ). However, expression of *TK1*, a key target gene involved in zidovudine activation, was comparable among iPSCs and NSCs. The expression level of *ADK*, key gene for abacavir metabolism, was instead increased in AGS1-derived NSC compared to AGS1-iPSC ( $P < 0.05$ ). *STING* mRNA expression was increased in NSC compared to iPSC in AGS- but not in BJ-derived stem cells (AGS1 ( $P < 0.05$ ), AGS2 ( $P < 0.00001$ ) and AGS7 ( $P < 0.05$ )). In AGS7-iPSC, treatment with cGAMP (4 ng/ $\mu\text{L}$ ) for 24 hours or baricitinib (10  $\mu\text{M}$ ) for 72 hours reduced *STING* expression levels compared to

untreated cells ( $P < 0.5$ ). In contrast, the exposure to baricitinib increases *STING* expression in AGS1- and AGS2-NSCs compared to the untreated condition ( $P < 0.01$  and  $P < 0.001$ , respectively).

With the aim to be capable of recognizing and quantifying JAK2 kinase activation *in vitro*, we set up a system based on the use of biosensor peptides (named  $P_{\text{JAK2-S}}$  and  $P_{\text{JAK2-L}}$ , whose sequence are published in literature) as artificial substrates for the kinase of interest, and on the detection of the biosensor phosphorylation by an ELISA method. The ELISA assay proposed could be useful as a "point-of-care" device to detect the alterations of kinases pathways in patient cells, but also to improve the personalized therapeutic approach by favoring the best choice of the tyrosine kinase inhibitor. For our purpose, we used immortalized hematopoietic cell lines having alterations in the JAK/STAT pathway: i.e., MHH-CALL-4, HEL and SET-2; the cell lines REH and K562 were used as negative controls. The constitutive protein expression and phosphorylation of the main components of the JAK/STAT signaling pathway (CRLF2, JAK2 and STAT5) was confirmed by western blot. A functional evaluation of the susceptibility to JAKi (ruxolitinib, baricitinib, tofacitinib and pacritinib) was also performed; by evaluating cytotoxicity in MTT assays, we confirmed that proliferation of cell lines with the overactivation of the JAK/STAT pathway relied on this pathway, differently from what observed for negative controls. Results of peptide-based ELISA assay did not show a different level of phosphorylation of the two peptides *versus* the background signal represented by the whole lysates. The lack of phosphorylation could be due to a lysate matrix effect, capable of interfering in the interaction between JAK2 and biosensors. We decided to perform the ELISA assay on JAK2, immunoprecipitated (IP) from HEL whole lysate. Preliminary results demonstrate that it was possible to detect an increase in  $P_{\text{JAK2-L}}$  phosphorylation signal compared to a baseline level condition (Fluorescence Intensity (FI)  $\pm$  SD in the absence of biosensor,  $2510.26 \pm 931.01$  versus FI in the presence of  $P_{\text{JAK2-L}}$ ,  $87710.99 \pm 3278.33$ ,  $P < 0.0001$ , Two-way ANOVA and Bonferroni's post-test) only when the immunoprecipitated JAK2 kinase was phosphorylated. In contrast,  $P_{\text{JAK2-S}}$  was never phosphorylated in IP combined ELISA assay, suggesting that only  $P_{\text{JAK2-L}}$  peptide is suitable as peptide biosensor. Several attempts to optimize the conditions of the  $P_{\text{JAK2-L}}$ -based ELISA assay followed, by modifying the main parameters of the conventional protocol that may influence peptide-lysate incubation steps, i.e. the temperature ( $25^{\circ}\text{C}$  vs  $37^{\circ}\text{C}$ ), the time of incubation (1 hour vs 2 hours), and the amount of whole lysate used ( $4 \mu\text{g}$  vs  $40 \mu\text{g}$ ). None of these changes enabled the detection of a signal for  $P_{\text{JAK2-L}}$  after whole lysate incubation. In the future, it may be useful to modify the  $P_{\text{JAK2-L}}$  sequence with the introduction of an additional amino acid sequence (targeting region) capable of increasing the affinity of the biosensor for JAK2, and to repeat the ELISA assay after adequate stimulation of the JAK/STAT pathway in immortalized cell lines.

# RIASSUNTO

---

Questa tesi fa parte di un ampio progetto incentrato sullo sviluppo di strategie molecolari per la medicina di precisione in ambito materno-infantile, focalizzato sugli inibitori delle tirosin chinasi della famiglia Janus (JAK). Lo studio si compone di due parti che mirano entrambe a sviluppare strumenti *in vitro* per migliorare la diagnosi, il monitoraggio clinico e la terapia di precisione per le malattie mediate da chinasi. Il primo obiettivo è creare modelli paziente-specifici della sindrome di Aicardi-Goutières (AGS), mediante differenziamento delle cellule staminali pluripotenti indotte dal paziente (iPSC) in staminali neuronali (NSC) e neuroni per studiare la sicurezza e l'efficacia dei farmaci JAK inibitori (JAKi) in questo contesto patogenetico. La seconda parte dello studio prevede invece lo sviluppo di un dispositivo *point-of-care* per la diagnosi e il monitoraggio clinico dell'attività enzimatica delle chinasi JAK aberranti nelle cellule dei pazienti, affetti da malattie mediate dalle stesse.

Le AGS sono malattie genetiche rare classificate come interferonopatie di tipo I e caratterizzate da un fenotipo neuroinfiammatorio e autoimmune. Ad oggi, il trattamento farmacologico dell'AGS è principalmente di supporto; recentemente i JAKi e gli antiretrovirali (RTI: abacavir, lamivudina, zidovudina) sono stati proposti come nuove potenziali terapie per l'AGS.

I modelli iPSC sono stati ottenuti riprogrammando i fibroblasti di 3 pazienti AGS con differenti mutazioni (AGS1, AGS2, AGS7) e differenziati in cellule staminali neurali (NSC). Come controllo sono stati generati modelli iPSC e corrispettive NSC da fibroblasti di un donatore sano (BJ). È stata eseguita una fase iniziale di caratterizzazione delle linee staminali, andando a valutare l'espressione dei marcatori genici di pluripotenza nelle iPSC e NSC mediante realtime-PCR (*OCT4*, *SOX1*, *SOX2*, *Nestin* e *PAX6*), e confermando il diverso grado di staminalità. Gli effetti citotossici dei JAKi (ruxolitinib, baricitinib, tofacitinib e pacritinib) e dei RTI sono stati studiati sui modelli iPSC e NSC derivati dai pazienti. Ad eccezione del pacritinib che si è dimostrato citotossico tanto per le iPSC che per le NSC (con valori di  $IC_{50}$  nel range 0,29-1,05  $\mu$ M), gli altri JAKi testati non compromettevano la vitalità cellulare delle cellule staminali. Al contrario, un'esposizione di 3 giorni ad alta concentrazione di ruxolitinib (2,5  $\mu$ M) ha aumentato la vitalità cellulare in AGS2-iPSC rispetto ai controlli BJ-iPSC ( $P < 0,05$ ); un risultato simile è stato osservato per AGS7-iPSC e per AGS7-iPSC a concentrazioni maggiori di 2,5  $\mu$ M di baricitinib ( $P < 0,05$ ). L'esposizione ad alte concentrazioni di ruxolitinib, baricitinib e tofacitinib ha aumentato la vitalità cellulare in AGS7-NSC rispetto a BJ-NSC ( $P < 0,05$ ); un risultato simile è stato osservato per AGS2-NSC e baricitinib a 0,6  $\mu$ M e 2,5  $\mu$ M ( $P < 0,001$ ) o tofacitinib a 2,5  $\mu$ M ( $P < 0,05$ ), ed anche per le AGS1-NSC trattate con tofacitinib a 10  $\mu$ M ( $P < 0,05$ ). L'espressione dei geni coinvolti nella farmacodinamica degli inibitori JAK (cioè *JAK1/STAT1*, *TYK2/STAT2*) è risultata paragonabile tra iPSC e NSC (ad eccezione di *STAT2* in AGS7, iPSC rispetto a NSC,  $P < 0,05$ , analisi t-test), ma anche tra tutte le NSC e tutte le iPSC.

Gli RTI non hanno mostrato citotossicità, ad eccezione delle AGS2-iPSC rispetto al controllo BJ-iPSC dopo trattamento con zidovudina ( $> 2,5 \mu$ M,  $P < 0,001$ ). Tuttavia, l'espressione di *TK1*, un gene bersaglio coinvolto nell'attivazione della zidovudina, è risultata paragonabile tra iPSC e NSC. Il livello di espressione di *ADK*, gene chiave per il metabolismo dell'abacavir, era invece aumentato nelle AGS1-NSC rispetto a AGS1-iPSC ( $P < 0,05$ ).

L'espressione dell'mRNA di *STING* è stata aumentata nelle NSC rispetto alle iPSC nei modelli AGS, ma non nelle linee staminali derivanti dal controllo BJ (AGS1 ( $P < 0,5$ ), AGS2 ( $P < 0,00001$ ) e AGS7 ( $P < 0,5$ )).

In AGS7-iPSC, il trattamento con cGAMP (4 ng/ $\mu$ L) per 24 ore o baricitinib (10  $\mu$ M) per 72 ore ha ridotto i livelli di espressione di *STING* rispetto alle cellule non trattate ( $P < 0,5$ ). Al contrario, l'esposizione a baricitinib aumenta l'espressione di *STING* nelle NSC AGS1 e AGS2 rispetto alla condizione non trattata (rispettivamente  $P < 0,01$  e  $P < 0,001$ ).

Con l'obiettivo di essere in grado di riconoscere e quantificare l'attivazione delle chinasi JAK2, abbiamo messo a punto un sistema basato sull'impiego di biosensori peptidici (denominati  $P_{JAK2-S}$  e  $P_{JAK2-L}$ , la cui sequenza è pubblicata in letteratura) come substrati artificiali per le chinasi di interesse e su una rilevazione della fosforilazione di tali biosensori mediante metodica ELISA. Il sistema così proposto potrebbe essere utile per lo sviluppo di un dispositivo "point-of-care" per rilevare le alterazioni delle chinasi nelle cellule dei pazienti, ma anche per migliorare l'approccio terapeutico favorendo fin da subito la scelta dell'inibitore delle tirosin chinasi da utilizzare per un approccio personalizzato. Per il nostro scopo, abbiamo utilizzato linee cellulari ematopoietiche immortalizzate con alterazioni nella pathway JAK2/STAT5: MHH-CALL-4, HEL e SET-2. Le linee leucemiche REH e K562, invece, sono state utilizzate come controlli negativi. Il coinvolgimento della via di segnalazione JAK2/STAT5 nelle linee cellulari è stato valutato e confermato mediante western blot, osservando l'espressione proteica costitutiva e la relativa fosforilazione dei componenti principali della via (CRLF2, JAK2 e STAT5). È stata inoltre eseguita una valutazione funzionale della sensibilità ai JAKi (ruxolitinib, baricitinib, tofacitinib e pacritinib) valutando la citotossicità di tali farmaci mediante saggi MTT; linee cellulari con iperattivazione della pathway JAK/STAT hanno dimostrato una proliferazione basata principalmente su questa via, a differenza di quanto osservato per i controlli negativi. I risultati ottenuti dal saggio ELISA non mostrano un diverso livello di fosforilazione dei due peptidi rispetto al segnale di fondo rappresentato dai lisati. La mancanza di un segnale potrebbe essere spiegata con l'esistenza di un effetto matrice del lisato, capace di interferire nell'interazione tra chinasi e peptide biosensore. Per verificare l'adeguatezza dei peptidi scelti, è stata eseguito il saggio ELISA sulla proteina JAK2 immunoprecipitata dal lisato della linea cellulare HEL. Così facendo, è stato possibile rilevare un aumento della fosforilazione del peptide  $P_{JAK2-L}$  (intensità di fluorescenza (IF)  $\pm$  SD in assenza di biosensore,  $2510,26 \pm 931,01$  contro IF in presenza di  $P_{JAK2-L}$ ,  $87710,99 \pm 3278,33$ ,  $P < 0,0001$ , ANOVA a due vie, Bonferroni post-test) solo quando la chinasi JAK2 immunoprecipitata risultava fosforilata (come verificato mediante western blot). Non è stata invece mai osservata la fosforilazione del peptide  $P_{JAK2-S}$ , suggerendo il peptide  $P_{JAK2-L}$  come più adatto ai nostri scopi. Sono stati quindi eseguiti diversi tentativi per ottimizzare il protocollo convenzionale del saggio ELISA basato su  $P_{JAK2-L}$ , modificando una alla volta i parametri principali che potrebbero influenzare le fasi di incubazione del peptide-lisato: quantità di lisato (4 vs 40  $\mu$ g), tempo (1 ora vs 2 ore) e temperatura di incubazione (25°C vs 37°C). Nessuna di queste modifiche ha consentito di rilevare una fosforilazione di  $P_{JAK2-L}$ . In futuro potrebbe essere utile procedere alla modifica della sequenza di  $P_{JAK2-L}$  con l'introduzione di una sequenza aminoacidica aggiuntiva (regione targeting) capace di aumentare l'affinità del biosensore per JAK2 e ripetere il saggio ELISA dopo adeguata stimolazione della pathway di JAK/STAT nelle linee cellulari immortalizzate.

# ***1 - INTRODUCTION***

---



## 1.1 JAK TYROSINE KINASES

Protein tyrosine kinases (TK) are a family of enzymes that catalyze the transfer of the  $\gamma$ -phosphate group from ATP to the hydroxyl group of a tyrosine residue of protein substrates. In addition to TKs, there are also serine or threonine kinases, which phosphorylate the hydroxyl group of serine or threonine respectively, and mixed kinases that phosphorylate both tyrosine and threonine residues [1]. Phosphorylation of amino acid residues is one of the key post-translational covalent modifications that occurs in eukaryotic cells. In this way, phosphorylation sites regulate the enzymatic activity and/or the conformation of target proteins, exposing binding sites for the recruitment and modulation of further downstream proteins. Thus, kinases are involved in a signaling transduction cascade in which external and internal activation signals are transmitted from the cell surface to the cytoplasmic proteins and from cytoplasmic proteins to the nucleus, regulating processes such as cell growth, differentiation and apoptosis [2, 3].

Among TK in mammalian cells, the family of JAK kinases is well known and consists of 4 members of intracellular non-receptor TK (namely JAK1, JAK2, JAK3 and TYK2). JAK kinases were discovered in the early '90s using PCR-based strategies or low-stringency hybridization technologies and due to their initial uncertain function, they were referred to as "Just Another Kinase", hence the name, but are ultimately best-known as "Janus kinase" [4-7].

In humans, the *JAK1* gene is located on chromosome 1p31.3, *JAK2* is on 9p24, *JAK3* and *TYK2* are on chromosome 19p13.1 and 19p13.2, respectively; *JAK1*, *JAK2* and *TYK2* are expressed ubiquitously, while the expression of *JAK3* occurs mainly in hematopoietic cells [8]. JAK proteins have seven homology regions (called homology domains (JH)1-7, Figure 1A-1B), organized in an N-terminal FERM domain (JH6-JH7), a Src-homology 2 (SH2) domain (JH3-JH4) and a carboxyl terminal domain containing the pseudo-kinase domain and the kinase domain (JH2 and JH1, respectively) [9]. Specifically, the FERM domain is responsible for protein-protein interactions, such as adaptor and scaffolding interactions with membrane associated proteins, while the SH2 domain mediates interactions with cytokine receptors and other signaling proteins. Sequential FERM and SH2 domains are thus responsible for distinct receptor interactions. JH2 domain is catalytically inactive but equally fundamental for modulating the activity of the kinase domain JH1 and contributing to the maintenance of the basal level of activity in absence of stimuli [10, 11]. Because of these two near-identical phosphate-transferring domains, one exhibiting the kinase activity while the other negatively regulating the kinase activity of the first, these kinases were named accordingly to the two-faced Roman god "Janus" of beginnings/endings and duality.

JAK kinases are identified as crucial proteins in cellular signaling, and are associated with important cytosolic downstream proteins, mainly the Signal Transducers and Transcription activators (STAT) [12]. Seven genes encoding for STAT proteins are located on 3 different chromosomes: *STAT1* and *STAT4* are located on chromosome 2 (2q32.2 and 2q32.2-2q32.3 respectively); *STAT3*, *STAT5A* and *STAT5B* are present on chromosome 17 (17q21, 17q1.2 and 17q1.2); in chromosome 12 (in loci 12q13.13 and 12q13) are present *STAT2* and *STAT6*, respectively [13]. As shown in Figure 1C-1D, STAT proteins share a common structure consisting in a N-terminal domain, a coiled-coil domain, a DNA binding

domain, a linker sequence, an SH2 and the transactivation domain (TAD). The N-terminal domain plays a role in nuclear translocation and protein interactions, the coiled-coil domain is involved in nuclear translocation and in the regulation of tyrosine phosphorylation; the DNA binding domain allows the recognition of the promoter sequences of the target genes. Finally, the carboxy-terminal region TAD is important for the recruitment of cofactors and for transcriptional responses [9]. The dimerization of JAK and STAT proteins is fundamental for their functional role: the active JAK dimer is complexed with the intracellular domain of the cytokine receptor, while STAT members need to form stable dimers to rapidly translocate to the nucleus and bind DNA [14].

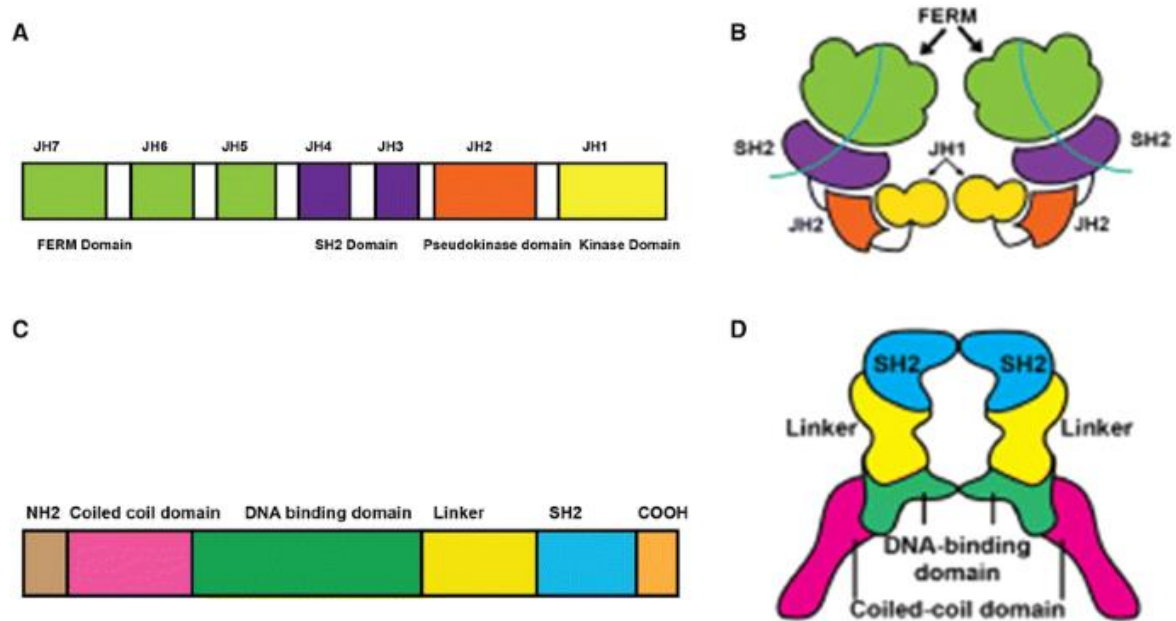


Figure 1. Schematic representation of the structure of JAK and STAT proteins. A) Linear structure of JAK: from the amino-terminal to the carboxy-terminal region, the JAK kinases are composed of the FERM, SH2, pseudo-kinase and kinase domains. B) Simplified image of the three-dimensional structure of JAK. C) Linear structure of STAT: from the amino-terminal to the carboxy-terminal region, they are composed of the N-terminal domain, the coiled-coil domain, the DNA binding domain, the linker sequence, SH2 and the TAD domain. D) Simplified image of the three-dimensional structure of STAT [14].

The JAK/STAT signaling pathway is described in Figure 2. The JAK/STAT pathway is involved in the signaling mechanism of a wide range of pro-inflammatory ligands, such as (TNF)- $\alpha$ , interleukins (IL) and interferons (IFN) [14, 15], and its activation regulates many biological processes, including cell proliferation, differentiation, apoptosis, immune cell development and regulation [16]. JAK2 ablation in mice results in embryonic lethality due to disruption of erythropoiesis in utero, underlying a critical need for JAK2 signaling in the development of the hematopoietic system [17]. The activation of the JAK/STAT pathway occurs when the binding of extracellular ligand to its receptor induces the multimerization of membrane receptor subunits [18]. JAK kinases are associated with the cytoplasmic domains of these receptors; the rearrangement induced by the ligand facilitates the trans-phosphorylation of the kinases themselves, determining their activation [19, 20]. Active JAK kinases, in turn, phosphorylate both the upstream receptor and the downstream STATs. Activated STAT proteins dimerize, translocate into the nucleus and bind, as dimers or complex oligomers, to specific sequences in target genes thus regulating

their transcription [19]. Among STAT target genes, there are genes involved in survival (e.g.: Bcl2, c-Myc), proliferation (e.g.: cyclin, Pim1/2), apoptosis (e.g.: caspase, p53) or cell cycle arrest (e.g.: p21, p27) [12].

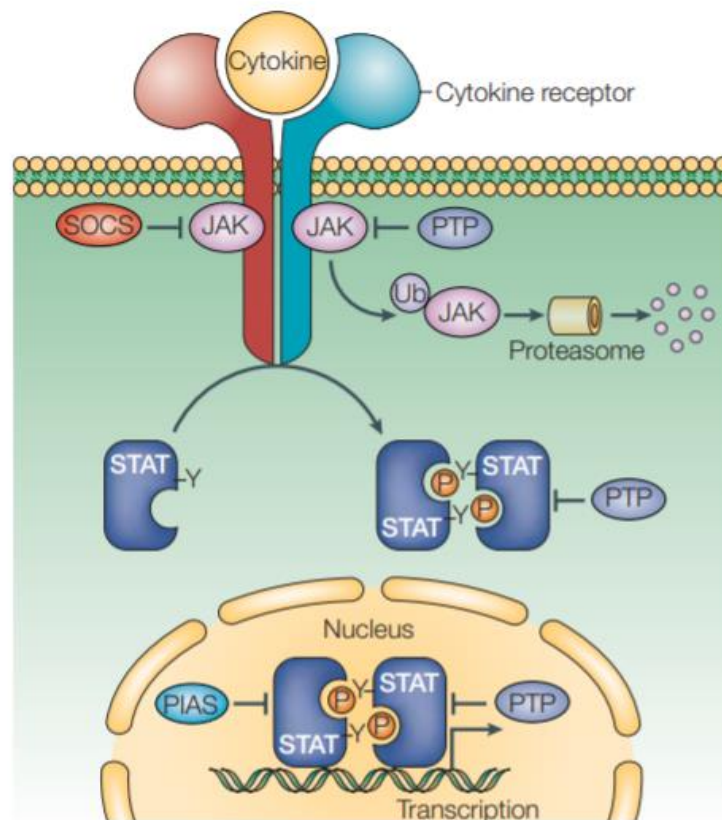


Figure 2. Description of the mechanisms involved in the activation and regulation of the JAK/STAT pathway. Receptor cytokines-binding activates JAK kinases. In turn, the active JAKs phosphorylate the receptor and the STAT proteins, determining their dimerization. Dimers translocate to the nucleus, where they act as transcription factors of target genes. SOCS, PIAS, and PTP proteins contribute to inhibiting JAK/STAT signaling through different mechanisms, blocking JAK kinases, STAT proteins, and dephosphorylating phosphorylated proteins, respectively [20].

A tight regulation of the signaling pathways is essential for the homeostasis of the cells, thus also the activity of JAK/STAT pathway is regulated at several levels (Figure 2). Several mechanisms contribute to the inhibition JAK/STAT signaling, including:

- the internalization of membrane receptors and their degradation by lysosome and proteasome.
- the recruitment of cytokine signal suppressors (SOCS), which operate through negative feedback loop on the JAK/STAT signaling pathway: activated STATs stimulate the transcription of SOCS genes and SOCS proteins bind to the phosphorylated JAK and receptor by turning them off.
- the interaction with the protein inhibitors of activated STAT (PIAS). PIAS proteins are constitutively expressed and inhibit the transcriptional activity of STAT.
- the recruitment of protein tyrosine phosphatase (PTP) which remove the phosphate group from the tyrosine residues of phosphorylated proteins [16].

Moreover, both JAK and STAT proteins present multiple phosphorylation sites, with complex, multi-level regulatory function on the kinase activity. As examples, the phosphorylation of Tyr119 in the JAK2 FERM domain destroys the JAK2-receptor interactions, whereas the phosphorylation of Tyr1007 and Tyr1008 residues in the in the activation loop of the kinase domain (JH1) plays an important role in the kinase activation [21, 22].

The pivotal role of JAKs in intracellular signaling is not limited in the JAK/STAT axis (Figure 3). Although the mechanism of JAK/STAT signaling is relatively simple in theory, the biological consequences of pathway activation are complicated by the crosstalk with other signaling pathways. The interaction between components in the JAK/STAT pathway and those in other well-known signaling pathways (such as TGF $\beta$ , MAPK, Notch, PI3K/AKT/mTOR, NF- $\kappa$ B and IRF signaling pathways) is complex and occurs at various levels, as described by Hu and collaborators in 2021 [23]. For example, in 2007, Levine and collaborators describe the role of JAK2 in myeloproliferative disorders and reported the activation of two other major signaling pathways, PI3K/Akt and Ras/Raf/MAPK/ERK, through JAK2 [24]. This evidence was later reported also by Birzniece et al. [25] as part of growth factor signaling and by Chiba et al. in Alzheimer's disease [26]. The crosstalk between components in the Notch signaling pathway is mainly thorough in organ development and also in breast cancer, in which the Notch signaling pathway is often hyperactivated, upregulating IL-6 expression when p53 is mutated or lost [27]. IL-6 is involved also in the connection between NF- $\kappa$ B signaling pathway with STAT3; the activation and interaction between STAT3 and NF- $\kappa$ B play vital roles in control of the communication between cancer cells and inflammatory cells [28]. Another example is given by the rearrangement t(9;22) encoding for the well-known Philadelphia Chromosome in Chronic Myeloid Leukemia (CML), which can lead to a persistent activation of STAT5, thanks to the interaction of BCR-ABL1 on JAK2 [29] and with high levels of STAT5 in the nucleus, as transcription factor [30, 31].

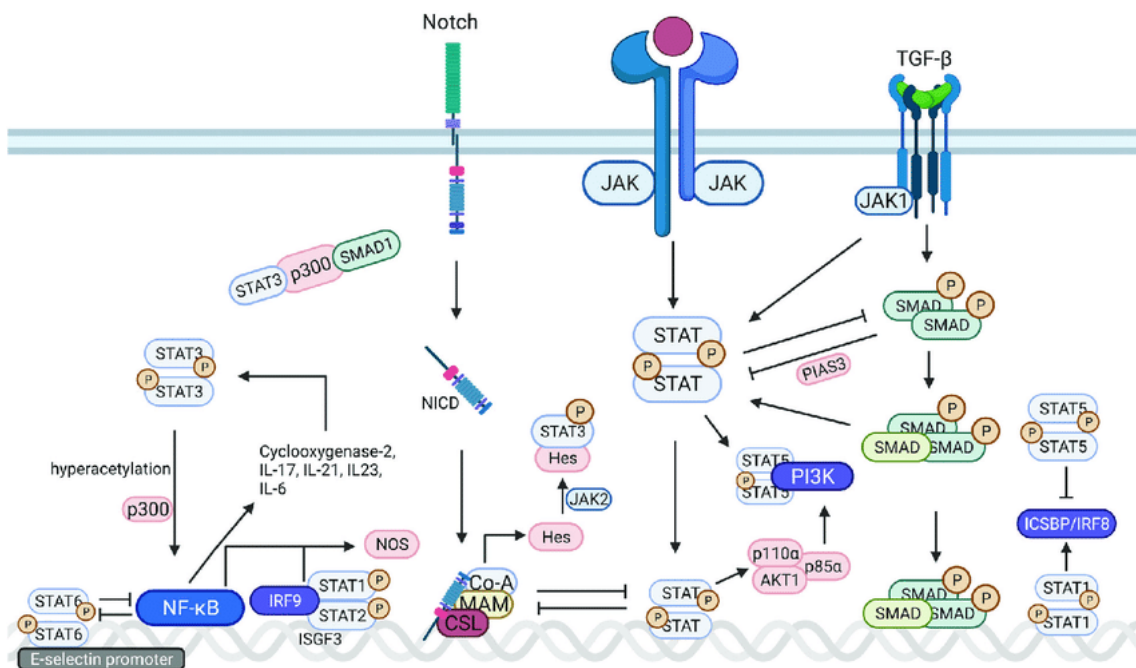


Figure 3. Signaling crosstalk between JAK/STAT and other signaling pathways [23].

## 1.2 JAK/STAT PATHWAY DEREGULATION

The deregulation of the JAK/STAT pathway can result in dramatic changes in physiological processes. Its aberrant activation is implicated in many immune-mediated diseases [32, 33], among which rheumatoid arthritis [34], psoriasis [35], dermatitis [36] and inflammatory bowel disease [37]. A common feature of these diseases is the abnormally elevated wide range of cytokines. Indeed, in immune-mediated chronic inflammation, the balance between pro-inflammatory and anti-inflammatory cytokines is skewed so that elevated levels of circulating pro-inflammatory cytokines such as IL-6, IL-12, IL-23 is favored leading to the involvement of the JAK/STAT pathway as a mediator of them [23, 38]. A recent investigation observed that IL-17 can activate the JAK1/2 and PI3K pathway, which coordinate with the NF- $\kappa$ B activation pathway of Act1/TRAF6/TAK1 for gene induction, especially for cell defense genes. host in human airway epithelial cells [39, 40]. Furthermore, JAKs can be strongly activated by IL-17-induced cytokines, such as IL-6.

Due to its essential role in the regulation of local and systemic inflammation, the JAK/STAT pathway is also relevant in response to viral infections and in type I interferonopathies characterized by constitutive activation of the antiviral type I interferon (IFN) axis [41]. IFNs are secreted molecules that represent one of the cell's first lines defense against viral and bacterial pathogens, as a part of the innate immune response triggered by the sensing of pathogen-associated nucleic acids. They are powerful inflammatory polypeptides, ubiquitously expressed by immune and non-immune cells, including macrophages, lymphocytes, dendritic cells, fibroblasts, and hematopoietic plasmacytoid dendritic cells [42]. Type I IFNs proteins (namely IFN $\alpha$  and IFN $\beta$ ) are encoded by a cluster of 13 IFN- $\alpha$  genes and one IFN- $\beta$  gene on chromosome 9. The secreted IFNs bind to their respective receptors and activate the JAK family members JAK1 and Tyk-2 with subsequent phosphorylation of STAT1 and STAT2, resulting in the expression of downstream antiviral IFN-stimulated genes (ISGs) [43]. Many ISGs encode molecules that have direct roles in the immune response, including viral interference as well as feedback regulatory mechanisms to inhibit viral replication [44].

Moreover, JAK/STAT signaling pathway is one of the critical factors that promotes neuroinflammation in neurodegenerative diseases as Alzheimer disease, Parkinson disease, and multiple sclerosis, especially due to myeloid cells and T cells switch to pathogenic phenotypes. In Alzheimer disease activated astrocytes and microglia are commonly observed around neurons and plaques; alongside, several pro-inflammatory cytokines or inflammatory markers were also shown to be overexpressed in patient's brains, as a response to the gradual accumulation of plaques. In particular, the JAK/STAT3 pathway appears to be a central player in the induction of astrocyte reactivity [45]. In Parkinson, the regulation of the *SNCA* (*Alpha-synuclein*) gene is affected by point mutations that lead to overexpression and aggregation of misfolded synuclein ( $\alpha$ -Syn) protein. The secretion of oligomeric  $\alpha$ -Syn induces toll-like-receptor-mediated activation of microglia and macrophages and leads to the production of pro-inflammatory mediators and SYN toxicity into brain. In *vitro*,  $\alpha$ -Syn exposure activated the JAK/STAT pathway in microglia and macrophages and in an *in vivo* rat model of Parkinson disease induced by viral overexpression of  $\alpha$ -SYN, JAKi treatment inhibited  $\alpha$ -SYN-induced neuroinflammation by suppressing microglial activation, macrophage and CD4<sup>+</sup> T-cell infiltration and production of proinflammatory

cytokines/chemokines. Importantly, inhibition of the JAK/STAT pathway prevented the degeneration of dopaminergic neurons *in vivo* [46].

Also in multiple sclerosis some investigators proposed a primary involvement of resident CNS glia, in particular, astrocytes and microglia, in disease pathogenesis. Clinical evidence suggests focal inflammatory infiltrates into the central nervous system, demyelinating lesions, axonal damage, and excessive cytokines (IL-12, IL-6, IL-21, IL-23, IL-17, granulocyte macrophage-colony stimulating factor, and IFN- $\gamma$ ) [47, 48]. As a result, while resident cells are anti-inflammatory in the physiologic state, they can switch to a pro-inflammatory phenotype in inflammatory conditions such as multiple sclerosis [49].

Besides, dysfunctional JAK/STAT pathway have also been associated with the development of different types and subtypes of human cancers, particularly several hematological diseases including myeloproliferative neoplasms (MPNs) and leukemias [50].

The most important example is given by the discovery in 2005 of the *JAK2* V617F somatic point mutation in Philadelphia (*BCR-ABL1*) negative MPNs. *JAK2* V617F (c.1849G>T, p.Val617Phe) is a gain-of-function mutation located in the pseudo-kinase domain of JAK2 (JH2) which negatively regulates the kinase domain of JH1 thereby causing constitutive tyrosine phosphorylation of JAK2. It is present in 96% of adult patients with polycythemia vera (PV), in 55% and 65% of patients with essential thrombocythemia (TE) and primary myelofibrosis (PMF), respectively [15, 51]. PV, TE and PMF are Philadelphia (*BCR-ABL1*) negative MPN, a heterogeneous group of hematopoietic stem cell diseases characterized by different risk grades of thrombotic complications and acute myeloid leukemia evolution. Patients with PV have aberrant production of red blood cells in the bone marrow and blood, and in the case of TE, there is a high number of platelets. PMF patients, on the other hand, have a bone marrow replaced by fibrous scar tissue [52]. The discovery of the *JAK2* V617F point mutation has led to an in-depth screening of the possible mutations present in JAK kinases and their frequencies among hematological tumors, for investigating the putative different molecular mechanisms underlying the constitutive activation of the JAK/STAT pathway. In addition to *JAK2* V617F, also missense mutations, small insertions, or deletions in exon 12 of *JAK2* were identified in 2007 (encountered in 2–3% of patients with PV and absent in ET and PMF). MPNs are also characterized by mutations in other genes, such as the *CALR* gene, which encodes for calreticulin (a calcium-binding chaperone of the endoplasmic reticulum), and the *MPLV* gene (myeloproliferative leukemia virus), a proto-oncogene encoding for the hematopoietic growth factor receptor of myeloid stem cells [53, 54]. Mutations in *CALR* are rare in PV but are present in 25-35% of patients with PMF and in 15-24% of patients with TE; mutations affecting *MPLV* also occur rarely in PV and in approximately in 4% and 8% of patients with TE and PMF, respectively [51]. *JAK2*, *CALR*, and *MPLV* mutations are considered as driver mutations; given their redundant effect, *MPLV* and *CALR* mutations rarely co-occur with *JAK2* mutations. On the other hand, the so-called "triple-negative" MPN patients even without a driver mutation in *JAK2*, *CALR* or *MPLV*, show activated JAK2 signaling; this highlights the significance of a crosstalk of JAK2 signaling with other pathways for the onset of MPN pathogenesis [55].

Compared to the predominance of *JAK2* V617F mutation in MPNs, the *JAK1*, *JAK2*, *JAK3* and *TYK2* mutations, described in other hematological diseases are more heterogeneous. *JAK2* genetic alterations characterize some forms of B-cells acute lymphoblastic leukemia (ALL) of the immunophenotype B

called *BCR-ABL1 like* [56]. *BCR-ABL1 like* ALL were first identified in 2009 as a new subgroup of B-ALL by the Dutch Childhood Oncology Group led by Professor Den Boer (Princess Máxima Center, Utrecht, The Netherlands) [57]. This form of leukemia takes its name from the *BCR-ABL1* ALL because of the transcriptional profile of *BCR-ABL1 like* leukemic cells that resembles that of true *BCR-ABL1* ALL cases; however, *BCR-ABL1 like* blasts do not show the chromosomal translocation t(9;22)(q34;q11.2) and thus do not present the *BCR-ABL1* fusion gene. Indeed, *BCR-ABL1 like* ALL are characterized by a heterogeneous molecular and genetic profile, characterized by the presence of mutations or rearrangement in several kinase-encoding genes (particularly *ABL1* or *JAK2*, linked to lymphoid signaling, or to their corresponding upstream membrane receptors (e.g.; *PDGFRβ* for *ABL1*; *CRFL2* and *EPOR* for *JAK2*) [58]. Approximately 10% of *BCR-ABL1 like* ALL patients have ABL-class related mutations [59].

JAK kinases are found to be mutated mainly in adult subjects with ALL *BCR-ABL1 like*, presenting *JAK2* rearrangements in 7% of cases (e.g., *BCR-JAK2*, *PAX5-JAK2*), or other alterations in different JAK/STAT pathway components (e.g., *CRLF2*, *IL7R*, *JAK1*, *JAK3*) in about 12% of cases [57].

In particular, *CRLF2* rearrangements are observed in approximately 50% of *BCR-ABL1 like* B-ALL patients. *CRLF2* encodes cytokine receptor-like factor 2, also known as the thymic stromal derived lymphopoietin receptor, which in combination with the interleukin 7 receptor  $\alpha$  chain (IL-7R) forms the receptor for thymic stromal lymphopoietin. *CRLF2* is an upstream receptor of the JAK/STAT pathway and commonly presents a translocation to the immunoglobulin heavy-chain enhancer region (*IGH-CRLF2*) or a deletion of upstream *PAR1* that leads to joining of *CRLF2* to adjacent *P2RY8*. *P2RY8-CRLF2* fusion encodes full-length *CRLF2*, which results in high expression of this cytokine receptor [59]. *CRLF2* rearrangements occur in 24% of children and up to 60% of adolescents with *BCR-ABL1 like* ALL; the *IGH/CRLF2* rearrangement is more present in the adult population: analyzing a group of patients aged >15 years with ALL *BCR-ABL1 like*, 66% of them have *CRLF2* overexpression, of which 76% have the *IGH/CRLF2* rearrangement, while only 17% have *P2RY8-CRLF2*. About 7% had an unknown fusion partner [56, 60].

### 1.3 JAK INHIBITORS (JAKi)

Thanks to genome-wide association studies, it was discovered that most cytokine receptors play an important role in the initiation and development of immune and inflammatory processes [25, 26]. For this reason, immunotherapeutic approaches were introduced and are critical to stop the abnormal signaling cascade. Monoclonal antibodies are effective in regulating cytokines and their receptors at an extracellular level, as well demonstrated by the use of infliximab in rheumatoid arthritis, psoriasis, and inflammatory bowel disease [61-64]. However, intracellular signaling proteins can also be targeted and so far, JAK inhibitors (JAKi) have been introduced, demonstrating an equivalent or even superior efficacy to biologics, overcoming many of their limitations [65, 66]. Monoclonal antibodies bind monospecifically to certain cells or proteins whereas the action of multiple cytokines is inhibited by the mode of action of JAKi and in comparison, with the treatment with biologicals, JAKi have the advantage of oral application [66].

Currently, regulatory authorities (e.g., European Medicines Agency (EMA) and U.S. Food and Drug Administration (FDA)) approved JAKi for treatment of rheumatologic, dermatologic, gastrointestinal, and neoplastic diseases. Many other JAKi and possible STAT inhibitors are under investigation in preclinical evaluations and clinical trials [67, 68].

Compounds of interest for our work, their chemical structure and affinities for JAK proteins are shown in Table 1.

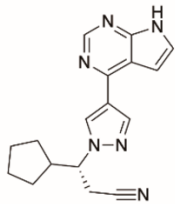
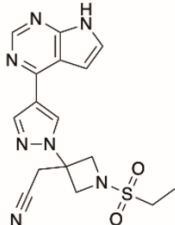
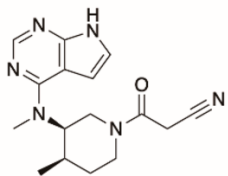
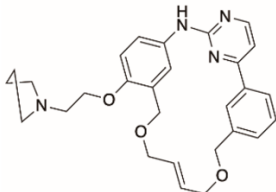
DRUG	JAK1 (IC <sub>50</sub> )*	JAK2 (IC <sub>50</sub> )*	JAK3 (IC <sub>50</sub> )*	TYK2 (IC <sub>50</sub> )*	REFERENCES
<b>RUXOLITINIB</b> 	3.3 nM	2.8 nM	NA	NA	[69]
<b>BARICITINIB</b> 	5.9 nM	5.7 nM	>400 nM	53 nM	[70]
<b>TOFACITINIB</b> 	112nM	20 nM	1 nM	NA	[71]
<b>PACRITINIB</b> 	NA	23 nM (V617F): 19 nM	520 nM	50 nM	[72]

Table 1. Main JAK inhibitors and their affinity to target kinases. \*Nanomolar (nM) concentrations refer to IC<sub>50</sub> values calculated in cell-free assays. NA: not assessed



The first JAKi to receive approval was the type I JAK inhibitor ruxolitinib, also known as Jakavi®. Ruxolitinib was approved in 2011 by the FDA and in 2012 by the EMA for the treatment of intermediate and high-risk MF (primary MF or post-PV/TE MF) and in 2014 for adult patients with PV who were resistant or intolerant to hydroxyurea. In these patients, therapy with ruxolitinib is not curative or capable of preventing disease progression. Consequently, treatment indications for PV, TE and PMF are primarily aimed to the prevention and treatment of thrombohemorrhagic events by low-dose aspirin, phlebotomy and hydroxyurea, while allogeneic stem cell transplantation represented the only curative approach in these patients [73, 74]. FDA and EMA approved ruxolitinib also for acute graft-versus-host disease (GVHD) in 2019 and for chronic GVHD in 2021, in patients older than 12 years who underwent transplantation and for whom corticosteroids or other systemic therapies are not effective. Approval was based on REACH-1 study (NCT02953678 [www.clinicaltrials.gov](http://www.clinicaltrials.gov)) and REACH-3 study (CINC424D2301; INCB 18424-365; NCT03112603) [75].

Baricitinib, known as Oluminant®, is JAK1/JAK2 inhibitor approved by FDA and EMA in 2017 for the treatment of rheumatoid arthritis and in 2022 for atopic dermatitis and alopecia areata [76-78].

It may be of interest also in MPNs treatment given its similarities with ruxolitinib and the longer half-life (12.5 hours) [79], and also for patients affected by systemic lupus erythematosus by attenuating autoimmune features as demonstrated by a phase II double-blind, randomized, placebo-controlled trial (NCT02708095) [80, 81].

Most recently, baricitinib has become a valuable therapeutic option in adult hospitalized patients with severe COVID-19 prognosis [82-85]. The therapeutic rationale is the treatment of COVID-19 related cytokine storm to contain systemic inflammation [65, 84] and the reduction of SARS-CoV-2 Coronavirus entry into lung cells. Indeed, baricitinib may interfere with AP2-associated kinase 1 AAK1 (AAK1) that regulates the angiotensin-converting enzyme 2 (ACE2) receptor involved in host viral endocytosis [86, 87]. Baricitinib does not decrease the length of patients' hospitalization but determine a reduced use of mechanical ventilation, a lower incidence of acute respiratory distress syndrome and a decreased risk of mortality. High costs and adverse events may be limiting aspects of JAKi treatments in COVID-19 [88].

Tofacitinib (CP-690550), commercial name Xeljanz®, belongs to the second-generation of selective JAKi targeting the JAK3 kinase; in 2019 it has been approved by FDA and EMA for rheumatoid arthritis, psoriatic arthritis, polyarticular course juvenile idiopathic arthritis and ulcerative colitis. In 2021, an extended-release version of tofacitinib has also been approved including treatment for ankylosing spondylitis [89-91].

Of interest is also pacritinib, approved in February 2022 as a type I inhibitor with specificity for JAK2, FLT2, FLT3, IRAK and CSF1R treatment of PMF and GVHD. The accelerated approval was based on results from the clinical trials PERSIST-1 and PERSIST-2 (NCT03645824, NCT02532010) demonstrating to be effective in PMF and acute myeloid leukemia patients [92-94].

Ruxolitinib, baricitinib and tofacitinib are first-generation type I JAKi. Type I inhibitors are ATP-competitive, blocking the ATP binding site and stabilizing the kinase in its active conformation [69-72]. The major limitation of this type of inhibitors is that chronic exposure leads to a loss of response as observed *in vitro*, in animal models and patients [74]. Ruxolitinib and baricitinib mainly inhibit JAK1 and

JAK2 [95]. Moreover, baricitinib seems to have a stronger inhibitory effect on JAK2/TYK2 activated by the IL-12/23 signaling than ruxolitinib [96]; only ruxolitinib has been proven to be capable of crossing the blood-brain barrier in humans [97]. Tofacitinib mainly inhibits JAK1 and JAK3 with mild selectivity on JAK2. Instead, pacritinib determines a potent inhibitory effect in both wild-type JAK2 and mutant JAK2 V617F, on TYK2 and on JAK3, with activity also towards the FMS tyrosine kinase 3 (FLT3); being a new generation JAKi.

There are also other types of JAKi, classified according to the structure of the enzyme-bound antagonist complex: Type II inhibitors (e.g. NVP-CHZ868, NVP-BBT594) bind to the ATP binding site of the TK domain, in the inactive conformation of the enzymes; allosteric inhibitors (e.g. LS104, ON044580) bind to a regulatory region (distinct from the kinase active site) where ligand binding can either positively or negatively affect the enzyme activity [98]. Allosteric molecules include type III inhibitors, which bind to an area near the ATP binding site, and type IV inhibitors, which instead hit an area distant from the ATP binding site. Finally, type V inhibitors recognize two sites of the kinase domain by a reversible binding and are therefore bivalent [79].

### 1.3.1 JAKi REPURPOSING

Evidence suggest JAKi as candidates for drug repurposing in different pathological conditions, as demonstrated by Trivedi et al in a recent study regarding type I diabetes affected patients [99], or in case of therapeutic management of hospitalized patients with COVID-19 [88].

Given the central role of the JAK-mediated cytokine signaling pathway in inflammatory and autoimmune disorders, it is not surprising that JAKi have recently been proposed as the most promising molecules for the treatment of these diseases and several clinical trials are currently ongoing for the approval of JAKi in other inflammatory and autoimmune diseases [65]. Evidence in literature regarding JAKi repurposing derives from the study conducted by Sanchez and collaborators: they repurposed baricitinib for patients with the monogenic interferonopathies CANDLE, SAVI, and other interferonopathies, demonstrating an improvement in clinical manifestations and inflammatory and IFN biomarkers [100]. Aicardi-Goutieres syndromes (named AGS) should be considered as a subtype of type I interferonopathies, given the lack of response to common autoinflammatory therapeutics including IL-1 and TNF blockade [74, 101, 102]. The role of JAK/STAT pathway and JAKi in another type I interferonopathies (the AGS) is better described in the paragraph below.

Among neoplastic diseases, *BCR-ABL1 like* ALL patients characterized by JAK/STAT overactivation may benefit from JAKi; *in vivo* studies have demonstrated the antileukemic activity of the type I inhibitor ruxolitinib given as monotherapy in xenograft models deriving from patients with *BCR-ABL1 like* ALL harboring JAK pathway aberrations [103]. A Phase I clinical trial (NCT01164163) demonstrated the safety of ruxolitinib monotherapy in children affected by relapsed or refractory tumors. In current clinical trials, however, ruxolitinib is given in combination with conventional chemotherapy from the consolidation phase to the end of maintenance therapy (NCT02883049, NCT02723994, NCT03117751) [104, 105]. To the best of our knowledge, *BCR-ABL1 like* ALL patients are not treated according to a specific target therapy. In Italy, the current AIEOP-BFM ALL 2017 protocol to treat pediatric *BCR-ABL1* negative ALL does not screen for *BCR-ABL1 like* genetic alterations, either of the ABL1 or JAK2 class. Indeed, the

heterogenic genetic background of *BCR-ABL1 like* ALL determine a challenge in diagnosis and considering high costs related to sequencing techniques, these can't be used routinely in clinical practice. The current need is thus related to the fast and accurate identifications of aberrant TK activity in lymphoblasts and for assessing their pharmacological response to tyrosine kinases inhibitors (either for ABL1 or JAK-class); for these purposes an innovative tool could become essential in the perspective of personalized therapy of this disease.

### **1.3.2 JAKi SIDE EFFECTS**

The JAKi treatments of patients with immune-mediated inflammatory diseases or hematopoietic neoplasms have substantially changed patients' outcome and advanced risk management. Although the effectiveness of JAKi treatment has given excellent results, data extracted from the World Health Organization database and published in 2022 by Hoisnard and collaborators, have clearly revealed the other side of the coin with respect to the use of these drugs. In fact, despite being considered safe, they are not free from having adverse effects, particularly in patients aged 65 years or above, in those at increased risk of major cardiovascular problems, in those who smoke or have done so for a long time in the past and in those at increased risk of cancer [106].

Recently, EMA has recommended and confirmed measures to minimize the risk of serious side effects associated with JAKi in several chronic inflammatory disorders (EMA/860610/2022). In particular, ruxolitinib, tofacitinib and baricitinib were commonly associated with infection (1-10% of patients) including fungal and mycobacterial infectious disorders; these drugs were also associated with musculoskeletal and connective tissue disorders and neoplasms (especially non-melanoma skin neoplasms) occurring in 0.1-1% of patients. Only tofacitinib was associated with gastrointestinal perforation events and peripheral neuropathy in patients with rheumatoid arthritis [107, 108]. After careful considerations EMA Committee for Medicinal Products for Human Use and the FDA added thrombosis (1-10% of patients) to the baricitinib and tofacitinib warnings and precautions in patients at high risk of blood clots (EMA/608520/2019).

Considering MPNs, the therapeutic value of JAKi is diminished by a nonspecific myelosuppressive effect as anemia, thrombocytopenia and neutropenia, occurring in more than 10% of patients affected by MF and PV. Common toxicity of pacritinib are gastrointestinal adverse events, thrombocytopenia, and anemia [109, 110].

In general, when possible, JAKi doses should be reduced in patient groups at risk.

## 1.4 TYPE I INTERFERONOPATHIES

Type I interferonopathies comprise a genetically and phenotypically heterogeneous group of inherited autoinflammatory and autoimmune disorders characterized by inappropriate activation of the IFN pathway, because of constitutive upregulation of its activation mechanisms or downregulation of negative regulatory systems, leading to severe inflammation.

The term “interferonopathy” first appeared in 2003, when some authors identified phenotypic overlaps between AGS encephalopathy, viral congenital infections, and some autoimmune diseases such as systemic lupus erythematosus, postulating an upregulation of IFN activity as a common pathological feature [111, 112]. While their phenotypic spectrum is broad, ranging from severe neurological impairment to mild cutaneous disease, systemic autoinflammation and autoimmunity are commonly shared signs of type I interferonopathies. According to the 2017 classification of the International Union of Immunological Societies, 13 type I interferonopathies were identified [113]; other monogenic syndromes were recognized, including proteasome-associated autoinflammatory syndromes, ISG15 deficiency, Singleton–Merten syndrome, and STING-associated vasculopathy with onset in infancy.

### 1.4.1 AICARDI-GOUTIÈRES SYNDROME (AGS)

AGS (Orphanet Orpha Number: ORPHA-51 ([www.orpha.net](http://www.orpha.net)), is a rare genetic neurological disorder classified as primary immunodeficiency [114], having an onset during infancy and early childhood. The prevalence is about 1-5 cases every 10000 person and various forms of this disease have been found in individuals of all ethnic origins; however, the actual AGS frequency is currently unknown. AGS has been described for the first time in 1984 in patients showing early-onset encephalopathy, basal ganglia calcification (therefore, various degrees of neurological impairment and deterioration) and persistent lymphocytosis in cerebro-spinal fluid (CSF) causing systemic inflammation [115, 116]. Clinically, AGS patients are characterized by immune manifestations, neurodevelopmental degeneration, and progressive impairments, leading to poor life expectation; tetraparesis occurs without other obvious causes in the first year of life, 92% of cases display mental delay, 75% dystonia, 63% microcephaly and 42% skin lesions similar to chilblains at fingers and toes [117]. The main neuropathological feature of the disease is abnormal myelination, probably caused by increased expression of proteases like cathepsin D, able to degrade myelin and brain tissue matrix [118, 119].

The presence of elevated levels of IFN I in CSF, serum and cardinal specific neuro-radiologic features are hallmarks typically associated to AGS [117, 120]. AGS patients demonstrate an increased expression of a set of interferon-stimulated genes (ISGs) in peripheral blood, the so-called “interferon signature”, commonly observed in CD4+T cells, monocytes, and monocyte-derived macrophages [121, 122].

This genetic disorder is an autosomal recessive inherited disease caused by biallelic mutations of at least one out of multiple genes involved in nucleic acid metabolism or sensing [123]. Originally, in 1984 Aicardi and Goutières reported 8 patients from 5 families who had a type of familial-onset encephalopathy and neurological manifestations revealing a certain clinical heterogeneity of the

syndrome [115]. Over the years and research it has found that there are at least 9 subtypes of the disease, involving mutations in different genes: DNA exonuclease 1 (*TREX1*) in AGS1; ribonuclease H2 subunit A (*RNASEH2A*) in AGS4, ribonuclease H2 subunit B (*RNASEH2B*) in AGS2, ribonuclease H2 subunit C (*RNASEH2C*) in AGS3; SAM and HD domain containing deoxynucleoside triphosphate triphosphohydrolase 1 (*SAMHD1*) in AGS5; RNA-specific adenosine deaminase-1 (*ADAR1*) in AGS6; cytosolic double-stranded RNA receptor gene *IFIH1* (also called MDA5) in AGS7 [124]. Recently, mutations in other two genes have been found, leading to new AGS subtypes: U7 Small Nuclear RNA Associated (*LSM11*) in AGS8 and U7 Small Nuclear 1 (*RNU7-1*) in AGS9, encoding components of the replication-dependent histone pre-mRNA processing complex, mutation of both leads to dysregulation of histone RNA [125]. Gene functions are summarized in Table 2.

In AGS, most frequently mutated genes are *RNASEH2B* (35-40% of AGS patients, usually of Italian and European origin) and *TREX1* (23-25%, often mutated in northern European families) [124]. *RNASEH2C* mutations are rarer (12-15%, almost exclusively found in the Pakistani population); 10-13% of patients have mutations in *SAMHD1* while mutations in *RNASEH2A* have been described in only 5% of cases. *ADAR1* and *IFIH1* have lower mutation rates, being found to be responsible for the disease in ~ 8% and ~4% of cases, respectively. As already indicated, in almost all cases the disease is inherited as an autosomal recessive trait; the exceptions are cases carrying *IFIH1* mutations (heterozygous and dominant) and cases of AGS caused by de novo heterozygous mutations of *TREX1* and *ADAR1* inherited as a dominant trait. In its most severe form, AGS is typically associated with mutations in *TREX1* [124].

AGS SUBTYPE	MUTATED GENE	CYTOGENETIC LOCATION	FUNCTION
AGS1	<i>TREX1</i>	3p21.31	DNA 3' to 5' exonuclease, prevents autoimmunity caused by endogenous retroelements.
AGS2	<i>RNASEH2B</i>	13q14.3	Beta subunit of the human ribonuclease H2 enzyme complex which cleaves ribonucleotides from RNA:DNA duplexes.
AGS3	<i>RNASEH2C</i>	11q13.1	Subunit C of the human ribonuclease H2 enzyme complex which cleaves ribonucleotides from RNA:DNA duplexes.
AGS4	<i>RNASEH2A</i>	19p13.13	Subunit A of the human ribonuclease H2 enzyme complex which cleaves ribonucleotides from RNA:DNA duplexes.
AGS5	<i>SAMHD1</i>	20q11.23	Converts deoxynucleoside triphosphates to constituent deoxynucleoside and inorganic triphosphate.
AGS6	<i>ADAR1</i>	1q21.3	Converts adenosine to inosine in double strand RNA.
AGS7	<i>IFIH1</i>	2q24.2	Encodes for a cytoplasmic receptor that senses dsRNA viral products to activate type I interferon signaling through the MAVS adaptor molecule.
AGS8	<i>LSM11</i>	5q33.3	Part of the U7 small nuclear ribonucleoprotein (snRNP) complex involved in the processing of RDH pre-mRNAs.
AGS9	<i>RNU7-1</i>	12p13.31	Role in processing the 3-prime stem-loop structure of replication-dependent histone pre-mRNAs.

Table 2. AGS subtypes and their genetic alterations (OMIM-Online Mendelian Inheritance in Man database).

AGS is thus associated with an abnormal response to endogenous nucleic acid stimuli, activating the type I IFN-dependent nucleic acid-sensing pathways (Figure 4). Specifically, the accumulation of cytosolic DNA activates the DNA sensor cyclic GMP-AMP synthase (cGAS). Upon binding to an endogenous nucleic acid fragment, cGAS converts AMP and GMP into cyclic 2'3' GMP-AMP (cGAMP) that acts as a second messenger: it mediates downstream immune responses through the interaction with the molecule STimulator of INterferon Genes (STING) localized on the endoplasmic reticulum [126]; STING translocates from the endoplasmic reticulum to the Golgi, where it recruits the TBK1 kinase and then the transcription factors IRF3, which translocate to the nucleus and upregulate the production and the release of type I IFN. The binding of the IFN to one receptor subunit induces the dimerization of IFN- $\alpha$  receptor 1 (IFNAR1) and IFNAR2 that in turn recruit JAK1 and TYK2 proteins. This activation further promotes the STAT1-STAT2 dimerization and the recruitment of IFN regulatory factors 9 (IRF9) to assemble the heterotrimeric interferon-stimulated gene factor 3 (ISGF3) transcription complex. In the nucleus, ISGF3 binds to IFN-stimulated response elements (ISRE) on DNA promoting the expression of ISGs [127-130].

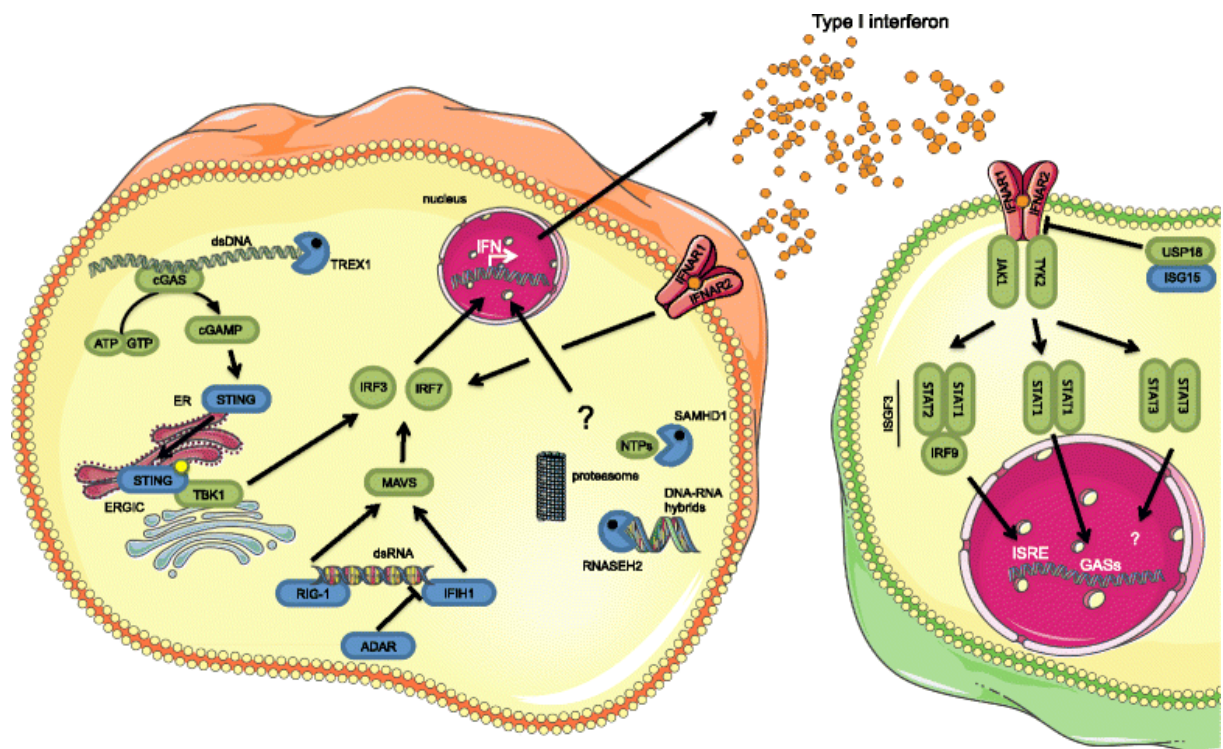


Figure 4. Cytoplasmic nucleic acid recognition and type I IFN pathway activation. Scheme of cytoplasmic nucleotide sensing, type I IFN secretion and autocrine and paracrine IFNAR activation [130].

## 1.4.2 AGS THERAPY

AGS is undoubtedly a severe disease; 19% of patients captured in the largest natural history study published to date had died, and 74% left profoundly disabled. Therefore, treatments are urgently needed [131]. To date, there are no effective cures for AGS and treatments are mainly supportive and symptomatic, improving the patient's quality of life particularly if started early, during the initial acute/subacute (active) phase of the diseases. Considering the involvement of the immune system in the pathogenesis of AGS, immunosuppressive and immunomodulatory therapies, based on glucocorticoids (dexamethasone) and thiopurines (mercaptopurine, thioguanine and azathioprine) or combined (prednisone + azathioprine, intravenous methylprednisolone + intravenous immunoglobulin (IVIG), isolated methylprednisolone or IVIG) have been tried empirically without a clear evidence of symptom resolution [132-135].

These therapies represent a "broad spectrum" approach directed to immune cells aimed at addressing the inflammatory basis of AGS, and judging the efficacy of these interventions is difficult because of the small numbers involved, the different regimens employed, and the stage of the disease process at which treatment was started. The fine characterization of the unraveled molecular mechanisms involved the type I IFN response in AGS have suggested other therapeutic targets for this orphan disease. Novel therapeutic strategies in AGS, including the use of JAKi, reverse transcriptase inhibitors (RTI), anti-IFN- $\alpha$  antibodies, anti-interleukin antibodies, antimalarial drugs (mepacrine) and other cGAS inhibitors were proposed for AGS patients, but their efficacy still needs to be proven [134]; the high heterogeneity of the diseases makes difficult to study targeted therapies.

Since JAK1 and TYK2 play a pivotal role in the type I IFN response, specific JAKi such as ruxolitinib and baricitinib, may be promising in blocking IFN activation and reducing the inflammatory reaction caused by the IFN overproduction [136]. JAKi have been already used to treat patients with distinct interferonopathies including AGS, on a compassionate basis. The rationale for using JAK inhibitors is that inhibiting JAK kinases should have the effect of reducing the inflammatory reaction caused by the IFN overproduction, typical of patients affected by type I interferonopathies [134]. In the past six years, literature has collected several reports of ruxolitinib treatment in AGS patients. In 2016, Tüngler et al. wrote about two AGS2 patients carrying biallelic mutations in *RNASEH2B* who presented severe developmental delay. Age at onset was not specified, but both patients were treated with ruxolitinib from the age of 23 months. The initial dosage was 0.2 mg/kg/day and after 1 week, 0.5 mg/kg/day. In both patients, an improvement of psychomotor delay with a reduction in dystonic movements was reported. Both showed a sustained reduction of the IFN score [137]. In 2018, another report by Kothur et al. described the use of ruxolitinib in a 8-months old child carrying an heterozygous p.Arg779Cys IFIH1 substitution (AGS7), demonstrating favorable therapeutic effects in reducing neuro-inflammation. The child kept a positive IFN signature, but no CSF lymphocytosis was found. Magnetic resonance showed a pattern of delayed myelination but no calcification or atrophy at 16 months, while cerebral computed tomography was not mentioned. At 16 months, treatment with oral prednisolone and intravenous immune globulin was started and a mild clinical improvement was observed in the form of reduction of irritability and sterile pyrexias, and acquisition of partial head and trunk control. At 32 months, oral ruxolitinib was started at a dosage of 2.5 mg twice a day, increased to 5 mg twice a day after 6 weeks. The introduction

of the JAKi coincided with an improvement of neurological conditions, with progressive reacquisition of the previously lost neurodevelopmental milestones, the improvement of the neuromotor scores, the lowering of IFN markers and inflammatory cytokine levels, and progressive improvement of myelination on magnetic resonance imaging [97]. In a recent case-report published in 2021, Cattalini et al described the use of ruxolitinib in a 5-year-old girl affected by AGS6 (*ADAR1* mutation). A limited, but distinct neurological improvement was observed. The girl's interferon score was compared with that of her older brother, suffering from the same disorder, who was not treated: the score of the girl was consistently lower than that measured in her brother. The authors suggested that starting JAKi at early age in children with AGS could mitigate the detrimental effects of type I interferon hyperproduction [138]. On the other hand, ruxolitinib treatment started pre-symptomatically in a *RNASEH2B*-mutated patient at diagnosis (4 months of age) did not prevent the onset of clinical signs at 14 months; this patient had also an affected older brother, thus was able to receive a genetic diagnosis prior to symptoms onset [131].

A *SAMHD1*-mutated patient treated with baricitinib was reported by Meesilpavikkai et al.; this young female was diagnosed at 19 years and presented as a case of AGS-related interferonopathy clinically characterized by subclinical hypothyroidism, mild intellectual disability and basal ganglia calcification. The authors described severe chilblains as the most prominent and disabling symptoms. After starting treatment with baricitinib at a dosage of 2 mg/day, the skin lesions significantly improved and the patient's IFN score decreased [139].

Two clinical trials are ongoing (Table 3). A currently ongoing clinical trial conducted at the Children's Hospital of Philadelphia (Pennsylvania, USA) is exploring baricitinib treatment in AGS and AGS-related interferonopathies: the primary aim is to determine if the administration of baricitinib results in an improvement or stability of the AGS scale at baseline and at 52 weeks (NCT03921554, [www.clinicaltrials.gov](http://www.clinicaltrials.gov)). Another trial in adult and pediatric Japanese participants with Nakajo-Nishimura syndrome (NNS)/CANDLE, SAVI, and AGS has the main purpose of evaluating the efficacy and safety of baricitinib over a 100-week period (NCT04517253). Both clinical trials are currently active with no results available. Nowadays, it is not clear whether inhibition of the JAK/STAT pathways will have similar efficacy and tolerability across AGS subtypes and, therefore, compassionate use of these drugs should be stricter. Depending on the results of the current studies, future clinical trials of JAK for the treatment of AGS might need to focus on specific genetic subtypes.



NCT NUMBER	DRUGS	PATHOLOGY	PARTECIPANTS	STATUS	CENTER
NCT03921554	Baricitinib	AGS	50	Ongoing	Children's Hospital of Philadelphia, Pennsylvania, United States
NCT04517253	Baricitinib	NNS; CANDLE; SAVI; AGS.	8	Ongoing	Hiroshima University Hospital; Hiroshima-shi, Hiroshima-ken, Japan; Nara Medical University Hospital; Kashihara, Nara, Japan; Tokyo Medical And Dental University Medical Hospital; Bunkyo, Tokyo, Japan.

Table 3: Clinical trial for JAKi in AGS treatment. NNS: Nakajo-Nishimura Syndrome; CANDLE: Chronic Atypical Neutrophilic Dermatosi s with Lipodystrophy and Elevated Temperature; SAVI: Stimulator of Interferon Genes (STING)-Associated Vasculopathy With Onset During Infancy.

Other novel therapeutic approaches, such as RTI (abacavir sulfate, lamivudine, zidovudine) provide substantial evidence of effectiveness in AGS patients clinical trials (completed clinical trial: NCT02363452, still ongoing clinical trial: NCT03304717). RTI can potentially disrupt the replication cycle of both exogenous retroviruses and endogenous retro-elements, reducing the accumulation of cytosolic DNA and are commonly prescribed drugs, widely used by HIV patients; for this reason, their pharmacodynamic, safety and toxicity profiles are already well characterized [133].

A recent single-center, open-label, study was conducted on 11 AGS patients treating them with a combination of 3 RTIs (abacavir sulfate, lamivudine, zidovudine) for 12 months, adopting the doses used in children's HIV treatment (NCT02363452, Table 4). Among the other inclusion criteria, it is important to highlight the recruitment of patients presenting only specific AGS pathogenic mutations such as *TREX1*, *RNASEH2A*, *RNASEH2B* and *SAMHD1*. The results showed that in 8 of the 11 patients there was a considerable reduction, without adverse reactions, in the INF score, which is given by calculating

the levels of 6 interferon stimulated genes. Furthermore, this effect showed to be greater among 4 patients presenting mutations in *RNASEH2A* and *RNASEH2B*. Despite a significant reduction in IFN score, clinical symptoms did not improve, as expected because patients were all in an advanced state of the disease. In fact, given the advanced state of the pathology of the recruited patients, improvement of their clinical picture was not the aim of the study. However, through magnetic resonance imaging it was possible to state how 3 patients, during the months of treatment, had increased cerebral blood flow, suggesting a possible benefit given by treatment with RTIs, perhaps also because of the combination with other drugs [140]. The aim of another currently ongoing trial, being conducted at the Children's Hospital of Philadelphia (NCT03304717, Table 4), is to explore the safety and the efficacy of two other RTIs (tenofovir and emtricitabine) administered for six months in children, aged 2-18 years, suffering from AGS and presenting a positive IFN signature. The primary endpoint is the change in IFN activation as measured by IFN signature. No results are yet available from this double-blind, placebo-controlled, two-arm, crossover trials [134].

<b>NCT NUMBER</b>	<b>DRUGS</b>	<b>PATHOLOGY</b>	<b>PARTECIPANTS</b>	<b>STATUS</b>	<b>CENTER</b>
<b>NCT02363452</b>	abacavir sulfate, lamivudine, zidovudine	AGS	11	Completed	Hôpital Necker - Enfants Malades Paris, France.
<b>NCT03304717</b>	abacavir sulfate, lamivudine, zidovudine	AGS	34	Ongoing	Children's Hospital of Philadelphia, Pennsylvania, United States.

Table 4: Clinical trial for RTIs in AGS treatment.

Other therapeutic approaches can also be envisaged, for example, anti-IFN antibodies or antibodies against the type I IFN receptor with the same therapeutic rationale of JAKi (i.e.: the strategy to block IFN signaling downstream of a nucleic acid stimulus). Alternative therapeutic approaches are represented by the antimalarial drug mepacrine, able to inhibit the binding between DNA and cGAS thus preventing the activation of the pathway [141], or by aspirin for the acetylation, thus the inhibition, of cyclic GMP-AMP synthase [142].

## 1.5 PRECISION MEDICINE

Precision medicine is broadly meant as the use of diagnostic tools and targeted treatments to the needs of the individual patient defined on the basis of molecular biomarkers. The term is often used interchangeably with “personalized medicine” that included delivering the right treatments, at the right time, every time to the right person. This novel perspective emerged as a critique of previous common medical practices characterized by a reductionist and oversimplified one-size-fits-all framework wherein all individuals presenting with some constellation of symptoms receive a similar treatment [143]. Despite presenting with similar symptoms, patients might have different underlying etiologies for the disease, as highlighted by the increasing knowledge of diseases biology. The identification of specific disease biomarkers can facilitate effective drug therapy, prompting a patient-oriented optimized therapy.

In this PhD thesis, two methodological approaches have been taken into accounts as tools to optimize the JAKi therapy: the application of the induced pluripotent stem cells (iPSC) technology in the context of AGS and the development of peptide biosensors *in vitro* system to monitor the aberrant JAK activity.

### 1.5.1 iPSC TECHNOLOGY

In the field of personalized medicine, a great opportunity is given by the iPSC technology. Patient-specific iPSCs represent a powerful application to better understand the underlying pathophysiological mechanisms of their diseases and to identify effective cures tailored to the individual, thanks to the possibility to preserve the patient-specific genetic background. In that regards, iPSCs recently emerged as an innovative and precious experimental tool for disease modeling and development of precision therapies, allowing the study both safety and efficacy drugs profile [144]. Easy-accessible patients' somatic cells such as fibroblasts can be reprogrammed to a pluripotent state, represented by iPSC, thanks to a transient overexpression of specific reprogramming transcription factors, known as Yamanaka factor genes (*OCT4*, *SOX2*, *KLF4* and *c-MYC*) because discovered by Takahashi and Yamanaka in 2006 [145]. Among the different methodologies showed in Figure 5, non-integrative methods are preferred and can include vector-based reprogramming systems, such Sendai virus, to simultaneously transfect all four classical Yamanaka factor genes into somatic cells. Fusaki and collaborators were the first to report the successful reprogramming of human fibroblasts using this technique [146]. The safety profile and transfection efficiency have made Sendai virus one of the most widely used systems for cell reprogramming, led to the currently on the market Sendai virus-based reprogramming system CytoTune™ 2.0 kit, which has higher efficiency, lower cytotoxicity, and faster viral clearance (ThermoFisher Scientific).

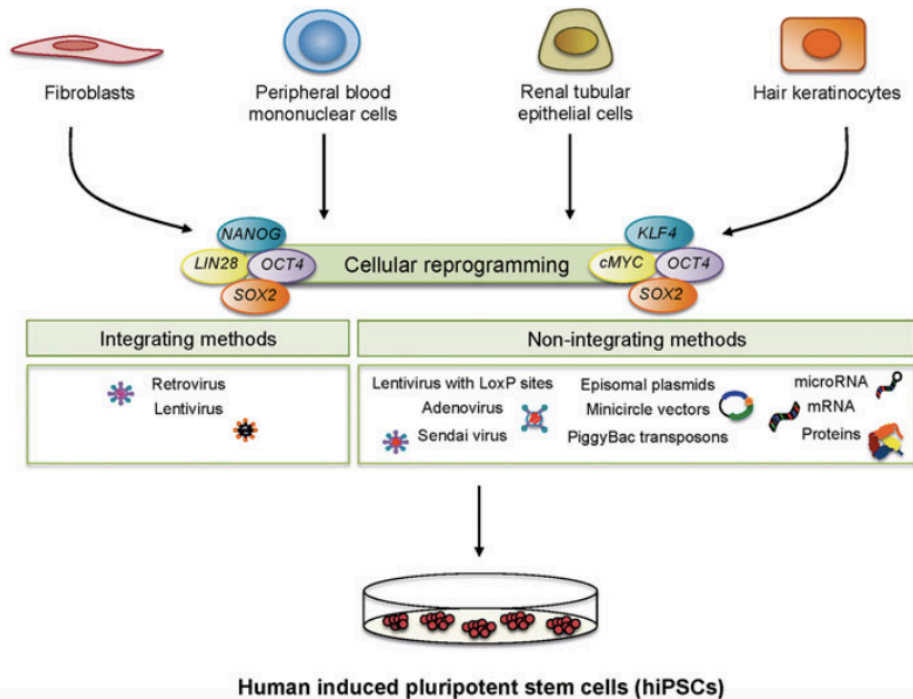


Figure 5: integrating and non-integrating methods to generate iPSCs form somatic cells [147].

Since 2006, when Yamanaka et al. discovered this powerful tool, the scientific community has been working on developing differentiation protocols to generate iPSC-derived somatic cells characterized by the maintenance of genetic heritage of the original donors. Under adequate stimuli, iPSCs are able to differentiate into any cell type of the three germ layers, such as cardiomyocytes [148], neurons [149] or keratinocytes [150], preserving patient-specific genetic background. That's why several diseases related to genetic disorders have been modeled according to this methodology, especially in the neurological and in the cardiac field as well as important primary immunodeficiencies. Moreover, patients'-derived cells can be used also during the drug screening process to assess the effects and the potential side effects of new compounds [151]. This application fits well with the concept of personalized medicine, which tries to identify the best therapy for each patient at the right dose and at the right time, thus limiting the possibility of adverse drug reactions development. iPSCs find possible application in drug discovery: in fact, the use of this technology brings with it several advantages such as reducing drug attrition rate and reducing costs for industries by being able to perform toxicity assays on more precise and predictive models [143].

iPSCs can eventually find a useful collocation also in the field of regenerative medicine. It may be possible to overcome the current transplantation approaches, which are mainly allogenic. iPSCs could be obtained from a patient, the cells could be engineered to repair pathogenic mutations through the mechanism of homologous recombination and could be differentiated into the cell type of interest that in turn could be transplanted into the patient. Numerous pre-clinical studies have been conducted to assess the potential of iPSCs-derived cells in cell therapy [152-154]. To date, a tangible example of clinical trial related to the use of donor-derived iPSCs (JMA-IIA00384) was conducted in 2008 at Kyoto University Hospital by Prof. Yun Takahashi with the aim of evaluating safety and efficacy in transplantation of

human iPSC-derived dopaminergic progenitor cells into the putamen of Parkinson's disease patients [155].

iPSCs are almost an inexhaustible source of cells avoiding the ethical problems related to embryonic stem cells, but limitations are related to their intrinsic properties. Epigenetic memory and clonal variability are two interesting points to discuss regarding iPSCs limits. iPSCs can present an epigenetic memory of the parent somatic cells that can influence the differentiation propensity and therefore the study outcomes. To perform drug screening, the clonal variability is a key point to keep in mind to set up useful standardized tools. Therefore, before the development of a model useful to predict patients' sensitivity, different clones should be first genetically checked to exclude for instance chromosomal aberrations, alterations in differentiation efficiency and variability in DNA methylation profiles. Also, the sensitivity to the drugs of interest should be analyzed in the different clones from the same patients, to exclude a variability in the response [144].

## **1.5.2 PATIENT-SPECIFIC iPSCs AS A MODEL FOR PRIMARY IMMUNODEFICIENCIES**

The possibility of differentiating iPSCs into central nervous system (CNS) cell types, otherwise inaccessible, gives a substantial advantage in the studies of immunodeficiencies affecting the CNS. An example is the recent work regarding AGS, which describes the generation of AGS patients-derived iPSCs (*TREX1* mutation) as human model to recapitulate AGS-relevant phenotypes [156]. In 2020 Genova et al. described AGS patients-derived iPSCs as an innovative *in vitro* model that is useful to investigate mechanisms of panel of immunomodulatory drugs potentially effective AGS treatment [151]. To date, no resolving therapies are available for AGS, and there is thus an increasing need for suitable, disease-relevant cell models for new potential therapeutic screening. For this purpose, animal systems such as gene specific knockout mice models are useful but have the limitation that they cannot recapitulate all phenotypic features of diseases [157]. Considering that brain damage in AGS mainly occurs in early phases of neuronal development, it is crucial to study on immature cells the safety profile of any drug proposed.

The use of iPSC allows to conduct safety studies on the AGS-iPSCs themselves, or in derived multipotent cellular model such as NSCs [144]. In addition, also pharmacological studies can be performed on the mature cell types involved in AGS pathogenesis, named neuronal cells and glial cells [156].

### 1.5.3 KINASE ACTIVITY MONITORING

The assessment of clinically relevant biomarkers associated with specific pathological mechanisms is the prerequisite for patients or disease stratification to improve precision medicine [158]. As mentioned above, kinases are widely involved in the inflammatory and autoimmune processes; understanding their contribution to the pathogenic mechanism of the diseases is complicated by the cross-talk of several signaling pathways. The ability to measure the activation of a single kinase in patients' cells can allow the understanding their role in disease progression and the choice of the most suitable kinase inhibitor to use in the single patient.

Historically, methodologies for quantitatively measuring kinase activity in purified protein were based on the use of radioactivity in radiometric assays exploiting the incorporation of [ $\gamma$ - $^{32}\text{P}$ ]- or [ $\gamma$ - $^{33}\text{P}$ ]-labeled ATP [159, 160]. However, the handling of radioactive tracers represents a limit given the high costs for maintenance and disposal of radioactive waste, as well as regarding the operator safety. Given these implications, non-radioactive methods of measuring kinase activity have become increasingly popular, employing fluorescent or luminescent peptide substrates and allowing studies of cell lysates and live cells, providing a more natural environment to study kinase activity of interest [161, 162]. A wide variety of these *in vitro* kinase tests are now available, but as far as we know, none are used in clinics [163]. To date, there are no tools that can be useful in the laboratory routine to measure the activation of signaling pathways linked to specific activated kinases.

#### 1.5.3.1 PEPTIDE BIOSENSORS

Approaches based on peptide biosensors may offer a valid method for the measurement of enzymatic phosphorylation activities. In the analytic setting, a biosensor is defined as a device comprising a receptor, that recognizes the analyte of interest, and a transducer, that triggers a measurable signal or catalyzes a reaction related to the concentration of the analyte to generate a signal [164]. Peptides are used as recognition elements in bio-detection thanks to their multiple properties: stability against denaturation, speed of synthesis, specificity, convenience, standard synthetic protocol, accessibility, easy modification, and versatility [165]. They are excellent candidates for the development of sensitive and affordable biosensors and are particularly useful for monitoring TK activity. In fact, exploiting the structural analogy with natural substrate proteins, specific peptides formed by short polymers of natural or synthetic amino acids with the appropriate sequence can become substrates of the TKs of interest. Sequence-specific peptides that have high affinity to kinases are obtained by screening and optimizing artificial peptide libraries by computational methods. Once the specific sequence for the analyte of interest has been identified, the synthesis of the biosensor peptide structure generally takes place using the Solid Phase Peptide Synthesis technique (SPPS). The SPPS protocol also offers the opportunity to link a wide range of functional molecules to the two terminal positions of a peptide sequence or to a particular amino acid, such as lysine, inside the sequence [164]. As an example, Wu and collaborators used such modified peptides to measure the level of kinase activity in ELISA assays [166]: a biotin was added to the lysine of the peptide biosensor and allowed its immobilization on a neutravidin-coated solid support; the peptide was phosphorylated on a tyrosine within its sequence by the incubation with the

analyte of interest (specifically a TK); finally the phosphorylated substrate was recognized by a primary antibody directed against the phosphorylated tyrosine, which in turn was recognized by a secondary antibody conjugated with an enzyme capable of emitting fluorescence signals. In this way, the detection methodology remained unchanged for the TK analyzed, except to change the peptide each time based on the optimal target sequence for the TK of interest. An ELISA based on a peptide biosensor is therefore potentially versatile and adaptable to any kinase to be analyzed. The *in vitro* kinase activity evaluation with peptide biosensors can be done using purified proteins or cell lysates. The use of cell lysates instead of purified kinases provides a more accurate estimate of inhibitor sensitivity and selectivity in a biological environment that comes closest to the complexity of intracellular conditions [166].

Pioneering work in the field of peptide biosensor was carried out by Dr. Parker and her research group (Purdue University, West Lafayette, Indiana, USA); they have developed a pipeline to generate biosensing peptides for several tyrosine kinases, including ABL1, JAK2 and Src-Family tyrosine kinases, and validated by *in vitro* KINATEST-ID™ (Kinase Terbium Emission Sensor Identification). Specific sequences were identified using proteomic data of endogenous kinase substrates and lanthanide binding sequences to build an “in silico” library, from which luminescence-detectable substrates could be selected [167, 168]. In the context of JAK kinase, two peptide biosensors with different validated sequences were identified for JAK2. In 2015 Lipchik and collaborators identified the peptide named JAStide-E, and structurally constituted as follows: GGDNDPDEYITLDEDGGK (in the text defined as P<sub>JAK2-L</sub> by P<sub>JAK2-LIPCHIK</sub>) [168]. The structure was identified from *in silico* analysis and is a specific substrate for JAK2 kinase and containing the phosphorylation site given by the presence of a tyrosine (Y). Furthermore, a small sequence belonging to the SH2 domain of STAT5, known to be an interaction domain with JAK2 and characterized by the presence of a specific phosphorylation site for this kinase, was also identified in literature. This second peptide, constituted as LAKAVDGYVKPQI sequence (in the text defined as P<sub>JAK2-S</sub> as P<sub>JAK2-SANZ</sub>), was highlighted following protein microarray studies in 2011, by Sanz and colleagues [169].

The possibility to introduce dedicated biosensors represent a novelty in immune-mediated and oncological conditions, thus contributing to the rational use of TKIs and to monitor therapy, potentially leading to more positive clinical outcomes in patients for which current therapies are unsatisfactory. Moreover, creating sets of peptide biosensors with individual enzyme activities could guarantee the detection of many kinases quickly and simultaneously, while ensuring a non-invasive approach. The clinical significance of peptide-based biosensors is very important since clinicians, thanks to the use of these tools, could begin to monitor the target kinase levels in patient cells before treatment, to establish an optimal amount of drug to use; in addition, the test could be repeated during and after treatment to assess changes over time. With this improved diagnosis, patients may be offered more targeted therapy to achieve better treatment outcome [165].

**2 - AIM**

---



In this PhD thesis, the focus was on JAKi into the context of precision medicine. Two methodological approaches have been taken into accounts as tools to optimize the therapy: the application of the iPSC technology in Aicardi–Goutières syndrome (AGS) and the development of peptide biosensors-based *in vitro* system to monitor the aberrant JAK enzymatic activities in the context of hematological neoplasms.

The first part comes from a collaborative project of the Pharmacogenetics Group of the University of Trieste (Italy), in collaboration with the Childrens' research hospital IRCCS Burlo Garofolo in Trieste (Italy) and the group of Professor Giliani at "A. Nocivelli" Institute of Molecular Medicine in Brescia (Italy). The overall objective of the study is to evaluate the safety and efficacy of a panel of drugs repurposed for AGS using patient-specific iPSCs and derived neurons because of their central role in this syndrome as an innovative preclinical model. Specific goal of the PhD project was the evaluation of cytotoxicity and efficacy of JAKi considered promising among innovative therapies for AGS on patient-specific iPSC and iPSC-derived NSCs *in vitro* models from three pediatric patients with distinct subtypes of Aicardi–Goutières syndrome (AGS1, AGS2, AGS7).. Additionally, the effect of RTIs were also investigated. Compared with current clinical practice, which involves the use of therapies aimed at containing symptoms, these drugs have the ambition to act directly on the pathogenic mechanism of AGS and therefore to improve patient's clinical outcome.

The second part of the PhD thesis is developed in the context of a project on tyrosine kinases to screen their aberrant activities in patient's cells, setting up peptide biosensors-based ELISA assays. Long-term goal of this project is to set up a point-of-care device to improve the diagnosis and clinical management of TK-driven diseases in clinics. Peptide biosensors will allow to select the best TKi to be used in patients and/or to monitor the effectiveness of the inhibitor chosen during therapy. The project of the Pharmacogenetics Group of the University of Trieste (Italy), in collaboration with Professor Sorio (University of Verona) begun in 2016, with a focus on the TK ABL1. In this PhD project, the aim was to develop and improve an ELISA *in vitro* system capable of recognizing and quantifying JAK kinase activity. The initial analyses were performed using two peptide biosensors for JAK2 kinase, whose sequences had been published by Lipchik et al. 2015 and Sanz et al. 2011 (named P<sub>JAK-L</sub> and P<sub>JAK-S</sub>, respectively). These sequences were highlighted thanks to protein microarray studies, including the specific binding and phosphorylation site for JAK2 kinase (tyrosine Y694). In this thesis, attempts were made to optimize the peptide-based ELISA assay using hematopoietic immortalized cell lines, harboring rearrangements activating JAK2 and an aberrant activation of JAK/STAT pathway. The set-up of right experimental condition could represent a proof-of-concept of the system, demonstrating its feasibility, and could be then applied to other peptide biosensors and other diseases in the future.

## ***3 - MATERIALS AND METHODS***

---

## 3.1 DRUG AND CHEMICALS

Ruxolitinib (Catalog Number: 11609, Cayman Chemical, USA), baricitinib (S2851, Selleckchem, USA), tofacitinib (S5001, Selleckchem, USA), pacritinib (SB1518, Selleck Chemicals, USA), 2'3'-cGAMP 69.60 mM (cyclic [G(2',5')pA(3',5')p])(cGAMP, tlr-nacga23-1, Invivogen, Italy), lamivudine (L1295, Sigma-Aldrich, Italy), abacavir sulfate (SML0089, Sigma-Aldrich, Italy), zidovudine (A2169, Sigma-Aldrich, Italy), were dissolved according to manufacturer instructions (Table 6).

## 3.2 AGS PATIENTS

Three pediatric patients with distinct forms of Aicardi-Goutières syndrome (i.e.; AGS1, AGS2, AGS7) were enrolled to generate patients specific cellular models. AGS1-iPSC cell line was generated from skin fibroblasts of a 5-years old male with a compound heterozygous *TREX1* mutation (c.[260insAG];[290G>A]) [170]. AGS2-iPSC cell line was generated from skin fibroblasts of a 10-years old female presenting a homozygous mutation in *RNASEH2B* (c. [529G>A]; [529G>A]) [171]. Lastly, AGS7-iPSC cell line was obtained through the reprogramming of fibroblasts of a 14-years old male with a dominant negative heterozygous mutation in *IFIH1* (c.[2471G>A]; wt) [172].

The study was approved by the Scientific Committee and by the Board of the Aziende Socio Sanitarie Territoriali Spedali Civili of Brescia, protocol numbers 1603 (AGS-CARIPLO study) and 3426 (iPSCREP study) and appropriate informed consent was obtained from patients' parents.

## 3.3 CELL CULTURES

Cells were cultured as described below, working under sterile conditions and keeping cell cultures in incubator at 37°C and 5% CO<sub>2</sub>.

### 3.3.1 AGS PATIENT DERIVED CELLS

#### 3.3.1.1 iPSCs REPROGRAMMING AND CULTURE

AGS patient-specific iPSCs were generated by Prof. Giliani's group at "A. Nocivelli" Institute of Molecular Medicine (Brescia, Italy) using the Cyto-Tune-iPS 2.0 Sendai Reprogramming Kit (A16517, ThermoFisher Scientific, Italy), a non-integrative technology based on three different vectors to deliver, efficiently and safely, Yamanaka Factors (*OCT4*, *SOX2*, *KLF4*, and *MYC*) into somatic cells to induce reprogramming towards iPSCs. An additional iPSC line from an healthy donor, used as control, was generated using the same technique described above, starting from the fibroblast commercial line BJ (human foreskin fibroblasts from a neonatal male, ATCC CRL-2522, American Type Culture Collection, Manassas, VA, USA). Karyotype stability was analyzed and confirmed by the "A. Nocivelli" group in parental cells and iPSCs at different time point of culture using Q-banding at 450 bands resolution according to the International System for Human Cytogenetic Nomenclature.

Patient-specific iPSCs and the control BJ-iPSC were maintained in StemMACS iPS-Brew XF (130-104-368, Miltenyi Biotec, Italy) on diluted Geltrex matrix coated plates (1 ml/well in 6-well plate, 833920 Sarstedt, Italy). Geltrex (A1413202, Gibco, ThermoFisher Scientific, Italy) was diluted 1:100 in DMEM/F12 medium (D8062, Sigma-Aldrich, Italy). Cells were passaged at 80% confluence: after 2 minutes exposure to Versene (15040066, Gibco, ThermoFisher Scientific, Italy) at 0.48 mM, cells were gently detached with the medium. Since iPSCs grow in clusters, the standard protocol of passaging used for long-term iPSCs cultures avoids the complete breakup of clusters. In contrast, when single cell culturing was required as to perform cytotoxicity assays, iPSCs were treated according to the same procedure but were exposed to Versene for 5–6 minutes. After each seeding, 10  $\mu$ M Rho-associated, coiled-coil containing protein kinase inhibitor (ROCK inhibitor, Y-27632, 130-103-922, Miltenyi Biotec, Italy) was added to the medium for 24 hours to facilitate cells adhesion.

### 3.3.1.2 NSCs INDUCTION AND CULTURE

iPSCs can be induced to NSCs under proper conditions. For NSCs differentiation, iPSCs colonies were seeded in StemMACS iPS-Brew XF medium on diluted Geltrex coated 6-wells plates at a density of  $3 \times 10^5$  cells/well and allowed to recover for 24 h at 37°C. Then, media was change to PSC Neural Induction medium (A1647801, Gibco, ThermoFisher Scientific, Italy) and for 7 days, medium was changed every other day, according to standard protocol provided by ThermoFisher Scientific (MAN0008031). Briefly, on day 0 of neural induction (about 24 hours after iPSCs splitting), the spent medium was removed and 2.5 mL of pre-warmed complete PSC Neural Induction Medium (A1647801, Gibco, ThermoFisher Scientific, Italy) were added into each well of 6-well plate. On day 2 of neural induction, the morphology of cell colonies was uniform; the spent medium was again replaced by 2.5 mL pre-warmed complete PSC Neural Induction Medium. On day 4 of neural induction, cells were reaching confluency; the spent medium was removed from each well and replaced it with 5 mL of pre-warmed complete PSC Neural Induction Medium. On day 6 of neural induction, cells were at near maximal confluence. After the removal of spent medium, 5 mL of pre-warmed complete PSC Neural Induction Medium were added into each well. Indeed, on day 7 of neural induction, NSCs (P0) are ready to be expanded, harvested and cryo-preserved (Figure 6). Neural markers expression was confirmed by qPCR and immunofluorescence staining (data not shown).

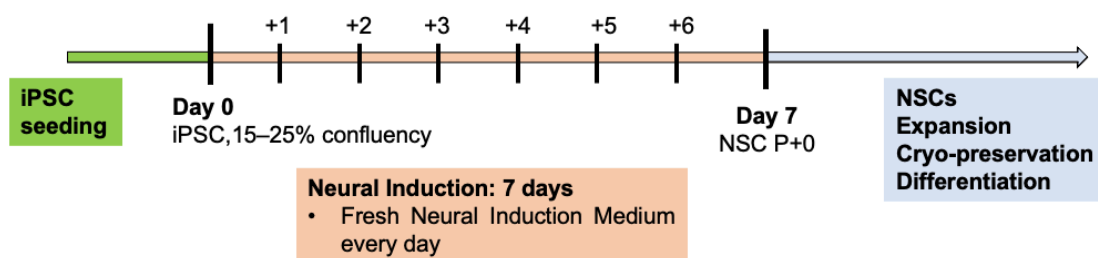


Figure 6: Workflow of NSCs derivation from iPSCs.

After NSC thawing, ROCK inhibitor (10  $\mu$ M) was added to the medium for 24 hours at each cell passaging for the first 3 passages. ROCK inhibitor was not further required afterwards. Patient-specific NSCs and the control BJ-NSC were maintained in a medium composed by same proportion of PSC Neural Induction Medium (A1647801, Gibco, ThermoFisher Scientific, Italy) and Advanced DMEM/F12 (12634010, Gibco, ThermoFisher), on diluted Geltrex matrix coated plates (1:100 Geltrex in DMEM/F12 medium), reaching 80% of confluence before cell passages. After 5 minutes exposure to StemPro Accutase Cell Dissociation Reagent (A11105, Gibco, ThermoFisher Scientific, Italy) at 37°C, cells were gently detached with PBS (D8537, Sigma-Aldrich, Italy) and filtered with a 100  $\mu$ m cell strainer (08-771-19, FisherScientific, Italy). After centrifugation at 300xg at room temperature for 4 minutes, cells were manually counted in a Burker chamber and seeded at  $0.3-1 \times 10^6$  cell/well in 6 well-plate for cell maintenance.

### 3.3.2 IMMORTALIZED HEMATOPOIETIC CELL LINES

The activity of JAK2 peptide biosensor was screened using three human hematopoietic cell lines: MHH-CALL-4 were kindly provided by Professor Monique Den Boer (Princess Máxima Center, Utrecht, Netherlands) whereas HEL and SET-2 cell lines were kindly supplied by Professor A. Vannucchi (Department of Experimental and Clinical Medicine, University of Florence). Additionally, K562 cell line, kindly provided by Professor Sorio (University of Verona) and REH (ACC 22) cell line purchased from the DSMZ GmbH (Germany), were included as controls.

MHH-CALL-4, HEL, SET-2 cell lines are characterized by genetic alterations involving the activation of the JAK/STAT pathway, in particular:

- MHH-CALL-4 cell line is a B-ALL *BCR-ABL1 like* model positive for the t(X;14) (p22;q32)/t(Y;14)(p11;q32) translocation which determine the fusion of two genes: *IGH* and *CRLF2*. This abnormality leads to a deregulated expression of the CRLF2 receptor. Overexpression of the receptor results in activation of the JAK/STAT pathway resulting in increased cell proliferation. In addition, this model has a JAK2 missense mutation in the pseudokinase domain (*JAK2* I682F) [173].
- HEL cell line is representative of erythroleukemia and carry the homozygous mutation *JAK2* V617F.
- SET-2 cell line is established from a patient with essential thrombocythemia at megakaryoblastic leukemic transformation; cells carry the *JAK2* V617F mutation in heterozygosity and the *DNMT3A* R882H mutation at the level of a DNA methyltransferase [174]. The latter has been identified in approximately 25% of patients with acute myeloid leukemia, and gives rise to an aberrant methylation pattern and increased cell proliferation [175].

The REH cell line, a human B-ALL cell line, does not show alterations in the pathway under study; cells harbor the t(12;21)(p13;q22) translocation and are positive for the *ETV6-RUNX1* fusion, known as TEL-AML1. The K562 cell line, on the other hand, is a CML model, positive for the translocation t(9;22)(q34;q11), known as the Philadelphia chromosome, which encodes the oncogenic fusion protein BCR-ABL1.

Cell lines characteristics are summarized in Table 5.

IMMORTALIZED CELL LINE	DISEASE MODEL	GENETIC ALTERATIONS	PATHWAY
MHH-CALL-4	B-ALL ( <i>BCR-ABL1 like</i> )	<i>IGH/CRLF2</i> <i>JAK2 I682F</i>	JAK/STAT
SET-2	MPN	<i>JAK2 V617F</i> (heterozygous)	JAK/STAT
HEL	MPN	<i>JAK2 V617F</i> (homozygous)	JAK/STAT
K562	CML	<i>BCR-ABL1</i>	ABL1
REH	B-ALL	<i>ETV6-RUNX1</i>	/

Table 5. Immortalized hematopoietic cell lines and their genetic alterations. B-ALL: Acute Lymphoblastic Leukemia B subtype; MPN: Myeloproliferative neoplasm; CML: chronic myeloid leukemia.

Cells were cultured in standard complete RPMI-1640 medium (ECB9006L, Euroclone, Italia) supplemented with 10-20% fetal bovine serum (FBS, F7524, Sigma-Aldrich, Italia), 2 mM L-glutamine (ECB3000D-20, Euroclone, Italy), 1X Penicillin-Streptomycin solution (P0781, Sigma-Aldrich, Italia); cell passages were performed according to standard procedures.

### 3.3.3 MYCOPLASMA DETECTION

*Mycoplasma* contamination is a well-known complication in cell culturing that can create several different biological effects on contaminated cell, such as alterations in the proliferation pattern, in cellular metabolism and cellular morphology [176]. Several studies have highlighted that *Mycoplasma* contamination negatively influences the reprogramming of cells, being a critical reason for failure of iPSCs generation.

iPSCs, NSCs and immortalized hematopoietic cell lines were tested for *Mycoplasma* contamination once thawed. To check the presence of *Mycoplasma*, a polymerase chain reaction (PCR) method was used to assess the presence of a 16S rRNA gene [177]. Cells have always tested negative for *Mycoplasma*.

## 3.4 CELL VIABILITY ASSAYS

### 3.4.1 MTT ASSAY

The cytotoxic effect of drugs was determined using the 3-(4,5-dimethylthiazol-2-yl)- 2,5-diphenyltetrazolium bromide (MTT, M2128-1G, Sigma-Aldrich, Italy) assay.

IPSC and NSC were first seeded on a Geltrex coated 96-well plate at different cell densities according to their different cell growth rate, to obtain similar cell densities at 72 hours. AGS2 patient-derived iPSCs

were seeded at  $3.0 \times 10^4$  cells/well in a final volume of 100  $\mu$ l while all the other iPSCs tested (AGS1, AGS7 and BJ-iPSC lines) were seeded at  $1.0 \times 10^4$  cells/well; all NSCs were seeded at  $1.0 \times 10^4$  cells/well. After 24h incubation, the medium was replaced with a medium containing drug at serial-diluted known concentration (Table 6). Experiments were repeated at least three times, and each experimental condition was seeded in triplicate. Immortalized hematopoietic cells were seeded at 12000 cells/well in a final volume of 200  $\mu$ l in 96-well plates in the presence of known concentration of drugs; the range of concentrations used for each drug is reported in Table 6. Treated cells were incubated for 72 hours at 37 °C; MTT was added in each well (0.5 mg/ml) four hours before the end of the incubation; cells were lysed with 100  $\mu$ l dimethyl sulfoxide (DMSO, 472301, Sigma-Aldrich, Italy). The absorbance was measured with a spectrophotometer (540-630 nm wavelength, Fluorostar Omega, BMG, Labtech Germany).

Cell metabolic activity was calculated as: % cell activity = (absorbance treated/absorbance control)\*100, and considered as a measurement of cell viability. Percentages were graphically reported as a function of the drug concentrations used, expressed in molarity and reported in a logarithmic scale, obtaining a sigmoid dose-response curve. The data analysis was performed using the GraphPad Prism® 9.4.1 software by means of a non-linear regression to extrapolate the IC<sub>50</sub>, which is the concentration of an enzyme inhibitor required to inhibit 50 percent of a target.

DRUG	SOLVENT	STOCK SOLUTION (nM)	CONCENTRATION RANGE TESTED IN MTT ASSAY (IPSCS/NSCS)	CONCENTRATION RANGE TESTED IN MTT ASSAY (HEMATOPOIETIC CELLS)
Ruxolitinib	EtOH	32.6	$9.77 \times 10^{-9}$ M – $2.0 \times 10^{-5}$ M	$1.6 \times 10^{-8}$ – $2.0 \times 10^{-5}$ M
Baricitinib	DMSO	50	$9.77 \times 10^{-9}$ M – $2.0 \times 10^{-5}$ M	$1.6 \times 10^{-8}$ – $2.0 \times 10^{-5}$ M
Tofacitinib	DMSO	50	$9.77 \times 10^{-9}$ M – $2.0 \times 10^{-5}$ M	$4.1 \times 10^{-8}$ – $3.1 \times 10^{-5}$ M
Pacritinib	DMSO	10	$7.0 \times 10^{-9}$ M – $5.0 \times 10^{-6}$ M	$4.1 \times 10^{-8}$ – $3.1 \times 10^{-5}$ M
cGAMP	H <sub>2</sub> O	69.60	$8.7 \times 10^{-8}$ M – $3.5 \times 10^{-5}$ M	NA
Lamivudine	H <sub>2</sub> O	43.61	$9.77 \times 10^{-9}$ M – $2.0 \times 10^{-5}$ M	NA
Abacavir Sulfate	H <sub>2</sub> O	44.22	$9.77 \times 10^{-9}$ M – $2.0 \times 10^{-5}$ M	NA
Zidovudine	H <sub>2</sub> O	187.09	$9.77 \times 10^{-9}$ M – $2.0 \times 10^{-5}$ M	NA

**Table 6.** Drugs and their concentration range used in MTT assays. In MTT assays the solvent percentage was adjusted considering the percentage present in the highest concentrated drug solution tested. NA: not assessed.

## 3.4.1 PROLIFERATION ASSAYS

### 3.4.1.1 [3H] THYMIDINE

Cell proliferation was determined by labeling metabolically active iPSCs and NSCs cells with (methyl-3H) thymidine (NET027X00 1MC, PerkinElmer, Italy). Cells were seeded on a Geltrex coated 96-well plate at different densities (500, 1000, 2500, 5000, 10000, 30000 cells/well), and after 91 hours of incubation, were pulsed with [methyl-3H] thymidine (2.5  $\mu$ Ci/mL) and incubated 5 hours more. Cells were then washed with PBS, collected, and the radioactivity of the samples was determined by a liquid scintillation analyzer (Wallac 1450 Microbeta liquid scintillation counter, PerkinElmer, Italy). Raw count per minute (CPM) data were analyzed.

### 3.4.1.2 CFSE

Carboxyfluorescein succinimidyl ester (CFSE, 65-0850, eBioscience™), is an ammine-reactive dye used in cell proliferation and *in vivo* cell tracking. Once CFSE crosses the cell membranes, intracellular esterases cleave the acetate groups to yield the fluorescent carboxyfluorescein molecule. The succinimidyl ester group reacts with primary amines, crosslinking the dye to intracellular proteins. Cell division can be measured as successive halving of the fluorescence intensity of CFSE.

CFSE (4.21 mM) was added to the cellular suspension ( $1 \times 10^6$  cells/ml) at the final concentration of 18  $\mu$ M and incubated for 5 minutes at 37° protected from light. Then, labeled cell suspension was washed 3-times with PBS, centrifuged at 300 xg 10 min, and seeded in 6-well plates in NSC specific culture medium. Cell proliferation was assessed after 24-48-72 hours, by flow cytometry. Cells were gently detached from the plate according to standard procedure, washed with PBS, centrifuged at 300 g 10 min at room temperature, and then fixed with 1% Paraformaldehyde (158127, Sigma-Aldrich, Italy) diluted in PBS. Samples were acquired with MACSQuant Analyzer 10 (Miltenyi Biotec) and analyzed with FlowLogic software (version 7.2.1, Inivai Technologies). The program calculates the proliferation index based on the dilution levels of CFSE detected in dividing cell.

## 3.5 CELL CYCLE ANALYSIS

Cell cycle of patient-specific AGS/BJ-iPSCs and a human immortalized hepatic cell line (IHH) were analyzed by flow-cytometry using the propidium iodide (P4170, Sigma-Aldrich, Italy) cellular uptake assay. Two million cells were fixed in 70% ethanol on ice, washed twice with PBS, and kept in PBS for 1 hour at 4°C. Cells were stained overnight with 2 mL of a PBS/EDTA 0.5 mM solution containing 200  $\mu$ L of propidium iodide (0.1 mg/mL, P4170, Sigma-Aldrich, Italy) and 25  $\mu$ L of 1 mg/mL RNase (R4875, Sigma-Aldrich, Italy). Samples were analyzed by the flow cytometer CYTOMICSTM FC500 (Beckman Coulter Inc. Fullerton, CA). All flow cytometric measurements were carried out on storage data as list mode files and were analyzed with the FCS Express V3.



## 3.6 TOTAL RNA ISOLATION AND REVERSE TRANSCRIPTION

Total RNA was extracted with TRIzol reagent (15596018, Invitrogen, ThermoFisher Scientific, Italy) and PureLink RNA mini KIT (12183018A, ThermoFisher Scientific, Italy) according to the manufacturer's instructions, and quantified using Nanodrop 2000 spectrophotometer (ThermoFisher Scientific, Italy). RNA was reversed-transcribed into cDNA using the High-Capacity RNA-to-cDNA kit (4387406, Applied Biosystem, ThermoFisher Scientific, Italy).

## 3.7 QUANTITATIVE REAL-TIME PCR

IPSCs and NSCs stemness determination and the analysis of genes involved in drug pathways were performed by real-time PCR using the KiCqStart SYBR Green qPCR Ready Mix (KCQS00, Sigma-Aldrich, Italy), in a Thermal Cycle Dice Real Time System (BIO-RAD, Italy), using pre-designed primers sequence (KSPQ12012, Sigma-Aldrich, Italy) (Table 7). Relative quantification is represented as  $2^{-\Delta Ct}$  with respect to the housekeeping gene beta-actin (*ACTB*), setting BJ-iPSC or BJ-NSC as calibrator. All experiments were carried out in triplicate and the reproducibility of the observations was confirmed in at least two independent experiments.

GENE	GENE FUNCTION	PRIMER	SEQUENCE 5'→3'
<b>ACTB</b>	House-keeping	Forward	CGCCGCCAGCTCACCATG
		Reverse	CACGATGGAGGGGAAGACGC
<b>SOX2</b>	IPSCs stemness gene	Forward	CCCAGCAGACTTCACATGT
		Reverse	CCTCCCATTTCCTCGTTTT
<b>OCT4</b>	IPSCs stemness gene	Forward	CCTCACTTCACTGCACTGTA
		Reverse	CAGGTTTTCTTCCCTAGCT
<b>NES</b>	NSCs stemness gene	Forward	ATGGAGACGTCGCTG
		Reverse	ACAGCCAGCTGGAAC
<b>SOX1</b>	NSCs stemness gene	Forward	TGCTTGTTCTGTTAACTCAC
		Reverse	AAAGAACCTCAGAGAGAGTC
<b>PAX6</b>	NSCs stemness gene	Forward	GAGTTTGAGAGAACCCATTATC
		Reverse	CATACCTGTATTCTTGCTTCAG
<b>JAK1</b>	Gene related to JAK/STAT signaling pathway	Forward	GAAAAACAAGATCCGGGAAG
		Reverse	TCCATTTTCTTGTTGTCCTG
<b>TYK2</b>	Gene related to JAK/STAT signaling pathway	Forward	CTCCTTGCTTCAATCTCTTTG
		Reverse	ACCTTATGCGAAATATAGC
<b>STAT1</b>	Gene related to JAK/STAT signaling pathway	Forward	ACCCAATCCAGATGTCTATG
		Reverse	GAGCCTGATTAATCTCTGG
<b>STAT2</b>	Gene related to JAK/STAT signaling pathway	Forward	ATATAAGATCCAGGCCAAAGG
		Reverse	CAGTAGCTCGATTAGGGTAG

<b>TK1</b>	Antiretroviral drugs target gene	Forward	AAAAGCACAGAGTTGATGAG
		Reverse	GAGTGTCTTTGGCATACTTG
<b>ADK</b>	Antiretroviral drugs target gene	Forward	CCAAAGATGAACTCAAAGAGG
		Reverse	AGAAAACCTCCAACAAATGC
<b>DCK</b>	Antiretroviral drugs target gene	Forward	GAGGAACTTACAATGTCTCAG
		Reverse	TGTTTGGAAGGTAAAAGACC

Table 7. Custom-designed primer sequences (Sigma-Aldrich, Italy) for real-time PCR analysis of iPSCs stemness genes (*ACTB*, beta-actin; *SOX2*, SRY-box 2; *OCT4*, POU class 5 homeobox 1), NSCs stemness genes (*NES*, Nestin; *SOX1*, SRY-box 1; *PAX6*, paired type homeobox 6), genes involved in type I IFN pathway activation (*JAK1*, Janus kinase 1; *TYK2*, Tyrosine kinase 2; *STAT1*, Signal transducer and activator of transcription 1; *STAT2*, Signal transducer and activator of transcription 2), antiretroviral drug pathway (*TK1*, thymidine kinase 1; *ADK*, adenosine kinase; *DCK*, Deoxycytidine Kinase; *JAK1*, Janus kinase 1; *TYK2*, Tyrosine kinase 2; *STAT1*, Signal transducer and activator of transcription 1; *STAT2*, Signal transducer and activator of transcription 2).

To explore the molecular mechanisms of these disorders, studies on *STING* gene expression, which has a key role in the interferon pathway, were performed.

We evaluated *STING* expression in untreated conditions and after baricitinib and pro-inflammatory stimulus cGAMP exposure. iPSCs and NSCs were treated with baricitinib 10  $\mu$ M for 72 hours and exposed to 4 ng/ $\mu$ L of the pro-inflammatory stimulus cGAMP, in the last 3, 6, 24, 48 hours before the end of incubation. After cell passage, 0.125x10<sup>6</sup> iPSCs and NSCs (except 0.3x10<sup>6</sup> of AGS2-iPSCs) were seeded in 12-wells plates. After 24 h at 37°C and 5% CO<sub>2</sub> with ROCK inhibitor (10  $\mu$ M, only for iPSC), cells were treated in nine different conditions as follow: baricitinib 10  $\mu$ M, cGAMP 4 ng/ $\mu$ l 3h, baricitinib 10  $\mu$ M + cGAMP 4 ng/ $\mu$ l 3h, cGAMP 4 ng/ $\mu$ l 6h, baricitinib 10  $\mu$ M + cGAMP 4 ng/ $\mu$ l 6h, cGAMP 4 ng/ $\mu$ l 24h, baricitinib 10  $\mu$ M + cGAMP 4 ng/ $\mu$ l 24h, cGAMP 4 ng/ $\mu$ l 48h, baricitinib 10  $\mu$ M + CGAMP 4 ng/ $\mu$ l 48h. An untreated control was always included. Treated and untreated cells were harvested to perform gene expression analysis.

For relative quantification analysis of *STING* expression by real time PCR, TaqMan Gene Expression Master Mix (4440047, Applied Biosystems, ThermoFisher Scientific, Italy) and TaqMan Gene Expression probes were employed ((4331182, ThermoFisher Scientific, Italy; housekeeping *HPRT*: Hs02800695\_m1, *STING-Tmem173*, Hs00736956\_m1), using Thermal Cycle Dice Real Time System (BIO-RAD, Italy) according to manufacturer's instructions.

## **3.8 CELL LYSATES PREPARATION FROM HEMATOPOIETIC CELL LINES**

Whole protein cell lysates from human hematopoietic cell lines were used for both western blot and peptide-based ELISA assays. The procedure of cell lysates has been optimized by Professor Sorio (University of Verona, Italy) and requires the use of kinase and phosphatase inhibitors to maintain the integrity of kinases. Twenty million cells were washed with PBS (D8537, Sigma-Aldrich, Italy), then lysed on ice with 150 µl of lysis buffer pipetting 20 times, vortexing and centrifuging at 4 °C for 30 min at 13000 g. The lysis buffer contains 50 mM Tris-HCl (pH 7.4), 1% Triton-X, 150 mM NaCl, 2 mM EDTA, with addition of LeukoProtect lysis buffer (AB Analytica, Padova, Italy), 1x PhosSTOP (4906845001, Sigma-Aldrich/Merk, Italy), sodium orthovanadate ( $\text{Na}_3\text{VO}_4$ ) 100 µM (S6508, Sigma-Aldrich, Italy), sodium fluoride (NaF) 10 mM (450022, Sigma-Aldrich, Italy) and 1 mM dithiothreitol (DTT, 43819, Sigma-Aldrich, Italy). Supernatant was frozen in liquid nitrogen and stored at -80 °C, until use. Protein concentrations were determined using the Bradford reagent (B6916, Sigma-Aldrich, Italy), according to manufacturer's instructions; absorbance at 570 nm was measured on a Fluorostar Omega (BMG, Labtech Germany).

## **3.9 IMMUNOPRECIPITATION**

Protein lysates from HEL and REH cell lines (100 µg) were incubated for 2 hours at 4°C on a rotating wheel, in 200 µl lysis buffer (TrisHCl 100 mM, NaCl 300 mM, EDTA 2 mM, Triton X 2%, with  $\text{Na}_3\text{VO}_4$  200 mM, DTT 2 mM, NaF 10 mM and 1x Roche) with an antibody against JAK2 (#3230 Cell Signaling Technology, dilution 1:200). Rabbit IgG polyclonal isotype (0.5 µg, ab37415, Abcam) was used as control. 15 µl of protein G-Dynabeads (Dynabeads, 10003D, ThermoFisher Scientific, Italy) were added and the mixture was incubated for 1 hour at 4°C on wheel. The immunocomplex was collected using a magnetic support (CS15000, ThermoFisher Scientific, Italy). Three one-minute washes each with 200 µl of Tyrosine Kinase Buffer (100 mM Tris-HCl pH 7.5, 50 mM  $\text{MgCl}_2$ , 0.25% TritonX without inhibitors) were performed. The immunoprecipitation product, containing the beads linked to the immunocomplex, was subsequently used in Western blot and in the ELISA assay with peptide biosensors.

## **3.10 WESTERN BLOT**

Cell lysates or immunoprecipitated complexes were suspended in 20 µL Bolt LDS Sample Buffer (B0008, ThermoFisher Scientific, Italy) diluted in lysis buffer, and added with Bolt Sample Reducing Agent 1X (B0004, ThermoFisher Scientific, Italy). After denaturation at 70°C for 10 minutes, samples were fractionated by SDS-PAGE using 10% NUPAGE Bis-Tris Gels 12-well (NW00102BOX, ThermoFisher Scientific, Italy) using 130 V, 150 mA for 60 minutes. Proteins were transblotted to nitrocellulose membranes (PB7320, ThermoFischer Scientific, Italy) using 2.5 A for 10 minutes (PB7320, ThermoFischer Scientific, Italy) through the Electrophoresis Power Supply (EPS301, ThermoFischer Scientific, Italy). After blocking for 1 hour at room temperature (RT) with 5% nonfat milk in T-TBS (Tris buffered saline (50 mM Tris-Cl, 150 mM NaCl, pH 7.5) with 0.1% Tween-20), membranes were incubated overnight at 4°C with rabbit primary antibodies against human proteins: CRLF2 (1:1000, ab186427,

Abcam, Italy), JAK2 (1:1000, #3230, Cell Signaling Technology, Italy), Phospho-JAK2 (Tyr1007/1008, 1:1000, #3776, Cell Signaling Technology, Italy), STAT5 (1:1000, Cell Signaling Technology, Italy), Phospho-STAT5 (Tyr694, 1:1000, #9359, Cell Signaling Technology, Italy), actin (1: 3000, ab218787, Abcam, Italy) and vinculin (1:10000, ab129002, Abcam, Italy). All primary antibodies dilution were made in T-TBS 5% nonfat milk. Membranes were washed with T-TBS three times for 5 minutes and then incubated 1 hour at 4 °C with a 1:10000 dilution in T-TBS 5% nonfat milk of horseradish peroxidase conjugated anti-rabbit antibodies (AP132P, Merk, Italy). Blots were developed with LiteAblo TURBO Extra Sensitive Chemiluminescent Substrate (EMP012001, Euroclone, Italy) and detection was performed using ChemiDoc MP Imaging System (Bio-Rad, Italy).

For each antibody, experiments were repeated twice with similar results and bands of interest were quantified with ImageJ software (NHI, USA), after normalizing with actin or vinculin.

## 3.11 *IN VITRO* ASSAY WITH PEPTIDE BIOSENSORS

### 3.11.1 PEPTIDE BIOSENSORS

Biotinylated peptide biosensors were synthesized by JPT Peptide Technologies (Berlin, Germany) with 98% purity and are shown in Table 8. P<sub>JAK2-L</sub> and P<sub>JAK2-S</sub> comprise a single tyrosine in their sequence, target of the JAK2 kinase activity. P<sub>PHOSPHO-JAK2</sub> is a fully phosphorylated version of P<sub>JAK2-L</sub>, used as internal control in the peptide biosensors-based ELISA assay. Peptides stabilities were routinely checked in mass spectrometry thank to the collaboration with Professor Tossi (University of Trieste).

PEPTIDES	SEQUENCE	MOLECULAR WEIGHT	REFERENCE
P <sub>JAK2-L</sub>	GGDNDPDEY <b>ITL</b> DEDGGK(biotin)GG	2250.28 Da	[168]
P <sub>JAK2-S</sub>	LAKAVDGYV <b>KPQI</b> --Ttds-Lys(biotin)	2057.52 Da	[169]
P <sub>PHOSPHO-JAK2</sub>	GGDNDPDEY( <b>P</b> )ITLDEDGGK(biotin)GG	2330.25 Da	[168]

Table 8. Peptide biosensors. Tyrosine and its modifications are shown in bold.

### 3.11.2 PEPTIDE BIOSENSORS-BASED ELISA ASSAY ON WHOLE PROTEIN CELL LYSATES

The peptide biosensor-based ELISA assay procedure is shown in Figure 7.

P<sub>JAK2-L</sub> and P<sub>JAK2-S</sub> contain a biotin tag that allows their anchoring to a neutravidine-coated plate (786-766, G-Bioscience, United States). Peptides were loaded onto the plate at a concentration 0.5 µM in PBS and shacked for 1 hour at RT. To avoid non specific signals, the plate was washed with a Quencher Buffer (100 µl /well; PBS with 0.1% Tween 20, pH 7.4 and 0.4% BSA) for 20 minutes in oscillation. 4µg of whole protein cell lysates in Tyrosine Kinase Buffer (4 mM Tris-HCl pH 7.5, 10 mM MgCl<sub>2</sub>, 0.1 mM

EDTA, 0.01% TritonX) with 100  $\mu\text{M}$  ATP, 1x Roche Inhibitors, 2 mM DTT, 0.1 mM  $\text{Na}_3\text{VO}_4$  and MilliQ water (final volume 100  $\mu\text{l}$ ) were then loaded into the plate and incubated for 1 hour at RT. The phosphorylation of the peptides was measured using an anti-phosphorylated tyrosine antibody (05-1050 4G10 Platinum, EDM Millipore Corporation, dilution 1:10000 in Quencher Buffer, incubated for 1 hour while shaking at RT) and detected with a secondary antibody conjugated with horseradish peroxidase (ECL Anti Mouse IgG, HRP from goat, 5210-0159, Sera-care, United States, dilution of 1: 6000 in Quencher Buffer, incubated for 1 hour while shaking at RT). The signal was detected by adding a solution of citrate buffer pH 6.0, 3%  $\text{H}_2\text{O}_2$ , Amplex Ultra Reagent Invitrogen 0.5% (A36006, ThermoFischer Scientific, Italy) and measured 25 times every 0.2 sec (excitation 544 nm, emission wavelengths 590 nm), using Fluorostar Omega fluorometer (BMG, Labtech Germany). Peptide phosphorylation was expressed as "fluorescence intensity" (FI), value that indicates the average of the intensity of the acquired fluorescence signals.  $\text{P}_{\text{PHOSPHO}}$ -peptides were included in each experiment and added to lysates of any cell line used as positive control and as a tool to measure the maximal fluorescent signal achievable on the biosensor.

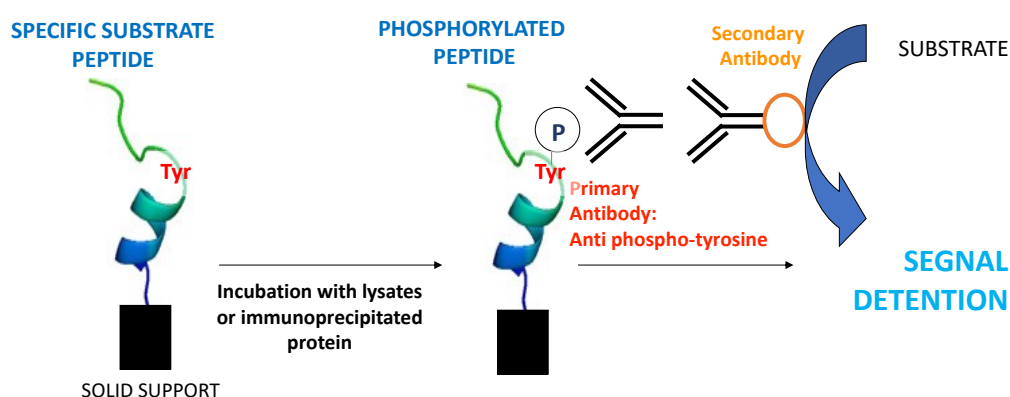


Figure 7. Schematic illustration of peptide-based ELISA assay. Biotinylated peptide is anchored on a neutravidin-coated plate and incubated with cell lysates with or immunoprecipitated protein. Fluorescence is detected through an anti phospho-tyrosine antibody [178].

### 3.11.3 PEPTIDE BIOSENSORS-BASED ELISA ASSAY ON IMMUNOPRECIPITATED JAK2 PROTEIN

Peptide biosensors was resuspended in kinase assay buffer (20mM Tris-HCl, 10mM  $\text{MgCl}_2$ , 0.05% Triton-X, 20 $\mu\text{M}$  ATP, 1mM DTT, 0.1mM  $\text{Na}_3\text{VO}_4$  in  $\text{H}_2\text{O}$ ) at the final concentration of 1  $\mu\text{M}$  ( $\text{P}_{\text{JAK2-L}}$  and  $\text{P}_{\text{JAK2-S}}$ ) or 0.5  $\mu\text{M}$  ( $\text{P}_{\text{PHOSPHO-JAK2}}$ ), and incubated on a rotating wheel with the immunoprecipitated products for 30 min at 4°C. After beads removal with a magnetic support, peptides were captured on neutravidine-coated plate in 30 minutes of incubation in oscillation at RT. After three washes, mouse monoclonal anti-phosphotyrosine antibody, was added and then incubated at 4°C overnight and the phosphorylation of the peptides was detected as mentioned above (see paragraph 3.11.2).

## 3.12 STATISTICAL ANALYSIS

Graphical representation and statistical analysis were performed using the GraphPad Prism® 9.4.1 program (GraphPad Software Inc.).

Data obtained from the MTT assay were analyzed using a nonlinear regression; results are presented as mean  $\pm$  standard error (SE) and  $IC_{50}$  was determined from the dose-response curve. To compare the results from MTT assay, western blot and ELISA assays Two-way ANOVA and by Bonferroni's post-test for multiple comparison was performed.

Real-time PCR data of relative gene expression of iPSC and NSC stemness, specific markers expression of genes related to JAK/STAT signaling pathway and *STING* basal expression were analyzed comparing patients' iPSCs versus NSCs by t-test analysis. *STING* expression of iPSCs and NSCs after treatments were analyzed by Two-way ANOVA and Bonferroni's post-test.

Statistical significance was set at  $P < 0.05$ .

## ***4 - RESULTS – PART I***

---

## 4.1 iPSCs AND NSCs CHARACTERIZATION

### 4.1.1 STEMNESS

Expression of pluripotency gene markers for different grade of stemness was assessed in both iPSCs and NSCs by real-time PCR (Figure 8). The expression of *OCT4* was significantly reduced in NSC compared to iPSC in both AGS and healthy donor derived cells (iPSC vs NSC: BJ, AGS1, AGS7,  $P < 0.0001$ ; AGS2,  $P < 0.01$ , t-test analysis) whereas the expression of neuronal markers *SOX1* (BJ, AGS7,  $P < 0.01$ ; AGS1, AGS2,  $P < 0.0001$ , t-test analysis) and *PAX6* were increased in NSCs compared to iPSCs, as expected (BJ,  $P < 0.01$ ; AGS1,  $P < 0.001$ ; AGS2, AGS7,  $P < 0.05$ , t-test analysis). There were no significant variations in *SOX2* and *Nestin* mRNA expression between iPSC and NSC in all cell lines considered.

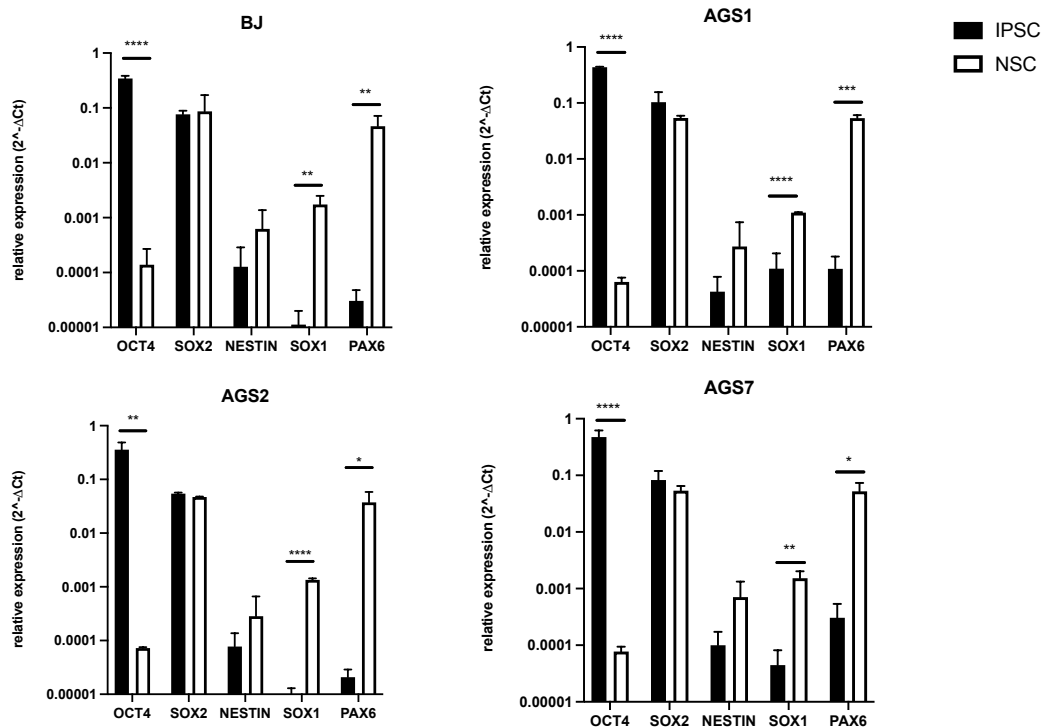


Figure 8: Expression levels of iPSC (*OCT4*, *SOX2*) and NSC stemness specific markers (*SOX1*, *Nestin*, *PAX6*) in iPSC and NSC. Gene expression was normalized to housekeeping  $\beta$ -actin gene expression, and relative expression was calculated as  $2^{-\Delta\Delta C_t}$ . P-value according to t-test analysis, \*  $P < 0.05$ , \*\*  $P < 0.001$ , \*\*\*\*  $P < 0.0001$ .



### 4.1.2 iPSCs PROLIFERATION BY [3H]-THYMIDINE INCORPORATION ASSAY

Cell proliferation of patient-derived AGS1-, AGS2-, AGS7-IPSC were analyzed by the [3H]-thymidine incorporation assay after 72 hours of culture (Figure 9). Results were compared to the proliferation rate of the BJ-iPSC healthy control line. As shown, thymidine incorporation of the AGS1- and AGS7-IPSCs was similar to the BJ-iPSC control line, at each cell seeding density tested. On the contrary, AGS2-IPSCs resulted significantly less proliferating in comparison to BJ-iPSC healthy control line showing a significant difference when seeded at  $0.5 \times 10^4$  and  $1.0 \times 10^4$  cell /well ( $P < 0.05$  and  $P < 0.001$ , respectively, Two-way ANOVA and Bonferroni's post-test). AGS2-IPSCs resulted less proliferating than others also when assessed subjectively by visual inspection (figure not shown).

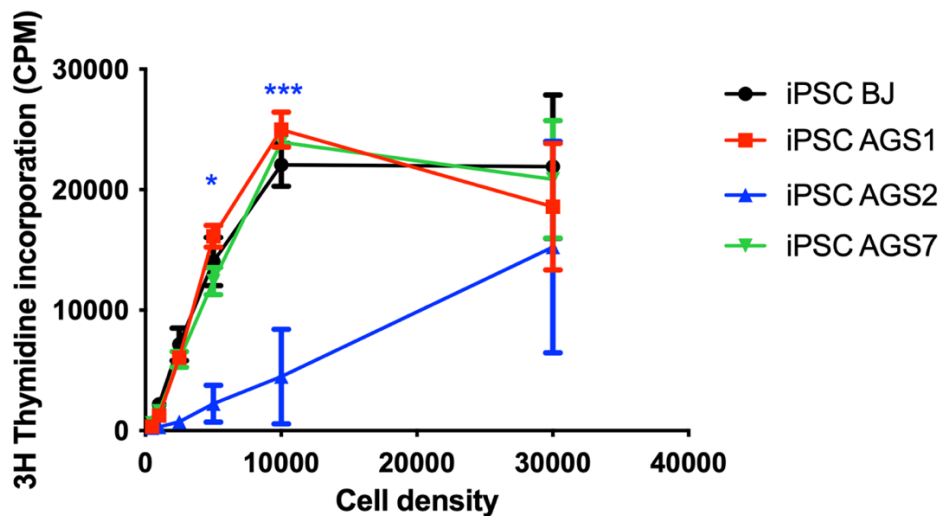


Figure 9: Cell proliferation of AGS1-, AGS2-, AGS7- and BJ-iPSC lines evaluated by the [3H]-thymidine incorporation assay. Data are reported as means  $\pm$  SE of 3 independent experiments performed in triplicate. [3H]-thymidine incorporation into DNA was expressed counts per minute (or CPM). Cell densities referred to initial cell/well seeding. Statistical analysis vs. BJ-iPSC control line: \*  $P < 0.05$ , \*\*\*  $P < 0.001$ , Two-way ANOVA, and Bonferroni's post-test.

### 4.1.3 iPSCs CELL CYCLE ANALYSIS

Cell cycle of iPSC and of a human immortalized hepatic cell line (IHH) was analyzed by measuring propidium iodide uptake by flow cytometry analysis after 72 hours of cell culture (Figure 10). Results were compared to the cell cycle of the BJ-iPSC healthy control line. The IHH line was chosen as additional control to compare cell cycle of iPSCs to that of immortalized cells.

Cell cycle G0 and S phases were comparable among patient-specific and healthy donor IPSC. In G2 phase, AGS2 showed significantly lower percentage of cells in G2 phase compared to BJ-iPSC (AGS2 26.2% vs BJ 35.8%,  $P < 0.05$ , Two-way ANOVA and Bonferroni's post-test). The IHH cell line was instead characterized by higher percentage of cells in the resting G0 phase compared to BJ-iPSCs (IHH 43.7% vs BJ 33.3%,  $P < 0.05$ , Two-way ANOVA and Bonferroni's post-test) and a lower percentage of cells in the G2 phase (IHH 22.9% vs BJ 35.8%,  $P < 0.001$  Two-way ANOVA and Bonferroni's post-test). No differences were observed in the S phase between iPSC and IHH.

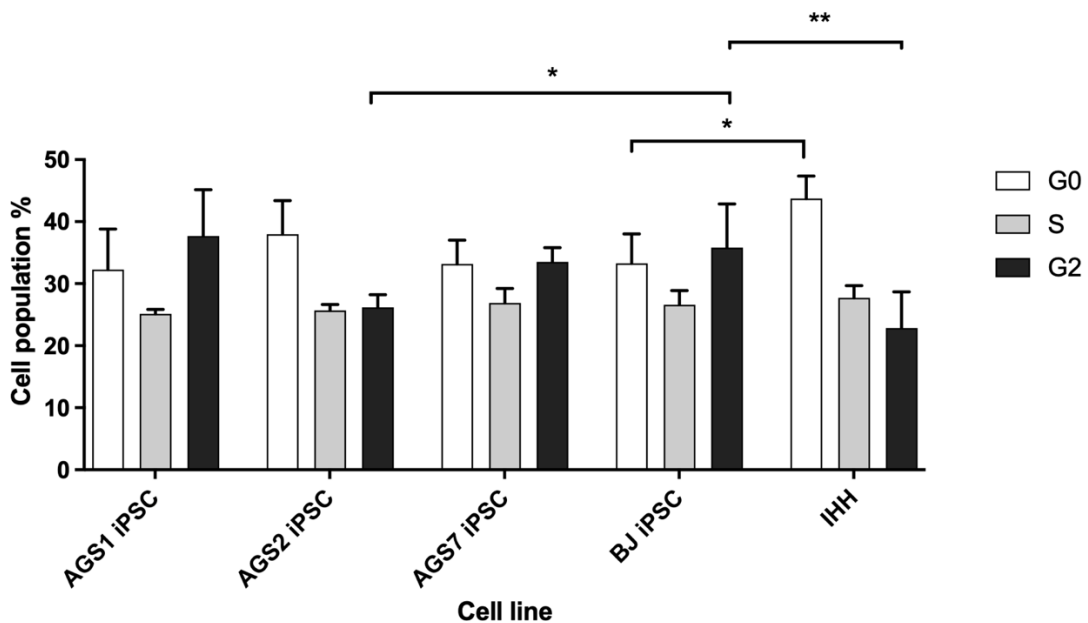


Figure 10: Cell cycle analyses of AGS1-, AGS2-, AGS7-, BJ-iPSCs and IHH immortalized cell line evaluated by propidium iodide cellular uptake. Results are reported as mean  $\pm$  SE of three replicates. Statistical analysis vs. BJ-iPSC control line: \*  $P < 0.05$ , \*\*  $P < 0.01$ , Two-way ANOVA, and Bonferroni's post-test.

#### 4.1.4 NSCs PROLIFERATION BY CFSE STAINING

We compared proliferation capability of untreated NSC by means of fluorescent intracellular staining dye CFSE. The rationale in changing the type of proliferative assay from [3H]-thymidine incorporation assay used for iPSC to CFSE was related to some aspects such as costs and laboriousness of the methods [179]. In fact, the CFSE proliferation assay requires the staining of cells with a non-radioactive dye and a cheaper and affordable cytofluorometer analysis, whereas in the [3H]-thymidine incorporation assay, the use of radioactive material is required and therefore dedicated protocols, instruments and laboratory are needed [180].

We performed the CFSE experiments three times on AGS- and BJ-NSC; however, results of these experiments were not comparable to each other showing a non-reproducible pattern of proliferation for each NSC line considered (Figure 11 represent one single experiment). No definitive conclusion could then be drawn. We can hypothesize that CFSE assay is not the ideal analysis to determine NSCs proliferation rate because of some technical issues such as an uncontrolled variability in cell seeding adhesion and growth.

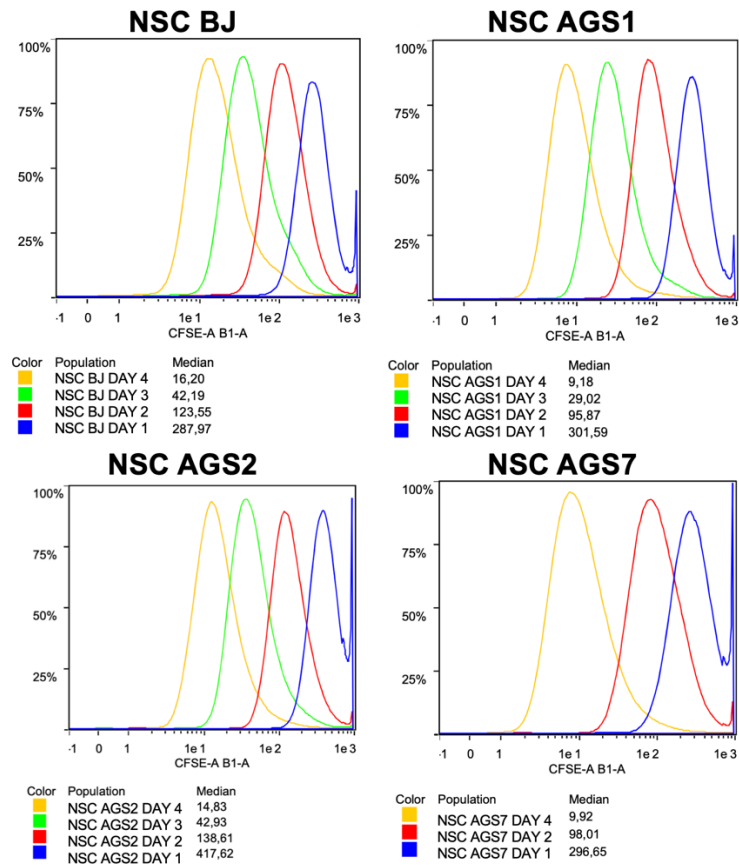


Figure 11: Cell proliferation analysis of AGS1-, AGS2-, AGS7-, BJ-NSCs evaluated by CFSE staining.

#### 4.1.5 NSCs VIABILITY BY MTT ASSAY

Viability of NSCs was measured by means of MTT assay after 72 hours growth in NSC culture medium and at different cell seeding density (range:  $5.0 \times 10^3$  -  $3.0 \times 10^4$  cells/well, Figure 12). Under these basal conditions, cell viability was comparable among NSCs. Results highlighted that optical density (OD) was about 0.5 when cells were seeded at  $5.0 \times 10^3$  cell/well; an OD close to 1 is generally taken as an optimal absorbance for untreated cells, so the absorbance obtained at this cell concentration was not considered ideal. For seeding concentrations  $\geq 1.0 \times 10^4$  cells/well, each NSC line achieved a stability in cell viability, with OD values ranging from 0.66 to 0.9; no difference among AGS- or BJ-derived cells was observed at each seeding density. A seeding concentration of  $1.0 \times 10^4$  cells/well was considered the best seeding condition to reach 80-90% confluence at the end of the 72 hours incubation and thus chosen for drug cytotoxicity assays.

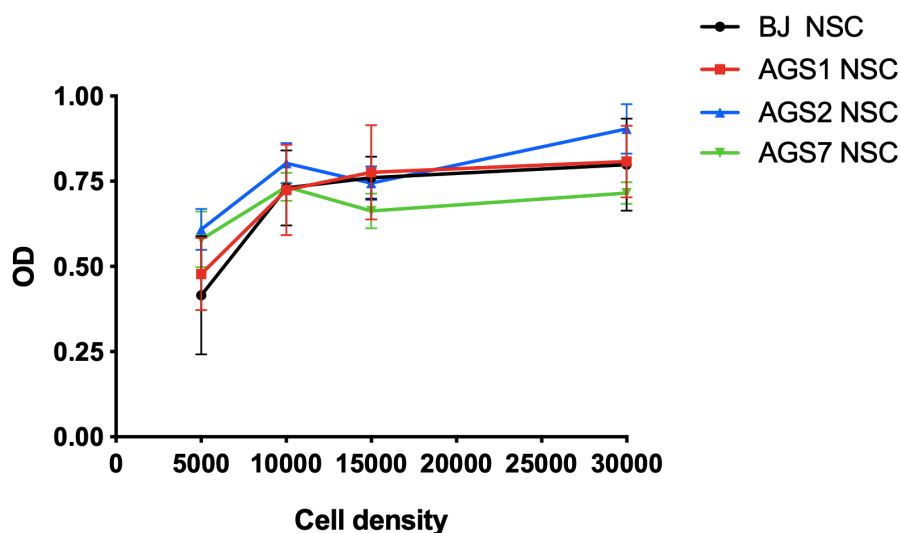


Figure 12: MTT assay under basal conditions on AGS1, AGS2, AGS7 and BJ-NSC lines. Cells, seeded at different concentrations, were incubated for 72 hours. Data represent the mean  $\pm$  SD (n=4). OD: optical density.

## 4.2 iPSCs AND NSCs CYTOTOXICITY ASSAYS

According to their different proliferation rate (for iPSC evaluated by the [3H]-thymidine incorporation assay) or survival rate (for NSC evaluated by MTT assay), AGS2-iPSCs were seeded at  $3.0 \times 10^4$  cells/well, while all other iPSCs at  $1.0 \times 10^4$  cells/well to obtain comparable OD of untreated cells after 72 hours of incubation; all NSC were seeded at  $1.0 \times 10^4$  cells/well.

MTT assay were performed to evaluate the cytotoxic effect of different drugs concentration on the AGS1-, AGS2-, AGS7-, and BJ-iPSC and NSC models, after 72 hours of exposure.

### 4.2.1 CYTOTOXIC EFFECT OF JAK INHIBITORS

With the exception of pacritinib, JAKi did not compromise iPSC and NSC viability (Figure 13 and Figure 14, respectively): the exposure to ruxolitinib, baricitinib, tofacitinib in the range of concentrations tested did not produce any significant cytotoxic response on iPSC and NSC, resulting resistant to these treatments ( $IC_{50} > 1 \times 10^{-5}$  M).

A 3-day exposure to high concentration of ruxolitinib ( $>2.5 \mu\text{M}$ ) increased cell viability in AGS7-iPSC compared to controls BJ-iPSC ( $P < 0.05$ , Two-way ANOVA and Bonferroni's post-test, Figure 13A); a similar result was observed for AGS7-iPSC and AGS2-iPSC when exposed to baricitinib at concentration of  $2.5 \mu\text{M}$  ( $P < 0.05$ , Two-way ANOVA and Bonferroni's post-test, Figure 13B). A slight viability reduction could be detected in patients derived iPSC compared to healthy control BJ-iPSCs after tofacitinib treatment at increasing concentrations (Figure 13C). Pacritinib was cytotoxic to all iPSC ( $IC_{50} \pm \text{SE}$ , BJ-iPSC:  $0.61 \pm 0.03 \mu\text{M}$ ; AGS1-iPSC:  $0.58 \pm 0.04 \mu\text{M}$ ; AGS2-iPSC:  $0.29 \pm 0.13 \mu\text{M}$ ; AGS7-iPSC:  $0.35 \pm 0.07 \mu\text{M}$ , Figure 13D); a significant decrease in cell viability was observed at  $0.56 \mu\text{M}$  in AGS2- or AGS7-iPSC compared to BJ-iPSC ( $P < 0.0001$ , Two-way ANOVA and Bonferroni's post-test).

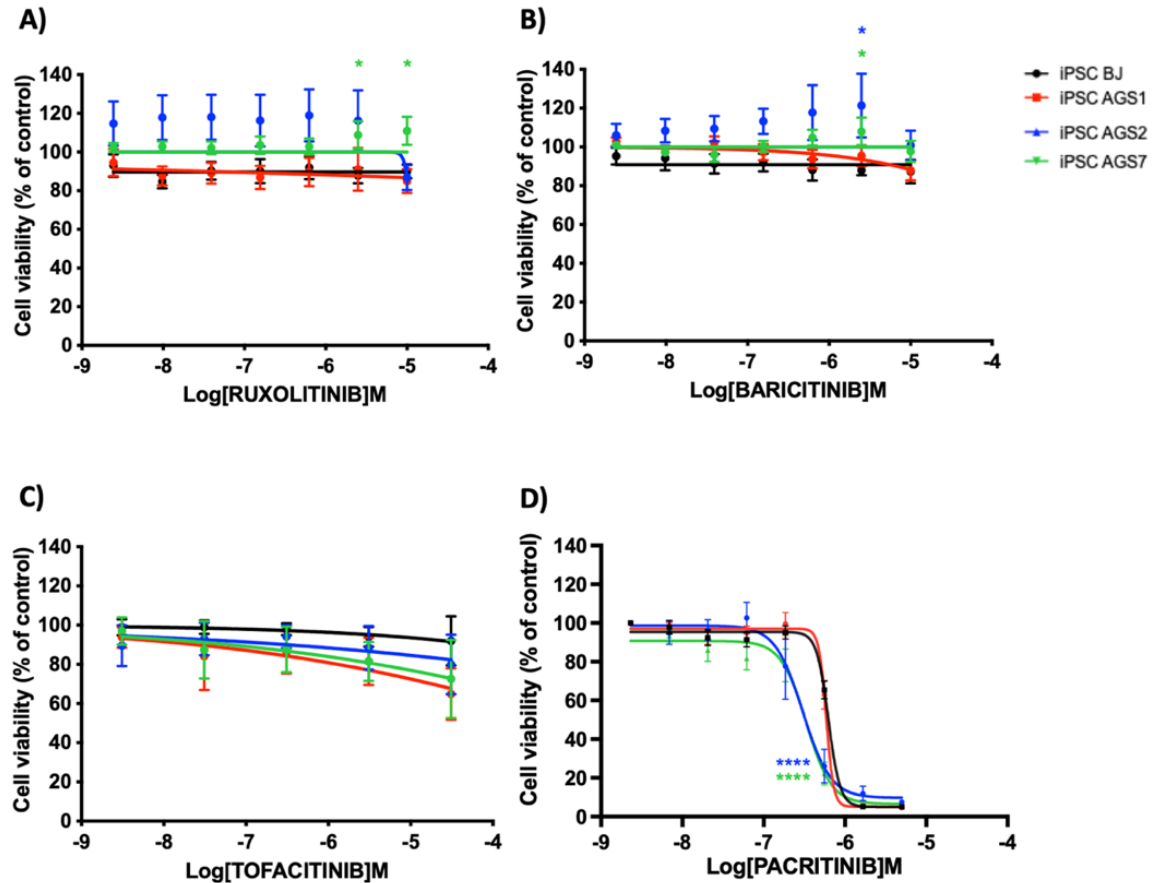


Figure 13. Dose-response curve after 72 hours exposure with A) ruxolitinib, B) baricitinib, C) tofacitinib, D) pacritinib. AGS1-, AGS7-, and BJ- iPSC lines were seeded at  $1.0 \times 10^4$  cells/well and AGS2-iPSC at  $3.0 \times 10^4$  cell/well. The data are reported as percentage of cell viability with respect to untreated cells and as means  $\pm$  standard error (SE) of 3 independent experiments performed in triplicate. Statistical analysis vs. BJ-iPSC control line: \*  $P < 0.05$ , \*\*\*\*  $P < 0.0001$ , Two-way ANOVA and Bonferroni's post-test. Green asterisks referred to AGS7-iPSC versus BJ-iPSC; blue asterisk to AGS2-iPSC versus BJ-iPSC.

The exposure to high concentrations of ruxolitinib ( $>10 \mu\text{M}$ ), baricitinib ( $>2.5 \mu\text{M}$ ) and tofacitinib ( $>10 \mu\text{M}$ ) increased cell viability in AGS7- NSC compared to BJ-NSC (Two-way ANOVA and Bonferroni's post-test,  $P < 0.05$ , Figure 14A, B and C); a similar result was observed for AGS2-NSC versus BJ-NSC treated with baricitinib at  $0.6 \mu\text{M}$  and  $2.5 \mu\text{M}$  ( $P < 0.05$ , Figure 14B) or tofacitinib at  $2.5 \mu\text{M}$  ( $P < 0.05$ , Figure 14C) and also for AGS1-NSC treated with tofacitinib at  $10 \mu\text{M}$  ( $P < 0.05$ , Figure 14C). Pacritinib was cytotoxic to all NSC (IC<sub>50</sub>  $\pm$  SE: BJ-NSC:  $0.63 \pm 0.13 \mu\text{M}$ ; AGS1-NSC:  $0.75 \pm 0.05 \mu\text{M}$ ; AGS2-NSC:  $1.05 \pm 0.34 \mu\text{M}$ ; AGS7-NSC:  $0.81 \pm 0.08 \mu\text{M}$  Figure 14D); AGS2-NSC were less sensitive than BJ-NSC to pacritinib (Two-way ANOVA and Bonferroni's post-test at  $0.06 \mu\text{M}$  ( $P < 0.05$ ) and  $0.56 \mu\text{M}$  ( $P < 0.0001$ ), Figure 14D).

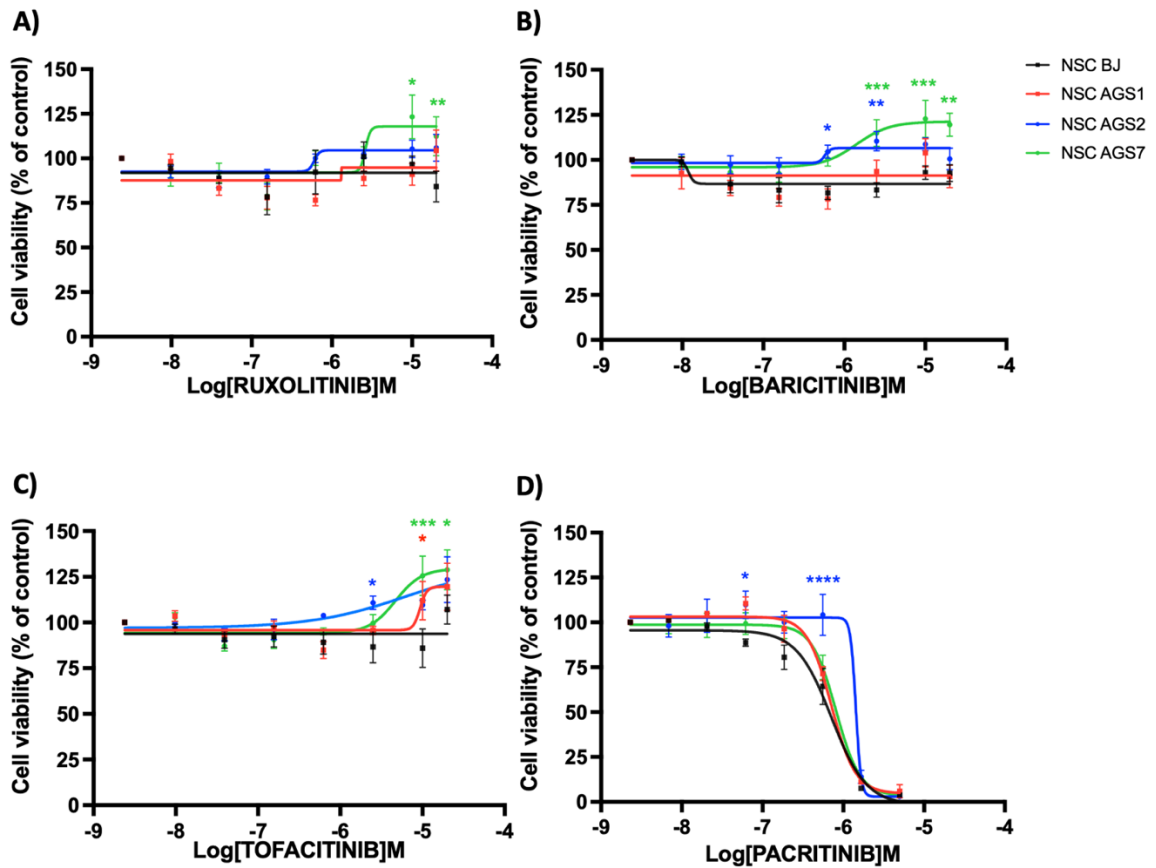


Figure 14. Dose-response curve after 72 hours exposure with A) ruxolitinib, B) baricitinib, C) tofacitinib, D) pacritinib. NSC lines were seeded at  $1.0 \times 10^4$  cells/well. The data are reported as percentage of cell viability with respect to untreated cells and as means  $\pm$  standard error (SE) of 3 independent experiments performed in triplicate. Statistical analysis vs. BJ-iPSC control line: \* P < 0.05, \*\* P < 0.01, \*\*\* P < 0.001, \*\*\*\* P < 0.0001, Two-way ANOVA and Bonferroni's post-test. Green asterisks referred to AGS7-NSC versus BJ-NSC, blue asterisk to AGS2-NSC versus BJ-NSC, red asterisk to AGS1-NSC versus BJ-NSC.

The expression of *JAK1/STAT1* and *TYK2/STAT2*, crucial molecular targets involved in the JAKi pharmacodynamics and activated by the IFN receptors, were evaluated in iPSC and NSC to understand whether the lack of *in vitro* drug cytotoxicity could be ascribable to the lack of expression of these key genes. *JAK1*, *STAT1*, *TYK2* and *STAT2* gene expression were comparable between iPSC and NSC, and among NSC and iPSC, except for *STAT2* that resulted higher in AGS7-iPSC compared to AGS7-NSC (Figure 15, t-test analysis).

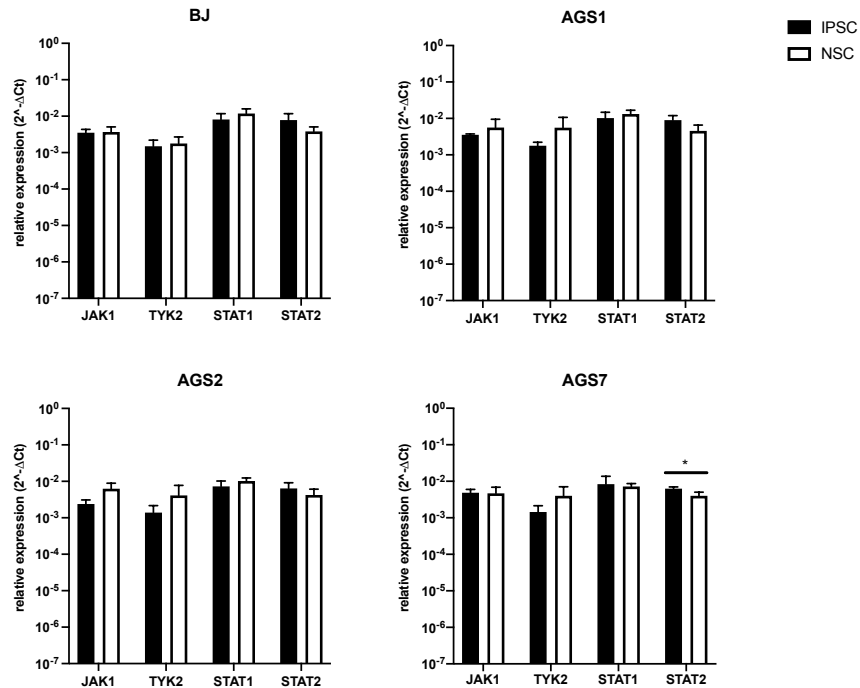


Figure 15. Gene expression analysis of *JAK1*, *STAT1*, *TYK2* and *STAT2*. Data are normalized to housekeeping  $\beta$ -actin gene expression, and relative expression was calculated as  $2^{-\Delta\Delta C_t}$ . P-value according to t-test analysis, \*  $P < 0.05$ .

## 4.2.2 CYTOTOXIC EFFECT OF ANTIRETROVIRALS

Cytotoxic assays on iPSC and NSC with RTIs (abacavir sulfate, lamivudine, zidovudine, Figure 16) showed that only AGS2-iPSCs were sensitive to zidovudine ( $>10 \mu\text{M}$ ) although  $IC_{50}$  could not be calculated in the range of concentrations tested ( $P < 0.001$  compared to controls BJ-iPSC, Two-way ANOVA and Bonferroni's post-test, Figure 16C-left panel); this sensitivity was lost in AGS2-NSC (Figure 16C-right panel).

A trend toward a dose-dependent increase of cell viability after RTIs exposure was observed in NSC. Survival of AGS2-NSC was significantly lower than BJ-NSC at the higher concentration tested of lamivudine ( $20 \mu\text{M}$ , Two-way ANOVA, Bonferroni's post-test,  $P < 0.05$ , Figure 16B-right panel).

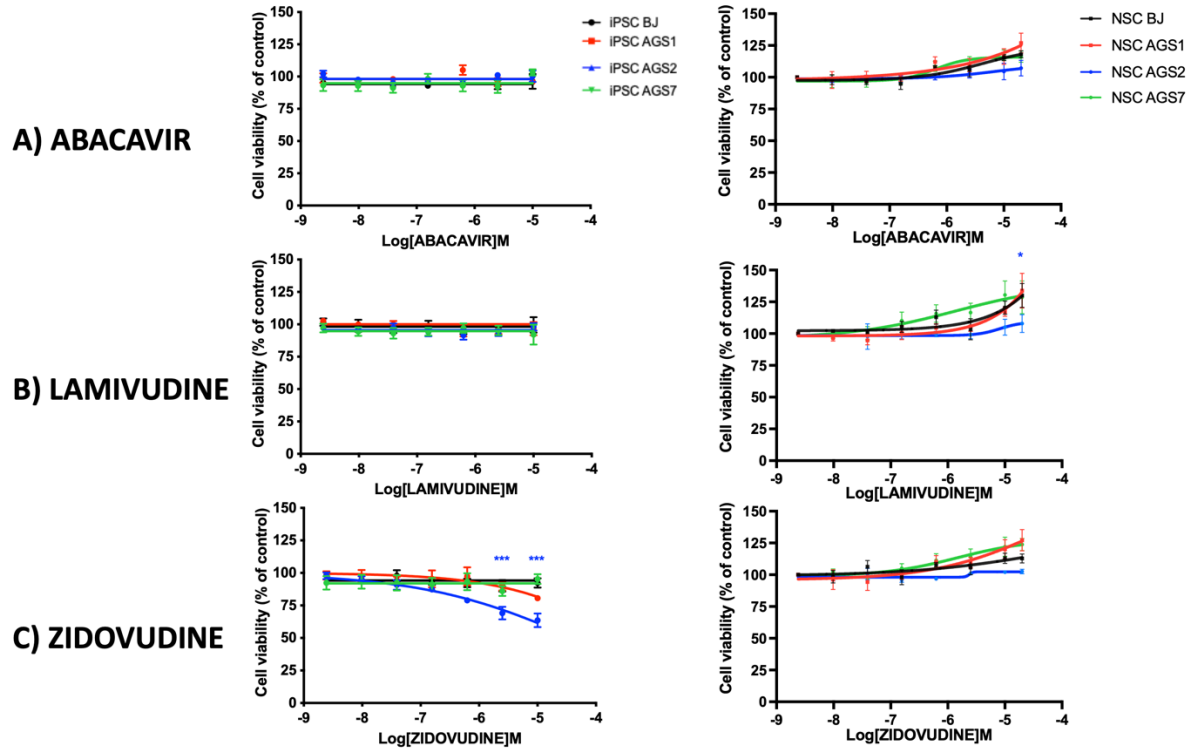


Figure 16: Dose-response curve after 72 hours exposure with A) abacavir, B) lamivudine, C) zidovudine, in iPSC (left panel) and NSC (right panel). The data are reported as percentage of cell viability with respect to untreated cells and as means  $\pm$  standard error (SE) of 3 independent experiments performed in triplicate. Statistical analysis vs. BJ-iPSC control line: \*  $P < 0.05$ , \*\*\*  $P < 0.001$ , Two-way ANOVA and Bonferroni's post-test. Blue asterisk referred to AGS2-NSC versus BJ-NSC.

The expression of key genes involved in the tested drug pathways (*ADK* for abacavir, *DCK* for lamivudine, *TK1* for zidovudine) was assessed in iPSCs and NSC by real-time PCR. Expressions were comparable between iPSC and NSC (Figure 17); intriguingly, *ADK* expression level increased in AGS1-NSC compared to AGS1-iPSC ( $P < 0.05$ ). However, no differences were found in terms of sensitivity to abacavir treatments.



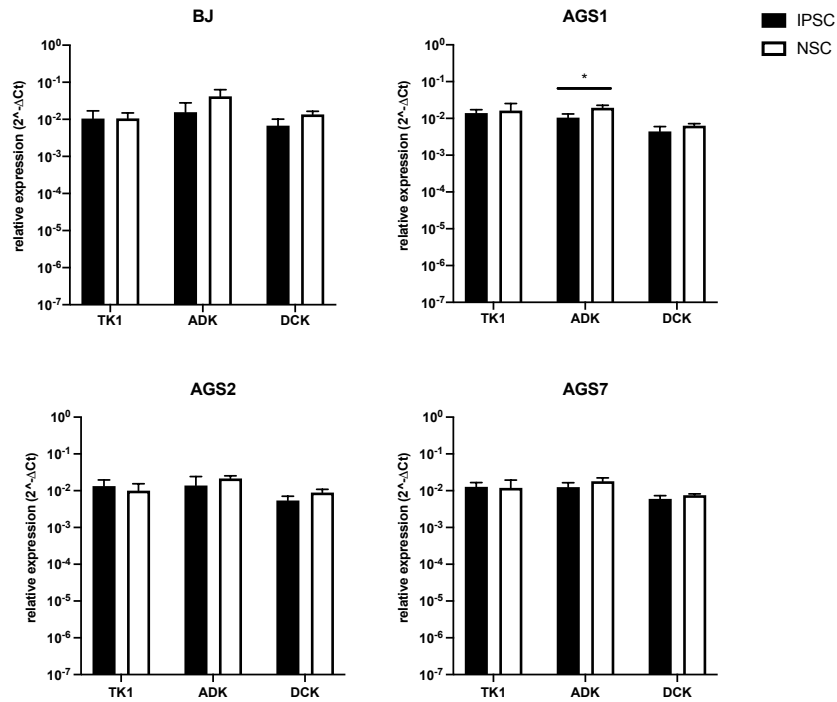


Figure 17: Gene expression analysis of RTIs key genes in iPSC and NSC cell lines. Data are normalized to housekeeping  $\beta$ -actin gene expression, and relative expression was calculated as  $2^{-\Delta C_t}$ . P-value according to t-test analysis, \* P<0.05

### 4.2.3 CYTOTOXICITY OF cGAMP

A 3-day exposure with cGAMP (range:  $8.7 \times 10^{-8}$  M –  $3.5 \times 10^{-5}$  M) did not show any cytotoxic activity in stem cell lines (Figure 18). Intriguingly, AGS2-NSC showed a significant increase in terms of viability at 0.348 nM compared to BJ-NSC (P<0.05, Two-way ANOVA and Bonferroni post-test).

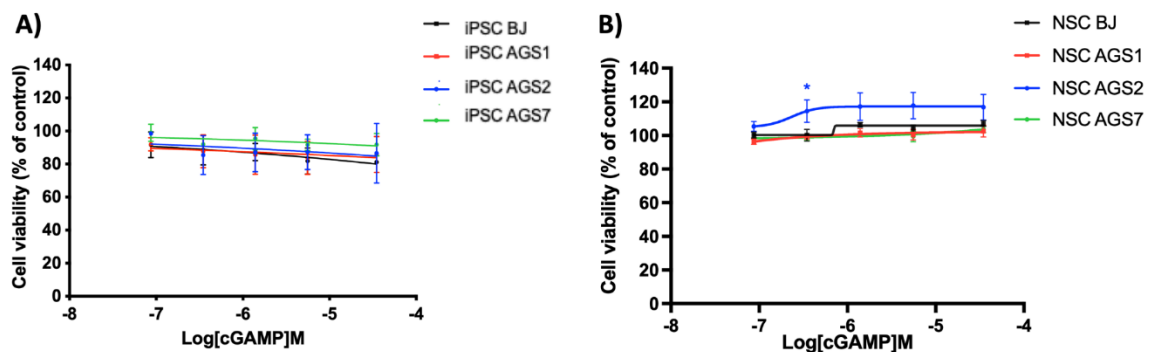


Figure 18: *In vitro* cytotoxicity of cGAMP on A) iPSC and B) NSC. Cells were exposed for 72h to cGAMP and cytotoxic effects were analyzed by MTT assay. Statistical analysis vs. BJ control line: \* P<0.05, Two-way ANOVA and Bonferroni's post-test.

### 4.3 ANALYSIS OF *STING* EXPRESSION

By real time PCR, we evaluated *STING* expression in iPSCs and NSCs models. *STING* expression was increased in patients'-derived NSC models compared to iPSC (t-test analysis: AGS1, AGS7:  $P < 0.5$ , AGS2:  $P < 0.0001$ , Figure 19).

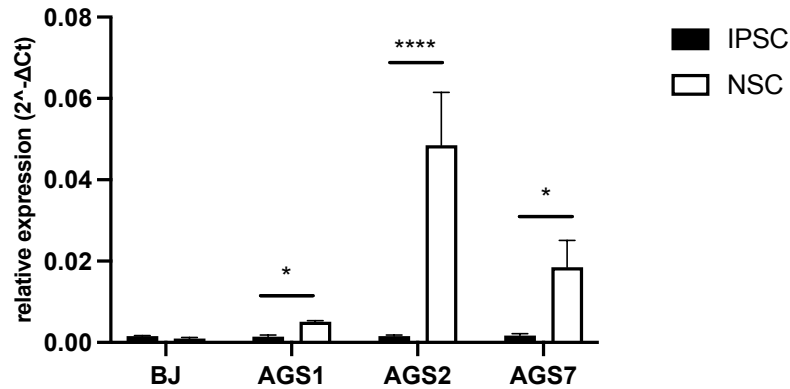


Figure 19: *STING* expression comparing iPSCs and NSCs. Data are shown as means  $\pm$  SE of three representative experiments and reported evaluating  $2^{-\Delta C_t}$  values, using the housekeeping gene HPRT1 as reference. P-value according to t-test analysis, \*  $P < 0.05$ , \*\*\*\*  $P < 0.0001$ .

Furthermore, we evaluated the expression of *STING* after 72 hours of culture in cells treated with baricitinib (10  $\mu$ M) and/or different time-exposure of the pro-inflammatory stimulus cGAMP (4 ng/ $\mu$ l), to verify whether these treatments can contribute to modulate the *STING* expression. Only in AGS7-iPSC, the treatment with cGAMP in the last 24 hours of incubation reduced *STING* expression levels compared to the condition without treatments ( $P < 0.05$ , Two-way ANOVA and Bonferroni's post-test). In the same cell line, the comparison between the untreated condition versus the condition with baricitinib was also significant ( $P < 0.05$ , Two-way ANOVA and Bonferroni's post-test) (Figure 20), showing a reduction in *STING* expression after drug exposure.

Interestingly, in AGS1- and AGS7-NSCs the presence of baricitinib, increased *STING* expression compared to the untreated condition ( $P < 0.01$  and  $P < 0.001$ , respectively, Two-way ANOVA and Bonferroni's post-test, Figure 21).

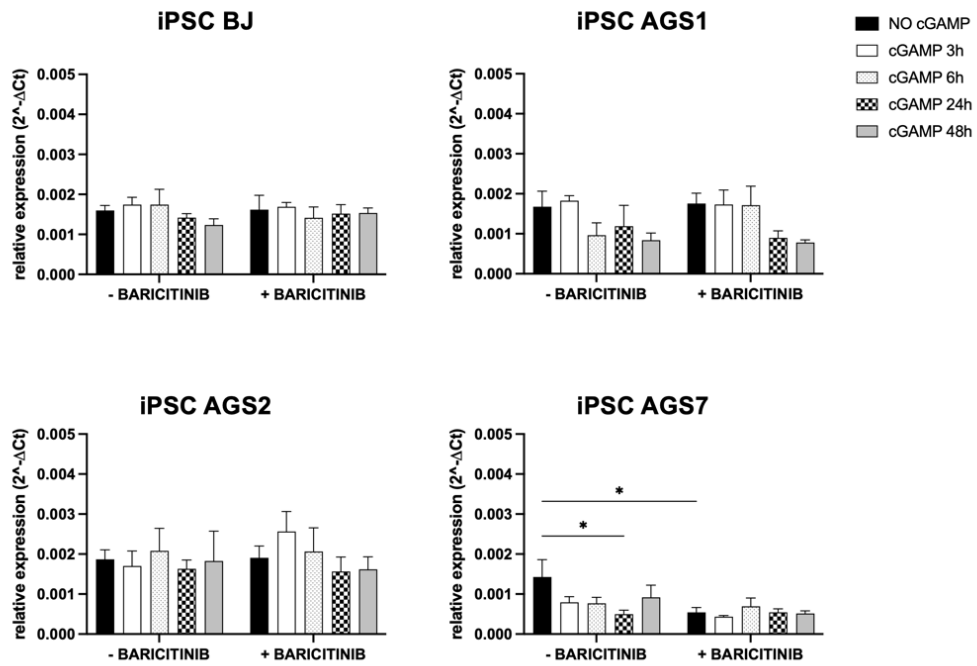


Figure 20: *STING* expression of iPSCs after 72h of cell culture in the presence of baricitinib (10  $\mu$ M) for 72 h and/or the pro-inflammatory stimulus cGAMP (4 ng/ $\mu$ l) for 3, 6, 24, 48 h of exposure. Data are shown as means  $\pm$  SE of three representative experiments and reported evaluating  $2^{-\Delta Ct}$  values, using the housekeeping gene *HPRT1* as reference. \*  $P < 0.05$ , \*\*  $P < 0.01$ , \*\*\*  $P < 0.001$ , Two-way ANOVA and Bonferroni's post-test.

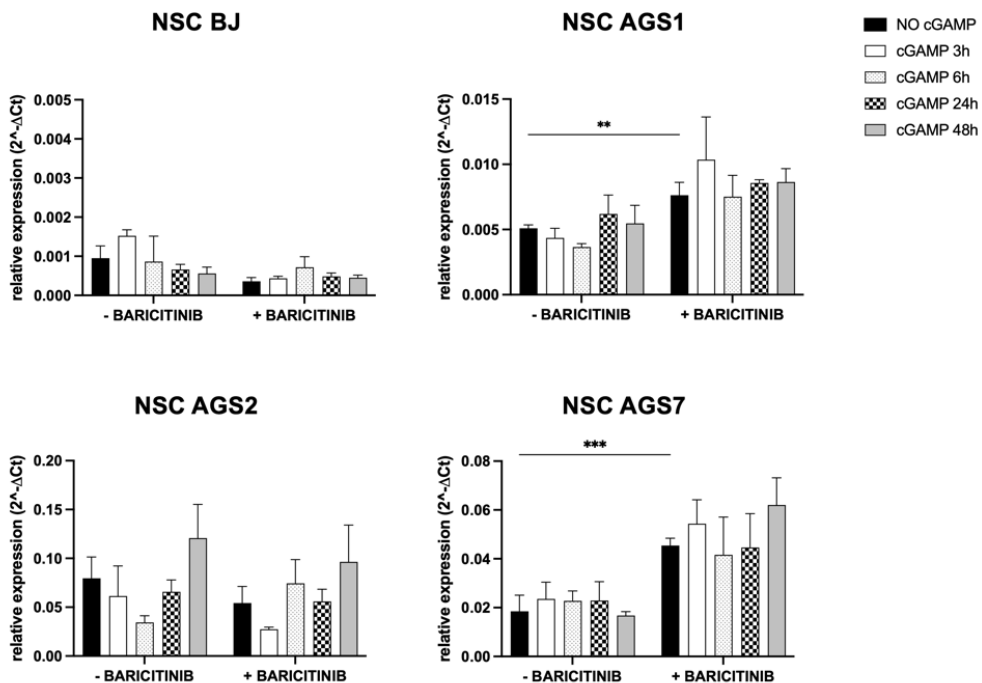


Figure 21: *STING* expression of NSCs after 72h of cell culture in the presence baricitinib (10  $\mu$ M) for 72 h and/or in presence of the pro-inflammatory stimulus cGAMP (4 ng/ $\mu$ l) for 3, 6, 24, 48 h of exposure. Data are shown as means  $\pm$  SE of three representative experiments and reported evaluating  $2^{-\Delta Ct}$  values, using the housekeeping gene *HPRT1* as reference. \*  $P < 0.05$ , \*\*  $P < 0.01$ , \*\*\*  $P < 0.001$ , Two-way ANOVA and Bonferroni's post-test.

## **5 - RESULTS – PART II**

---

## 5.1 CELL LINES CHARACTERIZATION

Human hematopoietic cell lines with different genetic backgrounds were initially characterized by western blot to verify the presence and expression of the CRLF2, JAK2 and STAT5 proteins. Cell lines were also functionally characterized for their sensitivity to JAKi (ruxolitinib, baricitinib, tofacitinib and pacritinib) by MTT cytotoxicity assay.

### 5.1.1 JAK2, STAT5 AND CRLF2 PROTEIN EXPRESSION IN HEMATOPOIETIC CELL LINES

JAK2 expression was comparable among REH, K562 and MHH-CALL-4; an higher and comparable JAK2 expression could be observed in the two MPN cell lines HEL and SET-2 (Figure 22A, HEL versus REH, K562 and MHH-CALL4,  $P < 0.01$ ; SET-2 versus REH, K562 and MHH-CALL-4,  $P < 0.01$ , HEL versus SET-2 non-significant Figure 22C). Phospho-JAK2 could be detected only in MHH-CALL4, HEL and SET-2 (Figure 18B; MHH-CALL4 versus REH,  $P < 0.05$ ; Two-way ANOVA, Bonferroni post-test, Figure 22C). JAK2 was phosphorylated at comparable levels in HEL and SET-2 (Figure 22B-C).

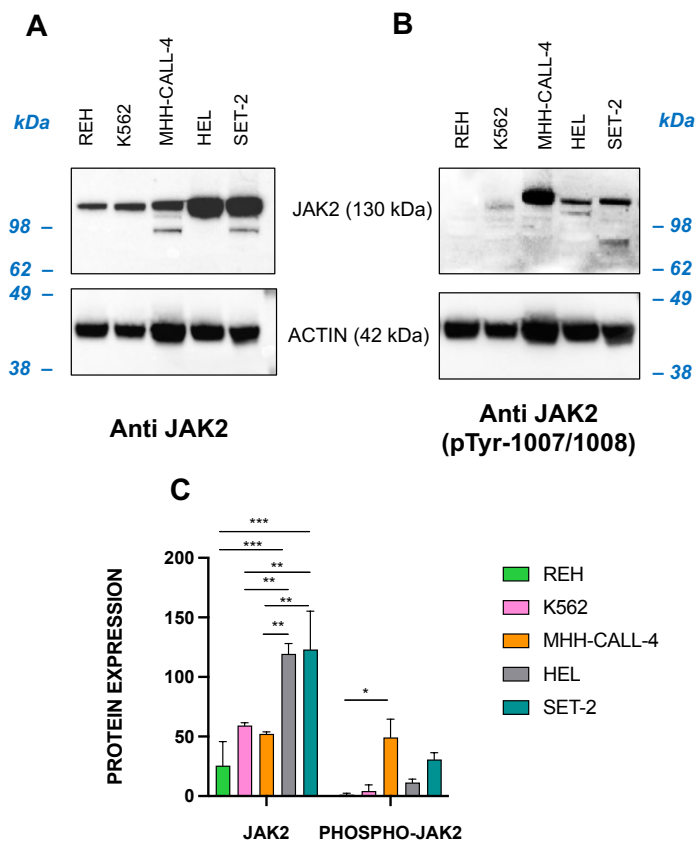


Figure 22. JAK2 protein expression in whole cell lysates. Representative images of 3 independent western blot performed using 25 $\mu$ g of cell lysate and A) anti human JAK2, B) anti human phospho-JAK2 (tyrosine 1007/1008) and C) protein expression normalized to actin used as loading control (mean  $\pm$  SE, n = 3): \*  $P < 0.05$ , \*\*  $P < 0.01$ , \*\*\*  $P < 0.001$ , Two-way ANOVA and Bonferroni's post-test.

The JAK2 kinase, when activated by trans-phosphorylation, phosphorylates the downstream transcription factor STAT5. To verify the aberrant activation of this pathway in hematopoietic cell lines, western blots were carried out using antibodies against STAT5 and STAT5 phosphorylated at the level of tyrosine 694. Figure 23A shows that the transcription factor was present in all cell lines, visible as a band at the expected molecular weight of 90 kDa. The analysis of the protein expression did not show significant differences between cell lines (Figure 23C). No phosphorylation of STAT5 was detected in the REH cell line, in contrast to other cells (Figure 23B; REH *versus* K562,  $P < 0.05$ ; Two-way ANOVA, Bonferroni's post-test, Figure 23C). K562, MHH-CALL-4, HEL and SET-2 showed comparable levels of phospho-STAT5.

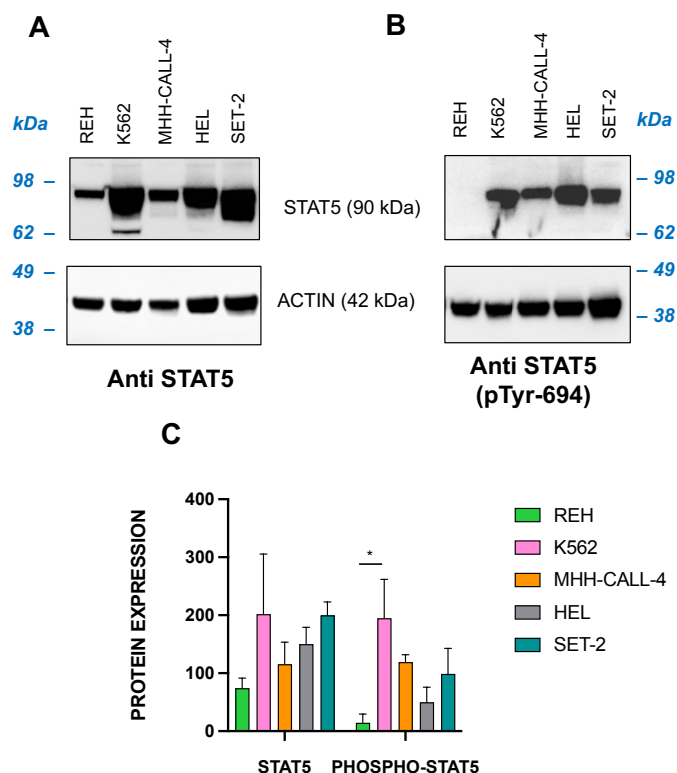


Figure 23. STAT5 protein expression in whole cell lysates. Representative images of 3 independent western blot performed using 25 $\mu$ g of cell lysate and A) anti human STAT5, B) anti human phospho-STAT5 (tyrosine 694) and C) protein expression normalized to actin used as loading control (mean  $\pm$  SE, n=3): \*  $P < 0.05$ , Two-way ANOVA and Bonferroni's post-test.

As shown in Figure 24A, CRLF2 (an upstream receptor of the JAK/STAT pathway) was present in all cell lines at the observed molecular weight of 49 kDa; in the myeloid cell lines K562 and HEL there was an additional lower molecular weight band (~38kDa), likely a truncated isoform of CRFL2.

After densitometric analysis of protein bands and normalization to vinculin used as internal loading control (124 kDa, Figure 24B), there was no difference in CRFL2 expression among cell lines, although K562 cells showed a slightly lower levels of protein.

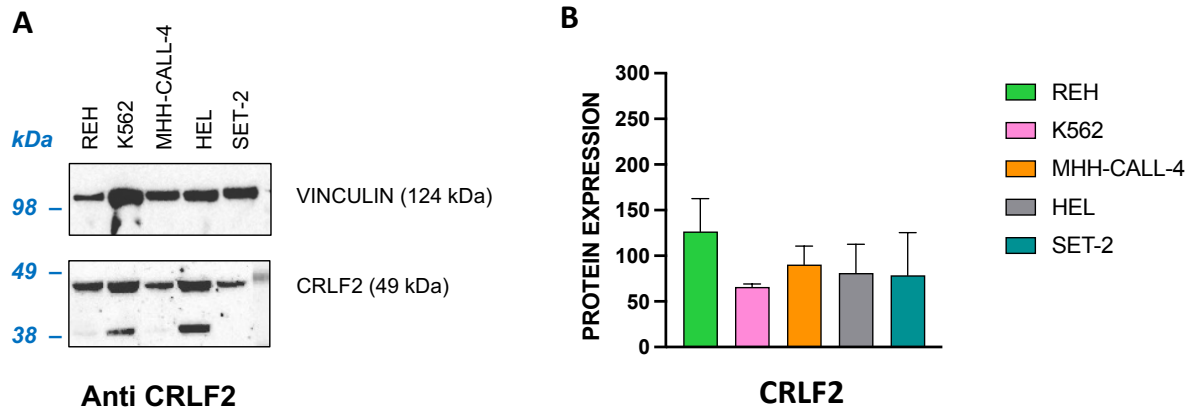


Figure 24. CRLF2 protein expression in whole cell lysates. A) Representative images of 3 independent western blot performed using 40µg of cell lysate and an antibody against the c-terminal portion of the human CRLF2 receptor. B) normalized CRLF2 protein expression to vinculin used as loading control (mean ± SE, n=3).

### 5.1.2 *IN VITRO* SENSITIVITY TO JAK INHIBITORS OF HEMATOPOIETIC CELL LINES

The cytotoxic effect of JAK inhibitors (ruxolitinib, baricitinib, tofacitinib and pacritinib) on cell lines was determined using the MTT viability assay and REH as control cell line (Figure 25). Ruxolitinib and baricitinib were not cytotoxic for REH, as expected, whereas tofacitinib increased REH viability in a dose-dependent manner and pacritinib impaired REH survival ( $IC_{50} \pm SE$ :  $0.28 \pm 0.02 \mu M$ ).

Among cell lines tested, SET-2 were the most sensitive to JAKi (SET-2,  $IC_{50} \pm SE$ , ruxolitinib:  $48.58 \pm 0.56$  nM; baricitinib:  $0.13 \pm 0.02 \mu M$ , tofacitinib  $0.50 \pm 0.14 \mu M$  and pacritinib  $0.41 \pm 0.06 \mu M$ ). With the exception of pacritinib, SET-2 and REH survival curves were significantly different from each other ( $P < 0.0001$ , Two-way ANOVA and Bonferroni's post-test). Viability of HEL was clearly less impaired than SET-2 when exposed to JAKi (HEL,  $IC_{50} \pm SE$ : ruxolitinib:  $1.19 \pm 0.33 \mu M$ ; tofacitinib  $10.87 \pm 1.7 \mu M$ ; pacritinib  $3.62 \pm 0.82 \mu M$ ; at 20 µM baricitinib, cell survival was 52.83%). A 3-day exposure to ruxolitinib, baricitinib and tofacitinib decreased cell viability in MHH-CALL-4, without killing more than half of cells at the highest concentration tested; MHH-CALL-4 were sensitive to pacritinib ( $IC_{50} \pm SE$ :  $0.37 \pm 0.06 \mu M$ ) with an overlapping dose dependence to REH.

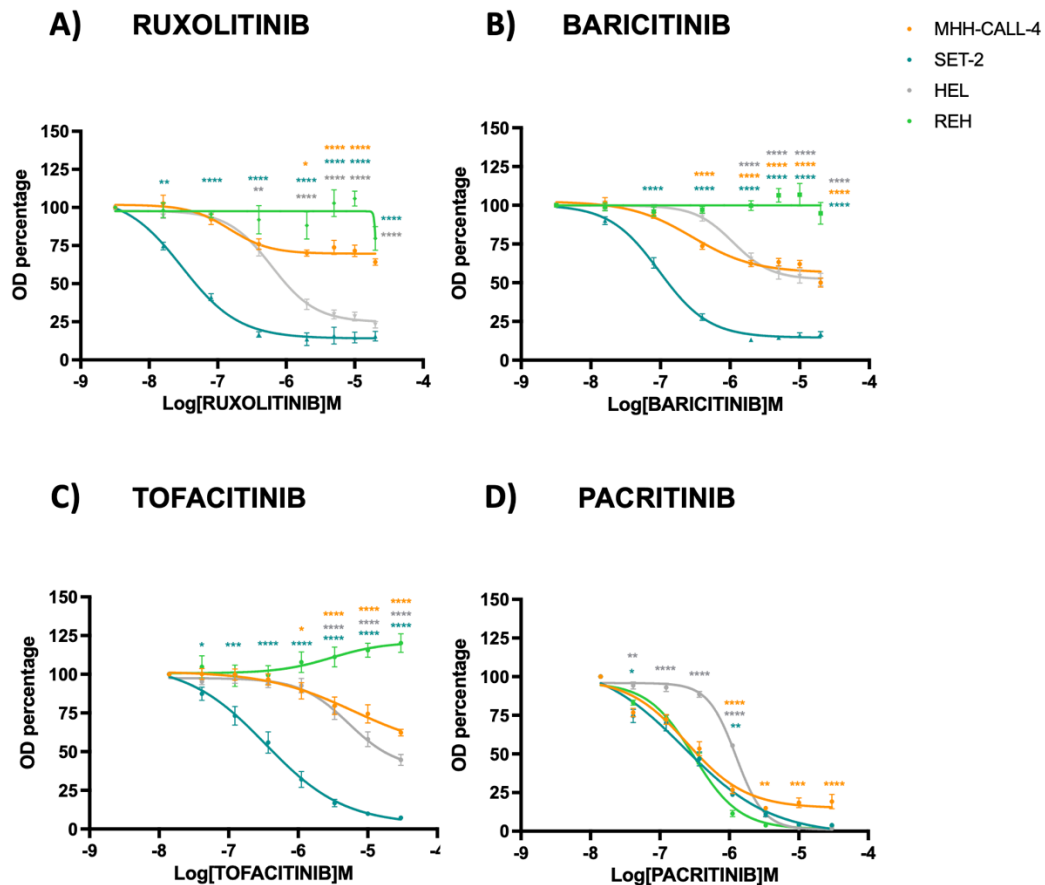


Figure 25. Dose-response curve with A) ruxolitinib, B) baricitinib, C) tofacitinib and D) pacritinib. Cell lines were seeded at 12,000 cells/well with a range of concentrations of 0.016  $\mu$ M – 20  $\mu$ M for ruxolitinib and baricitinib and of 0.041 – 30  $\mu$ M for tofacitinib and pacritinib. MTT assays were performed after 72 h of incubation. Error bars represent mean  $\pm$  SE (N=5). MHH-CALL-4, HEL, SET-2 versus REH: \* P<0.05, \*\* P<0.01, \*\*\* P<0.001, \*\*\*\* P<0.0001, Two-way ANOVA and Bonferroni's post-test.

## 5.2 PEPTIDE BIOSENSORS *IN VITRO* FUNCTIONAL ANALYSIS

### 5.2.1 PEPTIDE-BASED ELISA ASSAY ON WHOLE PROTEIN LYSATES

The peptide biosensor-based ELISA procedure on whole protein cell lysates was described by Montecchini et al. [178] and is referred to as “conventional protocol” in this manuscript. In this study, the procedure was applied for the first time to the P<sub>JAK2-L</sub> and P<sub>JAK2-S</sub> peptides and the MHH-CALL-4, HEL, SET-2, REH and K562 cell lysates, for measuring the kinase activity of JAK2 in cell lysates deriving from lines characterized by alterations in the JAK/STAT signaling pathway.

From results obtained and represented in Figure 26, there is no evidence of an increase in phosphorylation signaling for P<sub>JAK2-L</sub> and P<sub>JAK2-S</sub> beyond the baseline level of whole lysates. Only in the case of P<sub>PHOSPHO-JAK2</sub>, there are significantly different fluorescence values (P<0.0001, Two-way ANOVA



and Bonferroni's post-test). In fact, the latter peptide is used as an internal control of the ELISA assay, demonstrating the correct procedure execution.

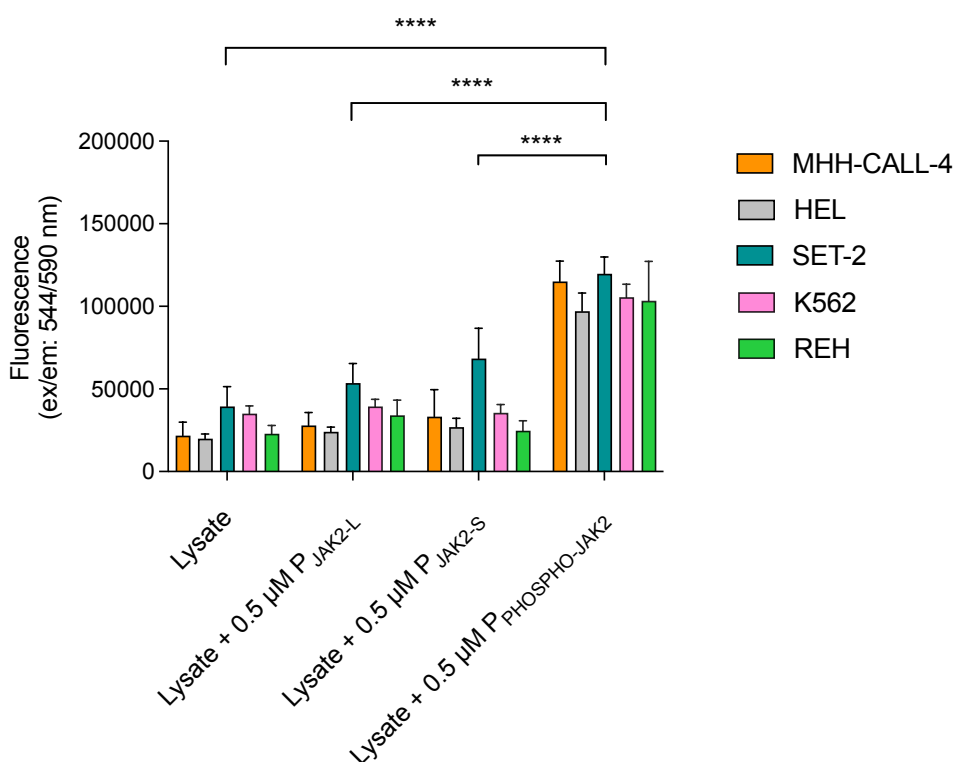


Figure 26. P<sub>JAK2</sub>-based ELISA assay. The graph compares the levels of P<sub>JAK2-L</sub> and P<sub>JAK2-S</sub> peptide phosphorylation by whole protein lysates obtained from cell lines. The highest FI (fluorescence intensity) is found as expected by P<sub>PHOSPHO-JAK2</sub> as internal control of the assay. The data obtained are the mean ± SE of at least N=3 experiments performed on different lysates; \*\*\*\* P<0.0001, Two-way ANOVA and Bonferroni's post-test.

## 5.2.2 PEPTIDE-BASED ELISA ASSAY ON IMMUNOPRECIPITATED PROTEIN

We perform the ELISA assay on purified JAK2 kinase by immunoprecipitation, assuming the presence of a possible "matrix effect" that could disturb and therefore mask the interaction of JAK2 with peptides biosensors in the whole lysates. The ELISA assay on immunoprecipitated proteins was also conducted with the aim of eliminating the non-specific background that could interfere with the specificity of the signal.

In this case, the HEL cell line was employed. Figure 27A shows the result of a first experiment performed using an antibody directed against JAK2, showing a band at 130 kDa, corresponding to the expected molecular weight of this kinase. Using an antibody against JAK2 phosphorylated at the level of tyrosine 1007/1008, it was possible to observe a band at about 130 kDa, thus confirming the presence of phosphorylated-JAK2 in the immunoprecipitated sample. A relevant phosphorylation signal over the background emerged after the incubation of P<sub>JAK2-L</sub> with the immunoprecipitated protein (FI in the absence of biosensor ± SD, 2510.26 ± 931.01 versus FI in the presence of P<sub>JAK2-L</sub>, 87710.99 ± 3278.33, P<0.0001 Two-way ANOVA and Bonferroni's post-test, Figure 27B). The incubation of P<sub>JAK2-S</sub> with the

immunoprecipitated product did not show a signal of phosphorylation compared to the condition without peptide (FI:  $2074.34 \pm 964.74$ ).  $P_{\text{PHOSPHO-JAK2}}$  was used as internal control of the assay (FI:  $165861.51 \pm 8152.81$ , Figure 27C) and represent the fully phosphorylated peptide. Compared to the control  $P_{\text{PHOSPHO-JAK2}}$  (100% phosphorylated), the amount of  $P_{\text{JAK2-L}}$  peptide phosphorylation was 53%.

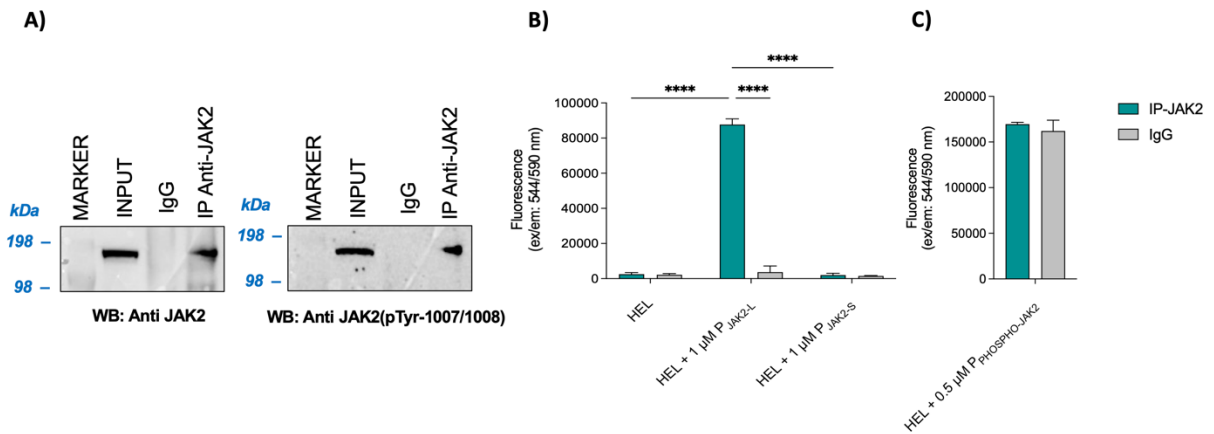


Figure 27. ELISA assay on immunoprecipitated JAK; A) Western blot performed using an antibody against JAK2 and against JAK2 phosphorylated tyrosine level 1007/1008. The input is represented by the cell lysate of the HEL line. B) The graph compares the phosphorylation levels of the  $P_{\text{JAK2-L}}$  and  $P_{\text{JAK2-S}}$  peptides by the immunoprecipitated JAK2 obtained from the HEL cell line. Absolute values of fluorescence are reported in ordinate.  $P_{\text{JAK2-L}}$  phosphorylation levels are higher than those obtained from the incubation condition in the absence of this peptide and with  $P_{\text{JAK2-S}}$ . (\*\*\*\*  $P < 0.0001$ , Two-way ANOVA and Bonferroni's post-test). C)  $P_{\text{PHOSPHO-JAK2}}$  is indicated as internal control of the assay.

An insufficient amount of activated JAK2 in the immunoprecipitate correspond to the lack of  $P_{\text{JAK2-L}}$  phosphorylation signal in the ELISA assay (Figure 28).

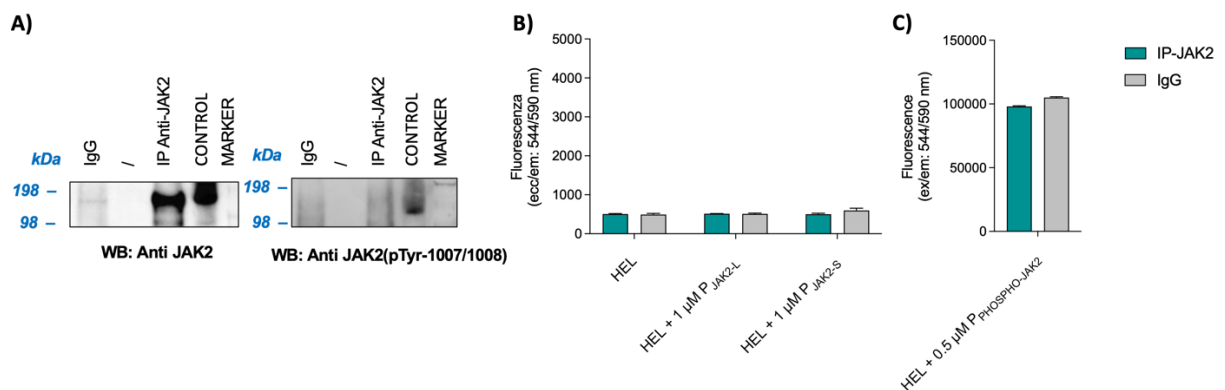


Figure 28. ELISA assay on immunoprecipitated JAK2; A) Western blot performed using an antibody against JAK2 and against JAK2 phosphorylated tyrosine level 1007/1008. Due to the lack of starting material, the input represented by the cell lysate of the HEL line is not present. However, a control was loaded, represented by the cell lysate deriving from the UT-7 hematopoietic line treated with granulocyte and macrophage growth factor, presenting phosphorylated JAK2 (#21104S, Cell Signaling Technologies). B) The graph compares the phosphorylation levels of the  $P_{\text{JAK2-L}}$  and  $P_{\text{JAK2-S}}$  peptides by the immunoprecipitated JAK2 obtained from the HEL cell line. The absolute values of fluorescence are reported in ordinate. C)  $P_{\text{PHOSPHO-JAK2}}$  is indicated as internal control of the assay to exclude technical error in the execution of the ELISA assay.

### 5.2.3 PEPTIDE-BASED ELISA ASSAY OPTIMIZATION ON WHOLE LYSATES AND P<sub>JAK-L</sub>

Thanks to ELISA assay performed on the immunoprecipitated samples, the P<sub>JAK2-L</sub> peptide was found to be the most promising peptide for the interaction with JAK2. Several attempts to optimize the conditions of the P<sub>JAK2-L</sub>-based ELISA assay in whole lysates followed, in particular by modifying the main parameters of the peptide-lysate incubation step, i.e. the temperature, the time of incubation, and the amount of whole lysate used.

To analyze the impact of the incubation temperature, two ELISA assays were performed in parallel, loading cell lysates on the neutravidin-coated plates with the pre-immobilized peptides (P<sub>JAK2-L</sub> and P<sub>PHOSPHO-JAK2</sub>) and keeping the plates for one hour, one at 25 °C (conventional protocol) and one at 37 °C; results are represented in Figure 29A. No significant differences in terms of P<sub>JAK2-L</sub> peptide phosphorylation signal were observed over background in any cell line. In MHH-CALL-4 and HEL, the P<sub>PHOSPHO-JAK2</sub> signal clearly emerged over the other two groups at both temperature conditions (P<0.05 and P<0.01, respectively, Two-way ANOVA and Bonferroni's post-test), while in the SET-2, there was no relevant difference among the three conditions tested at 25 °C and at 37 °C, likely because of the high experimental variability. The different incubation temperature did not improve phosphorylation and did not implement the signal detection.

Similarly, keeping the plates at room temperature (25°C) and increasing the peptide-lysate incubation time from 1 hour, as required by the conventional protocol, to 2 hours, did not affect P<sub>JAK2-L</sub> phosphorylation (Figure 29B). In MHH-CALL-4 and HEL, P<sub>PHOSPHO-JAK2</sub> fluorescence was significantly higher compared to background, at both incubation times, while in the SET-2 there was no relevant difference among the conditions tested.

The contribution of a variable amount of lysate was also investigated, comparing the 4 µg of lysate (conventional protocol) to a ten times higher quantity (40 µg), leaving the other parameters unchanged (25 °C; 1 hour) (Figure 29C). Incubation with 40 µg did not result in an increase in phosphorylation of the peptide biosensor over the background in MHH-CALL-4, HEL, and SET-2; fluorescence values were always comparable between 4 and 40 µg. P<sub>PHOSPHO-JAK2</sub> gave a relevant fluorescent signal at 4 µg. However, the incubation of 40 µg with P<sub>PHOSPHO-JAK2</sub> resulted in a signal reduction, in both cell lines for reasons not yet clarified. The hypothesis is that an insufficient amount of phosphatase inhibitors was present in the 40 µg lysate, since in the incubation of the 40 µg no adjustments were made to the concentrations of inhibitors with respect to the incubation of the 4 µg lysate.

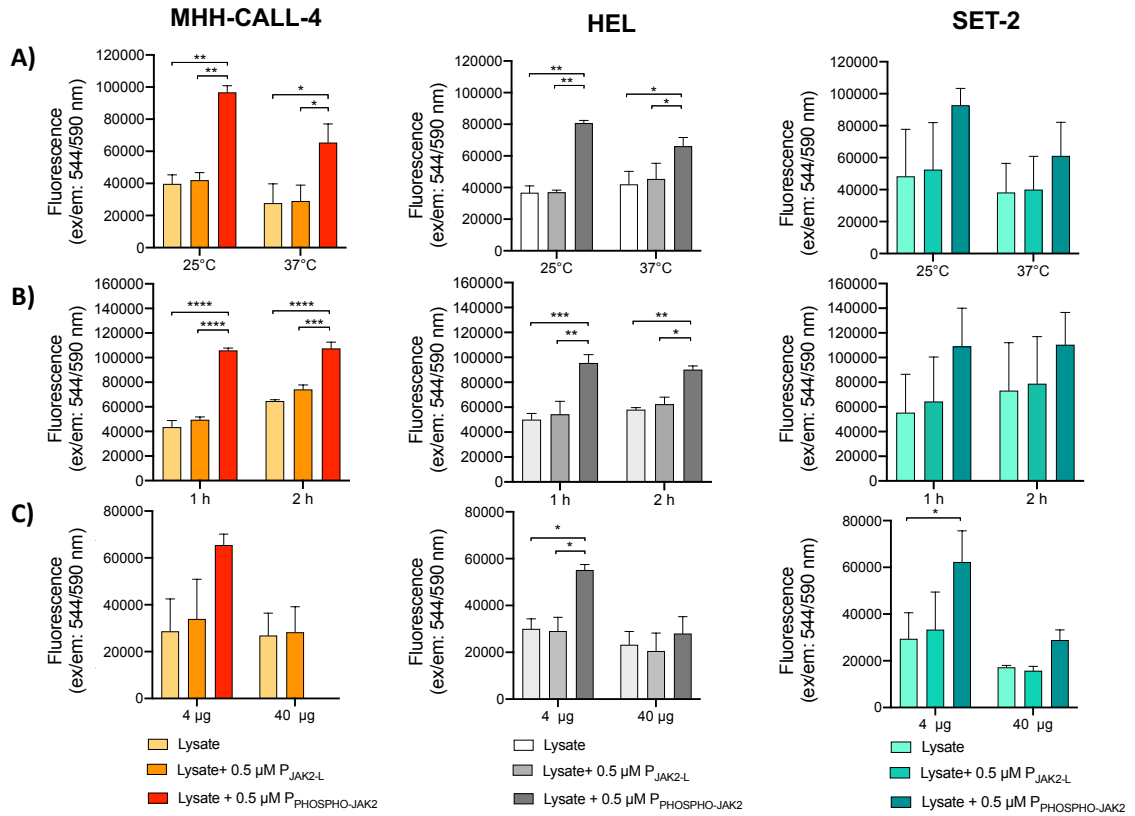


Figure 29. P<sub>JAK2-L</sub>-based ELISA assay optimization including A) different incubation temperature, B) incubation time and C) µg of lysate used. The absolute values of fluorescence are reported in ordinate. The data obtained are the mean ± SE of the experiments (n=2): \* P<0.05; \*\* P<0.01, \*\*\* P<0.001, \*\*\*\* P<0.0001, Two-way ANOVA and Bonferroni's post-test.

## **6 - *DISCUSSION***

---

As a rare disease, cure of AGS is challenging for clinicians for many reasons, including the difficulty in conducting clinical trials with an adequate number of patients. Judging the efficacy of the therapeutic interventions across published studies and case-reports is difficult because of the different regimens attempted, the heterogeneity of the AGS subtypes considered and the stage of the disease process at which treatment was started [131]. A further complication in AGS study is represented by the lack of adequate animal models. Indeed, a striking feature of all AGS mouse models generated is that they failed to recapitulate the strong CNS involvement seen in AGS [181-183]. Finally, the genetic heterogeneity of AGS requires knowledge of the full spectrum of disease mechanisms in order to provide individually tailored therapeutic intervention. The importance of creating patient-specific disease models to better understand inherited syndromes and to find ground-breaking therapies is becoming increasingly important in clinical and basic research. To accomplish these goals, powerful personalized cell models could be set up using the iPSC technology, as witness by the effort of 129 different clinical trials conducted, many of which consider iPSC as diseases model, around the world and currently registered on the public database [clinicaltrials.gov](http://clinicaltrials.gov) (web access on November 2022).

In this study, we used the previously generated iPSCs of AGS patients [170-172] and derived NSCs, to evaluate the safety and efficacy of a panel of drugs repurposed for AGS.

The expression of pluripotency gene markers for different grade of stemness was assessed in both iPSCs and NSCs. The decreased *OCT4* combined to the increased levels of *SOX1* and *PAX6* confirmed the proper differentiation of iPSC into NSCs. The transcription factor *OCT4* is essential to regain pluripotency in cell reprogramming and play a pivotal role in the maintenance of pluripotency. Due to the gradual methylation of its promoter and proximal enhancer region, the expression of *OCT4* significantly decreases during the consequent differentiation processes [184]. *SOX2* and *Nestin* levels of expression were found to be comparable between iPSCs and NSCs, as reported in literature [185], while the expression levels of *SOX1* and *PAX6* were increased in NSCs as expected [186].

We compared proliferation capability of iPSC lines, assessing both the growing rate and the percentage of cells at different stages of the cell cycle. Overall, the proliferation pattern of AGS1- and AGS7- iPSCs was comparable to that of the BJ-iPSC derived from fibroblasts of a healthy control. In contrast, AGS2-iPSCs resulted less proliferating in comparison to the other iPSCs tested, as assessed by [<sup>3</sup>H]-thymidine incorporation, but also as assessed subjectively by visual inspection (data not shown) as well as after viability assay (MTT assay), since it was necessary to seed three times more AGS2-iPSC to obtain comparable optical density (OD) of untreated cells after 72 hours in culture. AGS2-iPSC showed also a lower percentage of cells in G2 phase, suggesting a cell cycle arrest and/or dysregulation compared to other iPSCs. AGS2 patients are characterized by a reduction in *RNASEH2B* transcript and related protein levels. The lower proliferation of *RNASEH2B* deficient mice cells was also reported by Hiller and collaborators [187]. RNASE H2 is an endonuclease that degrades RNA within an RNA:DNA hybrids [188] and is specifically responsible for removing single ribonucleotides that are misincorporated into DNA during DNA replication [183]. *RNASEH2B* mutation leads to a reduction of RNASE H2 activity and, consequently, to elevated levels/aberrant accumulation of ribonucleotides into genomic DNA. It was demonstrated that RNASE H2 is able to exert its functions specifically in the G2 phase of the cell cycle [189].

The proliferation capability of untreated NSC was evaluated by means of fluorescent intracellular staining dye CFSE. The rationale in changing the type of proliferative assay from [3H]-thymidine incorporation assay to CFSE was related to some aspects such as costs and laboriousness of the methods [179]. In fact, the CFSE proliferation assay requires the staining of cells with a non-radioactive dye and a cheaper cytofluorometer analysis, whereas in the [3H]-thymidine incorporation assay, the use of radioactive material is required and therefore dedicated protocols, instruments and laboratory are needed [180]. We performed the CFSE experiments three times on AGS- and BJ-NSC; however, results of these experiments were not comparable each other showing a non-reproducible pattern of proliferation for each NSC line considered. No definitive conclusion could then be drawn. To our knowledge, CFSE analysis has never been used on stem cells to assess their proliferation, but it is routinely employed to assess patients' lymphocytes proliferation after stimulation, for diagnostics purposes [179]; additionally, this technique has been used to check the leukocytes proliferation in the presence of adult stem cells to evaluate their immunomodulatory properties [190]. Viability of NSCs was then measured by means of MTT assay after 72 hours growth in NSC culture medium and at different cell seeding density. Under these basal conditions, measured OD was comparable among NSC, including AGS2-NSC. In AGS-NSC, *RNASEH2B* deficient line did not show a slower proliferation rate compared to others and as observed in iPSC, for reasons that need to be further investigated.

AGS are inherited immunodeficiencies and affect the nervous tissue linking a degenerative pattern to an inflammatory phenotype; for this reason, initial empirical therapeutic approaches involved drugs active on the immune system. However, since the understanding of molecular pathogenic processes of the disease has advanced, the context of crucial cell mechanism-based events has become more important for therapeutic purposes, and pharmacological strategies have shifted towards more targeted approaches, including repurposing currently approved drugs in use for other diseases (i.e., JAKi and RTIs) [131, 151]. The anti-proliferative and suppressive effects of JAKi on immune cells are expected [134], whereas the efficacy and safety profiles of JAKi on patients NSC and neurons need to be better investigated. For decades, it was believed that the adult brain was a quiescent organ unable to produce new neurons but currently is well-known that new functional neurons could be generated thanks to the NSCs pool resident in neural niche [191]. The JAK/STAT signaling pathway plays a key role both in the balance between NSC quiescence and proliferation, neurogenesis versus gliogenesis lineage decisions and differentiation of NSC into mature neurons. NSC proliferation is known to be regulated by the JAK/STAT pathway [192-194], and JAK2 in particular is essential for NSC proliferation promoted by leptin receptor [192, 193]. In 1997, Bonni et al. demonstrated the involvement of JAK1 in astrocytic differentiation [195]. In embryonic cortical precursor cells, the activation of the ciliary neurotrophic factor receptor leads to the activation of JAK1, STAT1 and STAT3 triggering the differentiation into astrocytes. The differentiation of neural stem/progenitor cell into astrocytes can also be induced by microglia-derived IL-6 and leukemia inhibitory factor cytokines (named LIF) [195, 196]. Moreover, the modulation of JAK3 signaling is involved in differentiation since *knock-down* of JAK3 in neural progenitors induces their differentiation in neurons and oligodendrocytes [193]. Alongside, the JAK/STAT pathway is involved in synaptic plasticity in the brain. Nicolas et al. in 2013 have suggested the intriguing possibility of a non-nuclear role of STAT3 in synaptic plasticity [194, 197].

Recently, Yasuda et al. in 2021 have demonstrated that JAK2-STAT1 signaling in inactive axons and synapses is essential for their elimination [198]. In AGS patients, it is necessary to assess whether exposure of NSC to JAKi could be cytotoxic but also whether the treatment could interfere with the above-mentioned cellular mechanisms. Patients' neurons are not accessible, thus iPSC and derived-NSC offer an unprecedented opportunity to provide optimal patients cells surrogates, keeping the genetic background of the individuals. In a future perspective, it will be interesting to evaluate *in vitro* the impact of JAKi on neurons and macroglia generations from NSC, particularly on astrocytes. Astrocytes are the most abundant glial cells in the CNS having important homeostatic functions; they are one of the major sources of IFN in the CNS, together with microglia, and are proposed as key players in AGS pathology, becoming dysfunctional and participating in the pathogenesis [199-201].

With the exception of pacritinib, the exposure of all iPSC and NSC to JAKi did not produce a cytotoxic response. In contrast, a 3-day *in vitro* exposure of patients-derived cells to high concentration of JAKi (ruxolitinib, baricitinib, tofacitinib) leads to an increase in cell viability compared to the BJ-control lines. The increase was observed particularly in AGS7 derived models and was more pronounced in NSC compared to IPSC. The biological meaning of this finding is unclear and needs to be further investigated. First, it would be important to discriminate whether this increase was indicative of an increased number of actively dividing cells or metabolically active cells. A strong relationship between autoimmune diseases, neuroinflammation and mitochondrial dysfunctions has been reported by several authors [202-206]. It could therefore be hypothesized that in this complex interplay the use of JAKi can reduce the oxidative stress of the cell thus increasing metabolic response. In rheumatoid arthritis, tofacitinib significantly increased oxidative phosphorylation, ATP production, and the maximal respiratory capacity and the respiratory reserve in primary synovial fibroblasts, suggesting JAK/STAT signaling as a mediator of the complex interplay between inflammation and cellular metabolism [207]. Second, the exposure to high concentrations of ruxolitinib (>10  $\mu$ M), baricitinib (>2.5  $\mu$ M) and tofacitinib (>10  $\mu$ M) in the MTT assay are above the pharmacological ones. In healthy adult subjects receiving ruxolitinib 50 mg once daily, plasma concentrations are ~10 nM (FDA document number: 202192Orig1s000). Although JAKi are considered highly selective for some members of the JAK family, as the intracellular concentration of these drugs increases, a loss of selectivity is likely due to the interaction with ATP binding sites of other kinases [208]. Moreover, it is possible that in the defective genetic settings of AGS, the higher concentrations of JAKi altered the equilibrate cross-talk between the JAK/STAT signaling and other proliferative pathway, in favor of the latter.

Considering pacritinib, the significant cytotoxicity observed on iPSC and NSC suggest an unsafe use in clinics for AGS. The different cytotoxic profile of pacritinib can be attributed to its affinity for different targets such as IRAK1 and FLT3. In particular, FLT3 is a tyrosine kinase receptor expressed on the surface of multipotent stem cells (e.g.: hematopoietic stem cells), playing an important role in the survival and proliferation of these cells [209].

In addition to JAKi, also RTIs provide substantial evidence of effectiveness in AGS in patients in clinics. Using a combination of three RTIs – abacavir, lamivudine, and zidovudine – Rice and collaborators demonstrated a reduction in IFN signaling without evidence of side effects, leading to a reduction in IFN score, calculated as the median fold change of the six target ISGs [140]. In patients-derived iPSC lines, RTIs treatment did not affect AGS1-, AGS7 and BJ-iPSCs survival. AGS2-iPSCs were also not affected



to abacavir and lamivudine, but their viability significantly decreased after 3-day exposure at higher zidovudine concentrations. The reason of the increased sensitivity was thus unrelated to mRNA expression levels of *TK1* that was comparable among iPSCs. *TK1* is a key target gene involved in zidovudine activation because it converts the prodrug zidovudine into active triphosphate derivatives. The triphosphate derivatives efficiently inhibit HIV-1 reverse transcriptase by acting as a competitive inhibitor of normal nucleotides, thus being incorporated into cellular DNA and inhibiting retroviral replication [210, 211]. In addition, the triphosphates of zidovudine act also as weak inhibitors of mammalian DNA polymerases  $\alpha$ ,  $\beta$  and  $\gamma$ , which catalyze DNA replication *in vivo* [212]. Further analyses on zidovudine would be necessary to better understand the higher sensitivity of iPSC in the context of *RNASEH2B* mutation [183]. All together, the above mentioned mechanisms of zidovudine could explain the higher cytotoxic effect observed in AGS2-iPSC (the lowest proliferating iPSC) that could make these cells particularly sensitive to substances inhibiting DNA polymerases. In contrast, a trend toward a dose-dependent increase of cell viability after RTIs exposure was observed on NSC, and the decreased viability previously observed in AGS2-iPSC treated at higher zidovudine concentrations was no longer observable in AGS2-NSC. One possible explanation could be the very rapid cell cycle length of iPSC (16 -18 hours) and a very short G1 phase (~2.5 hours) [213]. Other acquired or intrinsic drug resistance mechanisms such as enhanced efflux through activation of transmembrane proteins, increased detoxification (e.g., via activation of glutathione transferases) and activation of survival pathway or cell cycle arrest could not be ruled out. Also apoptosis and autophagy process may be evaluated since NSCs undergo apoptotic cell death as an essential component of neural development [214]. All ROS production will be interesting to evaluate, comparing their production before and after JAKi treatment. Overall, based on our results we can hypothesize that RTIs could be safely administered in clinics without affecting NSC since they did not show cytotoxicity effects on these cells.

STING represents a major regulator of the innate-antiviral immune response, detecting abnormally high levels of nucleic acids and transmitting signals that activate type I IFN responses and subsequently the transcription of ISGs, resembling a congenital viral infection [215], to produce other antiviral effectors. Analysis of the ISGs in AGS patients' peripheral blood has shown, prolonged and persistently high expression of a specific subset of genes. This "interferon signature" and its readout measure, the IFN score, has been described as a marker of the biological activity of the disease and therefore used as a marker of therapeutic response.

We assessed *STING* expression levels in AGS- and BJ-derived models, comparing iPSC versus NSCs. Interestingly, *STING* was consistently more expressed in NSC compared to iPSC in patients- derived stem cells, but not in healthy donor stem cells, suggesting the hypothesis that an higher degree of differentiation shows more the functional impact of specific mutations in the cGAS-cGAMP-STING pathway. These data should be further investigated and correlated with the evaluation of IFN in the culture supernatant. Baricitinib could be useful in autoinflammatory conditions given its ability to modulate the expression of *STING* [216]. Of note, the effect of baricitinib on *STING* expression was different in AGS1-iPSC (no effect) and AGS1-NSC (increased expression) and was even opposite in AGS7-iPSC (decreased expression) and AGS7-NSC (increased expression), suggesting again a different profile in the cGAS-cGAMP-STING pathway according to the stage of differentiation.

Nowadays the procedure to obtain iPSC-derived neurons is quite long and complex, without obtaining a uniform neuronal pool for high-throughput screening. These are still the main limitations in working with iPSC-derived neurons [217]. Another limitation of these cell models regards the reproducibility between lines from the same patient considering that iPSC lines may accumulate point mutations or copy number variations in culture [218]. Therefore, it would be important to study different iPSC clones from a single patient in depth and evaluate a genome-wide expression profile and an epigenetic profile of clones. These important technical issues imply an increase in time and high costs [217]. It is important to recognize that the cytotoxic results obtained in iPSCs and NSCs may not be representative of the cytotoxic profiles of differentiated cells, due to various reasons, such as proliferation rate, cell cycle, epigenetics, relative density of drug target and enzyme expression profile [219]. However, iPSCs and NSCs carry the patient's specific genomic background and may still be informative of drug effects in the pathogenic context.

The second part of this work is based on the development of an ELISA assay based on peptide biosensors with the long-term goal of creating a point-of-care device to improve the diagnosis and clinical management of diseases caused by JAK aberrations in clinics. Our first experience in this field was related to the set up and the optimization of a novel ELISA-based peptide biosensor assay for screening the *in vitro* TK activity of ABL1 for precision therapy in leukemias, in particular in *BCR-ABL1* neoplasms and *BCR-ABL1 like* ALL of the ABL1-class. The peptide sequence used (named P<sub>ABL</sub>) was a novel artificial substrate designed to be specific for ABL1 and contains a reporter region including the tyrosine phosphorylation site, and a targeting region which increases the specificity for ABL1 [178]. The peptide-based ELISA assay is a potentially versatile and adaptable tool to any kinase of interest. To the best of our knowledge, peptide biosensors for JAK1, JAK3 and TYK2 are currently missing, whereas peptide biosensors specific for the JAK2 kinase have been already published (P<sub>JAK2-L</sub> [168] and P<sub>JAK2-S</sub> [169]), and attempts were made to optimize the ELISA assay using hematopoietic immortalized cell lines, harboring rearrangements activating JAK2 and an aberrant activation of JAK/STAT pathway. Hematopoietic immortalized cell lines were characterized to confirm the activation in the JAK/STAT pathway. MPN Philadelphia-negative cell lines HEL and SET-2 harbor the JAK2 V617F, in homozygosis and heterozygosis, respectively [220]. The point mutation in JAK2 V617F is known to result in kinase constitutive activation, being a gain-of-function mutation located in the pseudo-kinase domain of JAK2 (JH2). The JH2 domain is able to regulate the JH1 kinase domain and maintain the basal levels of JAK2 activity in the absence of cytokine stimulation, by phosphorylating two negative regulatory sites of JH1 (Ser523 and Tyr570); consequently, the mutation removes the negative regulatory capacity resulting in a constitutive phosphorylation of JAK2. The IGH/CRLF2 translocation, present in MHH-CALL-4, involves the disruption of a CpG site of *CRLF2* and of a V(D)J site in *IGH* with consequent rearrangement of the two genes; overexpression of the receptor results in activation of the JAK/STAT pathway resulting in increased cell proliferation [221]. The translocation does not determine a chimeric protein, but rather determines its homodimerization at the cell membrane level. This leads directly to the constitutive activation of the signaling pathway JAK2 / STAT5, PI3k / mTOR and SRC, again determining the stimulus to proliferation and survival [222]. However, in *BCR-ABL1 like* ALL patients with *CRLF2* rearrangement, flow cytometry analyzes were performed in the literature demonstrating the overexpression of *CRLF2* in

patients' blasts [223]. In contrast, K562 presents the *BCR-ABL1* fusion gene leading to the overactivation of the ABL1 pathway and REH cells are carriers of the *ETV6-RUNX1 (TEL-AML1)* gene fusion with no direct implication on the JAK2/STAT5 or ABL1 pathways. Our protein expression analysis reveal that the JAK/STAT pathway is activated in MHH-CALL-4, HEL and SET-2 cell lines, where the activation of STAT5 is linked to the phosphorylation of JAK2, as also highlighted by other authors [173]. The presence of phosphorylated STAT5 in K562 is explained by the activation due to BCR-ABL1 [29, 30]. It is known from the literature that the chimeric protein BCR-ABL1 can lead to a persistent activation of STAT5 directly, with interaction of BCR-ABL1 on JAK2 [29] and indirectly, with high levels of STAT5 as transcription factor in the nucleus [30]. In western blots, phosphorylation of JAK and STAT was not detectable in REH.

A greater sensitivity to JAKi was observed in SET-2 compared to HEL. The *JAK2 V617F* mutation results in an advantage in terms of survival and proliferation by altering the expression of mitogens, of antiapoptotic genes *BCL2*, *MCL1*, *BCL2L1* and of cell cycle regulatory proteins; these effects could be more pronounced in HEL (*JAK2 V617F* in homozygosity) compared to SET-2 (*JAK2 V617F* in *heterozygosity*) thus leading to greater resistance to JAK inhibitors for the HEL line [224-227].

Tofacitinib acts mainly inhibiting the kinase activity of JAK3 (IC<sub>50</sub>: 1 nM) and JAK1 (IC<sub>50</sub>: 112 nM) [228], however an inhibitory effect on the enzyme activity of the kinase was also found in the enzymatic assays on JAK2 purified protein (IC<sub>50</sub>: 20 nM) [71]. For this reason, it has been included in the panel of drugs to be tested despite the fact that the drug is not approved for the treatment of the oncohematological diseases. The sensitivity of REH to pacritinib was unexpected, being a cell line in which the JAK/STAT pathway is not hyperactive. However, pacritinib is not only an inhibitor for JAK2 but also acts as an inhibitor for FLT3 (IC<sub>50</sub><50 nM on purified protein) [229]. Tyrosine kinase-3 (FLT3) is a TK receptor expressed in hematopoietic progenitors and plays an important role in hematopoietic development by being involved in the pathogenesis of B-ALL [230]. The *FLT3 gene* is almost always wild type in lymphoblasts with the *TEL-AML1* gene fusion [231]. In particular, the REH cell line, B-ALL model with *TEL-AML1* rearrangement, expresses high levels of constitutively active FLT3 [232].

The peptide biosensor-based ELISA procedure on whole protein cell lysates was described in Montecchini, Braidotti et al. [178] and applied for the JAK2 peptide biosensors with no success: the greatest signal of phosphorylation was observed only by the P<sub>PHOSPHO-JAK2</sub> peptide, the internal control of the assay, whereas phosphorylation of candidate biosensors P<sub>JAK2-L</sub> or P<sub>JAK2-S</sub> did not exceed lysate background levels. We therefore tried to perform the ELISA assay on JAK2 kinase purified by immunoprecipitation, assuming the presence of a possible "matrix effect" that could interfere with the specificity of the signal and therefore mask the interaction of JAK2 with peptides biosensor in the whole lysates. Most matrix effects can be attributed to substances in the sample different from the analyte of interest, pH and salt concentrations, high viscosity or interaction between the protein of interest and other proteins in the sample [233]. The complexity of the "matrix effect" is acknowledged by the FDA document "Bioanalytical Method Validation" (FDA-2013-D-1020) and might have a confounding effect on the ELISA results.

Results obtained after the immunoprecipitation procedure indicate that P<sub>JAK2-L</sub> peptide is able to detect JAK2 V617F kinase activity by ELISA assay in HEL cell line. Although these results represent an advance with respect to the final goal of the project (i.e., the identification of a peptide substrate to be

used as biosensors in the ELISA assay), the introduction of protein purification is disadvantageous in practical terms, representing a complication in the execution and timing of the assay. For the final goal of creating a point of care device for TK monitoring, the introduction of an immunoprecipitation step may be less suitable with the need of a bedside device to be used routinely in hospital practice. Therefore, several attempts to optimize the conditions of the P<sub>JAK2-L</sub>-based ELISA assay in whole lysates followed, by modifying the main parameters that may influence peptide-lysate incubation steps, without success. The *in vitro* assays are an important tool for clinicians; the ability to measure JAK2 activity on patient tumor cells could be useful in guiding the choice of the best TKI to use on the patient, increasing the chance of survival and reducing the probability of exposing the patient to inadequate treatment. If the ELISA assay must be performed on the purified JAK2 protein from patients cells a careful evaluation of the basal level of JAK2 phosphorylation in the lysate should be performed. This is particularly important especially in patient's samples, where the degree of activation of the JAK/STAT pathway can also be conditioned by extracellular stimuli, such as for example by the presence of a persistent inflammatory state in the microenvironment of tumor cells [234]. Furthermore, the ELISA assay could also be proposed as a useful tool to promptly identify primary or acquired resistance to TKIs [94, 235, 236]. In fact, the major limitation of JAKi use is that chronic exposure may leads to a loss of response as observed *in vitro*, in animal models and patients [237].

Lysates used in the peptide-based ELISA assay were prepared from immortalized cell lines kept in basal conditions, i.e. in the absence of external stimuli, assuming that the JAK/STAT pathway was already activated by the genetic alterations present in these cell models, as reported in the literature and as demonstrated in part by western blots and cytotoxicity assays. However, this baseline activation may not be sufficient to allow a detectable phosphorylation of peptide biosensors. The JAK/STAT pathway could therefore be further stimulated with a targeted treatment, for example using TSLP, as a ligand of the CRLF2 membrane receptor present in all cell lines. In fact, preliminary results not shown in this thesis confirm a 25% cell growth stimulation in MHH-CALL-4 after 72 hours of treatment with 25 ng/ul of TSLP [238], not observed instead in REH (HEL and SET-2 not tested yet). After exposing the cells to different stimuli, cell lysates could then be prepared and tested again in the peptide-based ELISA assay, to see if it is possible to record an increase in the phosphorylation of the peptide linked to a greater activation of the JAK2 kinase. Finally, comparing the structure of the biosensor peptide P<sub>JAK2</sub> with that of the P<sub>ABL</sub> described in Montecchini, Braidotti et al. [178], it can be seen that P<sub>JAK2</sub> does not comprise a targeting sequence, present instead in P<sub>ABL</sub> and considered necessary to confer a greater binding specificity for the kinase of interest. The success of the P<sub>ABL</sub> has been proven in cell line model but also in lysates obtained from patient blasts [178, 239]. The proper targeting sequence for JAK2 could be searched through an accurate bioinformatics screening of the affinity sequences between JAK2 and STAT5, STAT5 being a substrate of kinase phosphorylation. These computational studies would not be sufficient by themselves to identify the ideal targeting sequence; experimental verifications would be necessary to evaluate the interaction between the new biosensor (consisting of a report sequence and a target sequence) and purified JAK2 protein with suitable techniques (for example through SPR-GCI or molecular docking).

Once these optimizations have been made, the assay may be able to detect peptide phosphorylation, and then the use of JAKi within the peptide-based ELISA assay will help us evaluate the specificity of

the result obtained. Furthermore, in order to be able to consider the bioanalytical assay valid and make it useful in the clinic, it will be necessary to validate the method according to the guidelines of the EMA (EMA/CHMP/ICH/172948/2019) in terms of sensitivity and accuracy, hoping that it can be integrated with the diagnostic methods currently in use to allow a more personalized therapy. On the basis of the acquired knowledge, it will then be possible to explore different peptide biosensor to detect the aberrant kinase activity of other JAK kinases.

## ***7 - CONCLUSION***

---

Both aspects proposed in my thesis work represent a step forward to a personalized approach for JAK kinase-mediated diseases.

The first part of the project highlights the importance in basic and clinical research of creating patient-specific disease models to better understand inherited syndromes and to deepen our knowledge on innovative therapeutic approaches. We used patient-specific iPSCs as model for AGS, obtained by reprogramming patients' primary cells and differentiated into NSCs. The *in vitro* model established has proven to be suitable for studying and investigating the safety profile of JAKi and RTIs on NSC, otherwise not available. As future prospective, it may be interesting to broaden the panel of drug tested on NSC and complete the efficacy and safety studies of all drugs used to treat AGS in clinics also in NSC-derived neuronal cells. In addition, given the involvement in AGS also of the immune component, it might be interesting to analyze the effects of these novel drugs also in NSC-derived neuronal co-cultured with cells of the immune system.

The second part of the project wants to underline the importance of measuring the activation of a single JAK kinase in the patient's cell to allow the choice of the most suitable inhibitor to use and provide important data for predicting clinical response. To date, there are no tools that can be useful in the laboratory routine to measure the activation of signaling pathways linked to specific activated kinases. Approaches based on biosensor peptides may offer a valid method for TK activity monitoring not only as a marker of disease progression, but also as a system for select patient-specific enzyme inhibitor drugs. The development of a point-of-care device, based on peptide biosensors-based ELISA assays, may improve the diagnosis and clinical management of TK-driven diseases, and will be useful both for the diagnosis and for the clinical monitoring, but also guiding the doctor to the choice of the best JAKi and monitor the clinical response. By identifying the best TKI to be used in treatment, the chances of survival for these patients would be optimized and the chances of developing severe toxicities linked to exposure to high doses of inadequate drugs would also be reduced. As proposed, the P<sub>JAK-L</sub>-based ELISA assay is not suitable for measuring JAK2 aberrant activity in whole cell lysates; however, results of this thesis suggest that P<sub>JAK-L</sub> is a promising peptide biosensor for JAK2 and that further optimization steps, such the introduction of targeting region to the peptide sequence, might be required.

## **8 - REFERENCES**

---



1. Fabbro, D., S.W. Cowan-Jacob, and H. Moebitz, *Ten things you should know about protein kinases: IUPHAR Review 14*. British Journal of Pharmacology, 2015. **172**(11): p. 2675-2700.
2. Hubbard, S.R. and J.H. Till, *Protein Tyrosine Kinase Structure and Function*. Annual Review of Biochemistry, 2000. **69**(1): p. 373-398.
3. Jiao, Q., et al., *Advances in studies of tyrosine kinase inhibitors and their acquired resistance*. Molecular Cancer, 2018. **17**(1): p. 36.
4. Seavey, M.M. and P. Dobrzanski, *The many faces of Janus kinase*. Biochemical Pharmacology, 2012. **83**(9): p. 1136-1145.
5. Wilks, A.F., et al., *Two novel protein-tyrosine kinases, each with a second phosphotransferase-related catalytic domain, define a new class of protein kinase*. Molecular and Cellular Biology, 1991. **11**(4): p. 2057-2065.
6. Riedy, M.C., et al., *Genomic Sequence, Organization, and Chromosomal Localization of Human JAK3*. Genomics, 1996. **37**(1): p. 57-61.
7. Firmbach-Kraft, I., et al., *tyk2, prototype of a novel class of non-receptor tyrosine kinase genes*. Oncogene, 1990. **5**(9): p. 1329-1336.
8. Yamaoka, K., et al., *The Janus kinases (Jaks)*. Genome biology, 2004. **5**(12): p. 253-253.
9. Liongue, C. and A.C. Ward, *Evolution of the JAK-STAT pathway*. JAK-STAT, 2013. **2**(1): p. e22756-e22756.
10. Alicea-Velázquez, N.L. and T.J. Boggon, *The use of structural biology in Janus kinase targeted drug discovery*. Current drug targets, 2011. **12**(4): p. 546-555.
11. Ungureanu, D., et al., *The pseudokinase domain of JAK2 is a dual-specificity protein kinase that negatively regulates cytokine signaling*. Nature structural & molecular biology, 2011. **18**(9): p. 971-976.
12. Bousoik, E. and H. Montazeri Aliabadi, *"Do We Know Jack" About JAK? A Closer Look at JAK/STAT Signaling Pathway*. Frontiers in oncology, 2018. **8**: p. 287-287.
13. Heim, M.H., *The STAT Protein Family*, in *Signal Transducers and Activators of Transcription (STATs): Activation and Biology*, P.B. Sehgal, D.E. Levy, and T. Hirano, Editors. 2003, Springer Netherlands: Dordrecht. p. 11-26.
14. Banerjee, S., et al., *JAK-STAT Signaling as a Target for Inflammatory and Autoimmune Diseases: Current and Future Prospects*. Drugs, 2017. **77**(5): p. 521-546.
15. Springuel, L., J.-C. Renaud, and L. Knoops, *JAK kinase targeting in hematologic malignancies: a sinuous pathway from identification of genetic alterations towards clinical indications*. Haematologica, 2015. **100**(10): p. 1240-1253.
16. Xin, P., et al., *The role of JAK/STAT signaling pathway and its inhibitors in diseases*. International Immunopharmacology, 2020. **80**: p. 106210.
17. Neubauer, H., et al., *Jak2 Deficiency Defines an Essential Developmental Checkpoint in Definitive Hematopoiesis*. Cell, 1998. **93**(3): p. 397-409.
18. Rawlings, J.S., K.M. Rosler, and D.A. Harrison, *The JAK/STAT signaling pathway*. Journal of Cell Science, 2004. **117**(8): p. 1281-1283.
19. Harrison, D.A., *The Jak/STAT pathway*. Cold Spring Harbor perspectives in biology, 2012. **4**(3): p. a011205.

20. Shuai, K. and B. Liu, *Regulation of JAK–STAT signalling in the immune system*. Nature Reviews Immunology, 2003. **3**(11): p. 900-911.
21. Robertson Scott, A., et al., *Regulation of Jak2 Function by Phosphorylation of Tyr317 and Tyr637 during Cytokine Signaling*. Molecular and Cellular Biology, 2009. **29**(12): p. 3367-3378.
22. Feng, J., et al., *Activation of Jak2 catalytic activity requires phosphorylation of Y1007 in the kinase activation loop*. Molecular and Cellular Biology, 1997. **17**(5): p. 2497-2501.
23. Hu, X., et al., *The JAK/STAT signaling pathway: from bench to clinic*. Signal Transduction and Targeted Therapy, 2021. **6**(1): p. 402.
24. Levine, R.L., et al., *Role of JAK2 in the pathogenesis and therapy of myeloproliferative disorders*. Nature Reviews Cancer, 2007. **7**(9): p. 673-683.
25. Birzniece, V., A. Sata, and K.K.Y. Ho, *Growth hormone receptor modulators*. Reviews in Endocrine and Metabolic Disorders, 2008. **10**(2): p. 145.
26. Chiba, T., M. Yamada, and S. Aiso, *Targeting the JAK2/STAT3 axis in Alzheimer's disease*. Expert Opinion on Therapeutic Targets, 2009. **13**(10): p. 1155-1167.
27. Jin, S., et al., *Non-canonical Notch signaling activates IL-6/JAK/STAT signaling in breast tumor cells and is controlled by p53 and IKK $\alpha$ /IKK $\beta$* . Oncogene, 2013. **32**(41): p. 4892-4902.
28. Fan, Y., R. Mao, and J. Yang, *NF- $\kappa$ B and STAT3 signaling pathways collaboratively link inflammation to cancer*. Protein & Cell, 2013. **4**(3): p. 176-185.
29. Recio, C., et al., *Signal transducer and activator of transcription (STAT)-5: an opportunity for drug development in oncohematology*. Oncogene, 2019. **38**(24): p. 4657-4668.
30. Wingelhofer, B., et al., *Implications of STAT3 and STAT5 signaling on gene regulation and chromatin remodeling in hematopoietic cancer*. Leukemia, 2018. **32**(8): p. 1713-1726.
31. Coppo, P., et al., *BCR–ABL activates STAT3 via JAK and MEK pathways in human cells*. British Journal of Haematology, 2006. **134**(2): p. 171-179.
32. Ferguson, F.M. and N.S. Gray, *Kinase inhibitors: the road ahead*. Nature Reviews Drug Discovery, 2018. **17**(5): p. 353-377.
33. Jamilloux, Y., et al., *JAK inhibitors for the treatment of autoimmune and inflammatory diseases*. Autoimmunity Reviews, 2019. **18**(11): p. 102390.
34. Ciobanu, D.A., et al., *JAK/STAT pathway in pathology of rheumatoid arthritis (Review)*. Exp Ther Med, 2020. **20**(4): p. 3498-3503.
35. Kvist-Hansen, A., P.R. Hansen, and L. Skov, *Systemic Treatment of Psoriasis with JAK Inhibitors: A Review*. Dermatology and Therapy, 2020. **10**(1): p. 29-42.
36. Bao, L., H. Zhang, and L.S. Chan, *The involvement of the JAK-STAT signaling pathway in chronic inflammatory skin disease atopic dermatitis*. JAK-STAT, 2013. **2**(3): p. e24137-e24137.
37. Salas, A., et al., *JAK–STAT pathway targeting for the treatment of inflammatory bowel disease*. Nature Reviews Gastroenterology & Hepatology, 2020. **17**(6): p. 323-337.
38. Malemud, J.C. and E. Pearlman, *Targeting JAK/STAT Signaling Pathway in Inflammatory Diseases*. Current Signal Transduction Therapy, 2009. **4**(3): p. 201-221.
39. Huang, F., et al., *Requirement for Both JAK-Mediated PI3K Signaling and ACT1/TRAF6/TAK1-Dependent NF- $\kappa$ B Activation by IL-17A in Enhancing Cytokine Expression in Human Airway Epithelial Cells*. The Journal of Immunology, 2007. **179**(10): p. 6504-6513.

40. Amatya, N., A.V. Garg, and S.L. Gaffen, *IL-17 Signaling: The Yin and the Yang*. Trends in Immunology, 2017. **38**(5): p. 310-322.
41. Majoros, A., et al., *Canonical and Non-Canonical Aspects of JAK–STAT Signaling: Lessons from Interferons for Cytokine Responses*. Frontiers in Immunology, 2017. **8**.
42. Sonnenfeld, G. and T.C. Merigan, *The role of interferon in viral infections*. Springer Seminars in Immunopathology, 1979. **2**(3): p. 311-338.
43. Ezeonwumelu, I.J., E. Garcia-Vidal, and E. Ballana *JAK-STAT Pathway: A Novel Target to Tackle Viral Infections*. Viruses, 2021. **13**.
44. Yang, E. and M.M.H. Li, *All About the RNA: Interferon-Stimulated Genes That Interfere With Viral RNA Processes*. Frontiers in Immunology, 2020. **11**.
45. Ben Haim, L., et al., *The JAK/STAT3 Pathway Is a Common Inducer of Astrocyte Reactivity in Alzheimer's and Huntington's Diseases*. The Journal of Neuroscience, 2015. **35**(6): p. 2817.
46. Qin, H., et al., *Inhibition of the JAK/STAT Pathway Protects Against  $\alpha$ -Synuclein-Induced Neuroinflammation and Dopaminergic Neurodegeneration*. The Journal of Neuroscience, 2016. **36**(18): p. 5144.
47. Benveniste, E.N., et al., *Involvement of the Janus Kinase/Signal Transducer and Activator of Transcription Signaling Pathway in Multiple Sclerosis and the Animal Model of Experimental Autoimmune Encephalomyelitis*. Journal of Interferon & Cytokine Research, 2014. **34**(8): p. 577-588.
48. Lashgari, N.-A., et al., *The involvement of JAK/STAT signaling pathway in the treatment of Parkinson's disease*. Journal of Neuroimmunology, 2021. **361**.
49. Jain, M., et al., *Role of JAK/STAT in the Neuroinflammation and its Association with Neurological Disorders*. Annals of neurosciences, 2021. **28**(3-4): p. 191-200.
50. Vainchenker, W., A. Dusa, and S.N. Constantinescu, *JAKs in pathology: Role of Janus kinases in hematopoietic malignancies and immunodeficiencies*. Seminars in Cell & Developmental Biology, 2008. **19**(4): p. 385-393.
51. Tefferi, A. and T. Barbui, *Polycythemia vera and essential thrombocythemia: 2021 update on diagnosis, risk-stratification and management*. American Journal of Hematology, 2020. **95**(12): p. 1599-1613.
52. Rumi, E., et al., *Clinical effect of driver mutations of JAK2, CALR, or MPL in primary myelofibrosis*. Blood, 2014. **124**(7): p. 1062-1069.
53. Luo, W. and Z. Yu, *Calreticulin (CALR) mutation in myeloproliferative neoplasms (MPNs)*. Stem cell investigation, 2015. **2**: p. 16-16.
54. Guglielmelli, P. and L. Calabresi, *Chapter Five - The MPL mutation*, in *International Review of Cell and Molecular Biology*, N. Bartalucci and L. Galluzzi, Editors. 2021, Academic Press. p. 163-178.
55. Bader, M.S. and S.C. Meyer, *JAK2 in Myeloproliferative Neoplasms: Still a Protagonist*. Pharmaceuticals (Basel, Switzerland), 2022. **15**(2): p. 160.
56. Shiraz, P., K.J. Payne, and L. Muffly, *The Current Genomic and Molecular Landscape of Philadelphia-like Acute Lymphoblastic Leukemia*. Int J Mol Sci, 2020. **21**(6).
57. Den Boer, M.L., et al., *A subtype of childhood acute lymphoblastic leukaemia with poor treatment outcome: a genome-wide classification study*. Lancet Oncol, 2009. **10**(2): p. 125-34.

58. Bernt, K.M. and S.P. Hunger, *Current concepts in pediatric Philadelphia chromosome-positive acute lymphoblastic leukemia*. *Front Oncol*, 2014. **4**: p. 54.
59. Jain, S. and A. Abraham, *BCR-ABL1-like B-Acute Lymphoblastic Leukemia/Lymphoma: A Comprehensive Review*. *Archives of Pathology & Laboratory Medicine*, 2019. **144**(2): p. 150-155.
60. Jain, N., et al., *Ph-like acute lymphoblastic leukemia: a high-risk subtype in adults*. *Blood*, 2017. **129**(5): p. 572-581.
61. Kotsovilis, S. and E. Andreakos, *Therapeutic Human Monoclonal Antibodies in Inflammatory Diseases*, in *Human Monoclonal Antibodies: Methods and Protocols*, M. Steinitz, Editor. 2014, Humana Press: Totowa, NJ. p. 37-59.
62. Perdriger, A., *Infliximab in the treatment of rheumatoid arthritis*. *Biologics : targets & therapy*, 2009. **3**: p. 183-191.
63. Leman, J. and A. Burden, *Treatment of severe psoriasis with infliximab*. *Therapeutics and clinical risk management*, 2008. **4**(6): p. 1165-1176.
64. Papamichael, K., et al., *Infliximab in inflammatory bowel disease*. *Therapeutic advances in chronic disease*, 2019. **10**: p. 2040622319838443-2040622319838443.
65. Spinelli, F.R., et al., *JAK inhibitors: Ten years after*. *European Journal of Immunology*, 2021. **51**(7): p. 1615-1627.
66. Sung, Y.-K. and Y.H. Lee, *Comparative effectiveness and safety of non-tumour necrosis factor biologics and Janus kinase inhibitors in patients with active rheumatoid arthritis showing insufficient response to tumour necrosis factor inhibitors: A Bayesian network meta-analysis of randomized controlled trials*. *Journal of Clinical Pharmacy and Therapeutics*, 2021. **46**(4): p. 984-992.
67. O'Shea, J.J., et al., *The JAK-STAT pathway: impact on human disease and therapeutic intervention*. *Annual review of medicine*, 2015. **66**: p. 311-328.
68. Bechman, K., M. Yates, and J.B. Galloway, *The new entries in the therapeutic armamentarium: The small molecule JAK inhibitors*. *Pharmacological Research*, 2019. **147**: p. 104392.
69. Quintas-Cardama, A., et al., *Preclinical characterization of the selective JAK1/2 inhibitor INCB018424: therapeutic implications for the treatment of myeloproliferative neoplasms*. *Blood*, 2010. **115**(15): p. 3109-17.
70. Fridman, J.S., et al., *Selective Inhibition of JAK1 and JAK2 Is Efficacious in Rodent Models of Arthritis: Preclinical Characterization of INCB028050*. *The Journal of Immunology*, 2010. **184**(9): p. 5298.
71. Changelian Paul, S., et al., *Prevention of Organ Allograft Rejection by a Specific Janus Kinase 3 Inhibitor*. *Science*, 2003. **302**(5646): p. 875-878.
72. Hart, S., et al., *SB1518, a novel macrocyclic pyrimidine-based JAK2 inhibitor for the treatment of myeloid and lymphoid malignancies*. *Leukemia*, 2011. **25**(11): p. 1751-1759.
73. Tefferi, A., *Myeloproliferative neoplasms: A decade of discoveries and treatment advances*. *American Journal of Hematology*, 2016. **91**(1): p. 50-58.
74. Meyer, S.C. and R.L. Levine, *Molecular pathways: molecular basis for sensitivity and resistance to JAK kinase inhibitors*. *Clinical cancer research : an official journal of the American Association for Cancer Research*, 2014. **20**(8): p. 2051-2059.
75. Aschenbrenner, D.S., *New Indication for Ruxolitinib*. *AJN The American Journal of Nursing*, 2022. **122**(1).

76. Markham, A., *Baricitinib: First Global Approval*. *Drugs*, 2017. **77**(6): p. 697-704.
77. Radi, G., et al., *Baricitinib: The First Jak Inhibitor Approved in Europe for the Treatment of Moderate to Severe Atopic Dermatitis in Adult Patients*. *Healthcare (Basel, Switzerland)*, 2021. **9**(11): p. 1575.
78. Ali, E., et al., *Olumiant (Baricitinib) oral tablets: An insight into FDA-approved systemic treatment for Alopecia Areata*. *Annals of medicine and surgery (2012)*, 2022. **80**: p. 104157-104157.
79. Vainchenker, W., et al., *JAK inhibitors for the treatment of myeloproliferative neoplasms and other disorders*. *F1000Research*, 2018. **7**: p. 82-82.
80. Dörner, T., et al., *Baricitinib decreases anti-dsDNA in patients with systemic lupus erythematosus: results from a phase II double-blind, randomized, placebo-controlled trial*. *Arthritis research & therapy*, 2022. **24**(1): p. 112-112.
81. Dörner, T., et al., *Mechanism of action of baricitinib and identification of biomarkers and key immune pathways in patients with active systemic lupus erythematosus*. *Annals of the Rheumatic Diseases*, 2022. **81**(9): p. 1267.
82. Wijaya, I., et al., *The use of Janus Kinase inhibitors in hospitalized patients with COVID-19: Systematic review and meta-analysis*. *Clinical epidemiology and global health*, 2021. **11**: p. 100755-100755.
83. Chen, C.-x., et al., *JAK-inhibitors for coronavirus disease-2019 (COVID-19): a meta-analysis*. *Leukemia*, 2021. **35**(9): p. 2616-2620.
84. Levy, G., et al., *JAK inhibitors and COVID-19*. *Journal for immunotherapy of cancer*, 2022. **10**(4): p. e002838.
85. Zhang, X., et al., *The Efficacy and Safety of Janus Kinase Inhibitors for Patients With COVID-19: A Living Systematic Review and Meta-Analysis*. *Frontiers in medicine*, 2022. **8**: p. 800492-800492.
86. Richardson, P., et al., *Baricitinib as potential treatment for 2019-nCoV acute respiratory disease*. *Lancet (London, England)*, 2020. **395**(10223): p. e30-e31.
87. Praveen, D., R.C. Puvvada, and V.A. M., *Janus kinase inhibitor baricitinib is not an ideal option for management of COVID-19*. *International Journal of Antimicrobial Agents*, 2020. **55**(5): p. 105967.
88. Seif, F., et al., *JAK Inhibition as a New Treatment Strategy for Patients with COVID-19*. *International archives of allergy and immunology*, 2020. **181**(6): p. 467-475.
89. Ogdie, A., et al., *Efficacy of tofacitinib in reducing pain in patients with rheumatoid arthritis, psoriatic arthritis or ankylosing spondylitis*. *RMD Open*, 2020. **6**(1): p. e001042.
90. Ruperto, N., et al., *Tofacitinib in juvenile idiopathic arthritis: a double-blind, placebo-controlled, withdrawal phase 3 randomised trial*. *The Lancet*, 2021. **398**(10315): p. 1984-1996.
91. Sedano, R., et al., *Janus Kinase Inhibitors for the Management of Patients With Inflammatory Bowel Disease*. *Gastroenterology & hepatology*, 2022. **18**(1): p. 14-27.
92. Yang, E.G., et al., *Design and Synthesis of Janus Kinase 2 (JAK2) and Histone Deacetylase (HDAC) Bispecific Inhibitors Based on Pacritinib and Evidence of Dual Pathway Inhibition in Hematological Cell Lines*. *Journal of Medicinal Chemistry*, 2016. **59**(18): p. 8233-8262.
93. Lamb, Y.N., *Pacritinib: First Approval*. *Drugs*, 2022. **82**(7): p. 831-838.

94. Patel, A.A. and O. Odenike, *The Next Generation of JAK Inhibitors: an Update on Fedratinib, Momelotonib, and Pacritinib*. Current Hematologic Malignancy Reports, 2020. **15**(6): p. 409-418.
95. Ghoreschi, K. and M. Gadina, *Jakpot! New small molecules in autoimmune and inflammatory diseases*. Experimental dermatology, 2014. **23**(1): p. 7-11.
96. Clark, J.D., M.E. Flanagan, and J.-B. Telliez, *Discovery and Development of Janus Kinase (JAK) Inhibitors for Inflammatory Diseases*. Journal of Medicinal Chemistry, 2014. **57**(12): p. 5023-5038.
97. Kothur, K., et al., *An open-label trial of JAK 1/2 blockade in progressive IFIH1-associated neuroinflammation*. Neurology, 2018. **90**(6): p. 289.
98. Leroy, E. and S.N. Constantinescu, *Rethinking JAK2 inhibition: towards novel strategies of more specific and versatile janus kinase inhibition*. Leukemia, 2017. **31**(5): p. 1023-1038.
99. Trivedi, P.M., et al., *Repurposed JAK1/JAK2 Inhibitor Reverses Established Autoimmune Insulinitis in NOD Mice*. Diabetes, 2017. **66**(6): p. 1650-1660.
100. Sanchez, G.A.M., et al., *JAK1/2 inhibition with baricitinib in the treatment of autoinflammatory interferonopathies*. The Journal of clinical investigation, 2018. **128**(7): p. 3041-3052.
101. Cohen, P., D. Cross, and P.A. Jänne, *Kinase drug discovery 20 years after imatinib: progress and future directions*. Nature Reviews Drug Discovery, 2021. **20**(7): p. 551-569.
102. Hoffman, H.M. and L. Broderick, *JAK inhibitors in autoinflammation*. The Journal of clinical investigation, 2018. **128**(7): p. 2760-2762.
103. Tasian, S.K., et al., *Potent efficacy of combined PI3K/mTOR and JAK or ABL inhibition in murine xenograft models of Ph-like acute lymphoblastic leukemia*. Blood, 2017. **129**(2): p. 177-187.
104. Maese, L., S.K. Tasian, and E.A. Raetz, *How is the Ph-like signature being incorporated into ALL therapy?* Best Practice & Research Clinical Haematology, 2017. **30**(3): p. 222-228.
105. Cario, G., et al., *BCR-ABL1-like acute lymphoblastic leukemia in childhood and targeted therapy*. Haematologica, 2020. **105**(9): p. 2200-2204.
106. Hoisnard, L., et al., *Adverse events associated with JAK inhibitors in 126,815 reports from the WHO pharmacovigilance database*. Scientific Reports, 2022. **12**(1): p. 7140.
107. Xie, F., et al., *Brief Report: Risk of Gastrointestinal Perforation Among Rheumatoid Arthritis Patients Receiving Tofacitinib, Tocilizumab, or Other Biologic Treatments*. Arthritis & rheumatology (Hoboken, N.J.), 2016. **68**(11): p. 2612-2617.
108. Navarro, E.P., et al., *Tofacitinib and Risk of Peripheral Neuropathy? Experience of 2 Cases in Patients With Rheumatoid Arthritis*. JCR: Journal of Clinical Rheumatology, 2021. **27**(2).
109. Duenas-Perez, A.B. and A.J. Mead, *Clinical potential of pacritinib in the treatment of myelofibrosis*. Therapeutic Advances in Hematology, 2015. **6**(4): p. 186-201.
110. Mascarenhas, J., et al., *Pacritinib vs Best Available Therapy, Including Ruxolitinib, in Patients With Myelofibrosis: A Randomized Clinical Trial*. JAMA Oncology, 2018. **4**(5): p. 652-659.
111. Crow, Y.J., et al., *Cree encephalitis is allelic with Aicardi-Goutières syndrome: implications for the pathogenesis of disorders of interferon alpha metabolism*. Journal of Medical Genetics, 2003. **40**(3): p. 183.
112. Crow, Y.J., *Type I interferonopathies: a novel set of inborn errors of immunity*. Annals of the New York Academy of Sciences, 2011. **1238**(1): p. 91-98.

113. Picard, C., et al., *International Union of Immunological Societies: 2017 Primary Immunodeficiency Diseases Committee Report on Inborn Errors of Immunity*. Journal of clinical immunology, 2018. **38**(1): p. 96-128.
114. Landrieu, P., J. Baets, and P. De Jonghe, *Chapter 146 - Hereditary motor-sensory, motor, and sensory neuropathies in childhood*, in *Handbook of Clinical Neurology*, O. Dulac, M. Lasseonde, and H.B. Sarnat, Editors. 2013, Elsevier. p. 1413-1432.
115. Aicardi, J. and F. Goutières, *A Progressive familial encephalopathy in infancy with calcifications of the basal ganglia and chronic cerebrospinal fluid lymphocytosis*. Annals of Neurology, 1984. **15**(1): p. 49-54.
116. Lebon, P., et al., *Intrathecal synthesis of interferon-alpha in infants with progressive familial encephalopathy*. Journal of the Neurological Sciences, 1988. **84**(2): p. 201-208.
117. Al Mutairi, F., et al., *Phenotypic and Molecular Spectrum of Aicardi-Goutières Syndrome: A Study of 24 Patients*. Pediatric Neurology, 2018. **78**: p. 35-40.
118. Vanderver, A., et al., *Early-Onset Aicardi-Goutières Syndrome: Magnetic Resonance Imaging (MRI) Pattern Recognition*. Journal of child neurology, 2015. **30**(10): p. 1343-1348.
119. Pulliero, A., et al., *Inhibition of the de-myelinating properties of Aicardi-Goutières Syndrome lymphocytes by cathepsin D silencing*. Biochemical and Biophysical Research Communications, 2013. **430**(3): p. 957-962.
120. La Piana, R., et al., *Neuroradiologic patterns and novel imaging findings in Aicardi-Goutières syndrome*. Neurology, 2016. **86**(1): p. 28-35.
121. Rice, G.I., et al., *Assessment of interferon-related biomarkers in Aicardi-Goutières syndrome associated with mutations in TREX1, RNASEH2A, RNASEH2B, RNASEH2C, SAMHD1, and ADAR: a case-control study*. The Lancet. Neurology, 2013. **12**(12): p. 1159-1169.
122. Aso, H., et al., *Comparative Description of the Expression Profile of Interferon-Stimulated Genes in Multiple Cell Lineages Targeted by HIV-1 Infection*. Frontiers in microbiology, 2019. **10**: p. 429-429.
123. Livingston, J.H. and Y.J. Crow, *Neurologic Phenotypes Associated with Mutations in TREX1, RNASEH2A, RNASEH2B, RNASEH2C, SAMHD1, ADAR1, and IFIH1: Aicardi-Goutières Syndrome and Beyond*. Neuropediatrics, 2016. **47**(06): p. 355-360.
124. Crow, Y.J., et al., *Characterization of human disease phenotypes associated with mutations in TREX1, RNASEH2A, RNASEH2B, RNASEH2C, SAMHD1, ADAR, and IFIH1*. American Journal of Medical Genetics Part A, 2015. **167**(2): p. 296-312.
125. Uggenti, C., et al., *cGAS-mediated induction of type I interferon due to inborn errors of histone pre-mRNA processing*. Nature Genetics, 2020. **52**(12): p. 1364-1372.
126. Sun, L., et al., *Cyclic GMP-AMP Synthase Is a Cytosolic DNA Sensor That Activates the Type I Interferon Pathway*. Science, 2013. **339**(6121): p. 786-791.
127. Michalska, A., et al., *A Positive Feedback Amplifier Circuit That Regulates Interferon (IFN)-Stimulated Gene Expression and Controls Type I and Type II IFN Responses*. Frontiers in Immunology, 2018. **9**.
128. Schneider, W.M., M.D. Chevillotte, and C.M. Rice, *Interferon-stimulated genes: a complex web of host defenses*. Annual review of immunology, 2014. **32**: p. 513-545.
129. Fryer, A.L., et al., *The Complexity of the cGAS-STING Pathway in CNS Pathologies*. Frontiers in neuroscience, 2021. **15**: p. 621501-621501.

130. Volpi, S., et al., *Type I interferonopathies in pediatric rheumatology*. *Pediatric Rheumatology*, 2016. **14**(1): p. 35.
131. Crow, Y.J., J. Shetty, and J.H. Livingston, *Treatments in Aicardi–Goutières syndrome*. *Developmental Medicine & Child Neurology*, 2020. **62**(1): p. 42-47.
132. Crow, M.K., *Introduction Type I Interferon and Autoimmune Disease*. *Autoimmunity*, 2003. **36**(8): p. 445-446.
133. Crow, Y.J., et al., *Therapies in Aicardi–Goutières syndrome*. *Clinical and Experimental Immunology*, 2014. **175**(1): p. 1-8.
134. Tonduti, D., et al., *Novel and emerging treatments for Aicardi-Goutières syndrome*. *Expert Review of Clinical Immunology*, 2020. **16**(2): p. 189-198.
135. Iro, M.A., et al., *Intravenous immunoglobulin for the treatment of childhood encephalitis*. *The Cochrane database of systematic reviews*, 2017. **10**(10): p. CD011367-CD011367.
136. Vanderver, A., et al., *Janus Kinase Inhibition in the Aicardi-Goutières Syndrome*. *The New England journal of medicine*, 2020. **383**(10): p. 986-989.
137. Tüngler, V., et al., *Response to: 'JAK inhibition in STING-associated interferonopathy' by Crow et al*. *Annals of the Rheumatic Diseases*, 2016. **75**(12): p. e76.
138. Cattalini, M., et al., *Case Report: The JAK-Inhibitor Ruxolitinib Use in Aicardi-Goutieres Syndrome Due to ADAR1 Mutation*. *Frontiers in pediatrics*, 2021. **9**: p. 725868-725868.
139. Meesilpavikkai, K., et al., *Efficacy of Baricitinib in the Treatment of Chilblains Associated With Aicardi-Goutières Syndrome, a Type I Interferonopathy*. *Arthritis & Rheumatology*, 2019. **71**(5): p. 829-831.
140. Rice, G.I., et al., *Reverse-Transcriptase Inhibitors in the Aicardi–Goutières Syndrome*. *New England Journal of Medicine*, 2018. **379**(23): p. 2275-2277.
141. An, J., et al., *Antimalarial Drugs as Immune Modulators: New Mechanisms for Old Drugs*. *Annual Review of Medicine*, 2017. **68**(1): p. 317-330.
142. Dai, J., et al., *Acetylation Blocks cGAS Activity and Inhibits Self-DNA-Induced Autoimmunity*. *Cell*, 2019. **176**(6): p. 1447-1460.e14.
143. Sayed, N., C. Liu, and J.C. Wu, *Translation of Human-Induced Pluripotent Stem Cells: From Clinical Trial in a Dish to Precision Medicine*. *Journal of the American College of Cardiology*, 2016. **67**(18): p. 2161-2176.
144. Genova, E., et al., *Induced pluripotent stem cells for therapy personalization in pediatric patients: Focus on drug-induced adverse events*. *World journal of stem cells*, 2019. **11**(12): p. 1020-1044.
145. Takahashi, K. and S. Yamanaka, *Induction of Pluripotent Stem Cells from Mouse Embryonic and Adult Fibroblast Cultures by Defined Factors*. *Cell*, 2006. **126**(4): p. 663-676.
146. Fusaki, N., et al., *Efficient induction of transgene-free human pluripotent stem cells using a vector based on Sendai virus, an RNA virus that does not integrate into the host genome*. *Proceedings of the Japan Academy, Series B*, 2009. **85**(8): p. 348-362.
147. Pane, L.S., I. My, and A. Moretti, *Induced Pluripotent Stem Cells in Regenerative Medicine*, in *Regenerative Medicine - from Protocol to Patient: 2. Stem Cell Science and Technology*, G. Steinhoff, Editor. 2016, Springer International Publishing: Cham. p. 51-75.
148. Han, L., J. Mich-Basso, and B. Kühn, *Generation of Human Induced Pluripotent Stem Cells and Differentiation into Cardiomyocytes*, in *Cardiac Regeneration: Methods and Protocols*, K.D. Poss and B. Kühn, Editors. 2021, Springer US: New York, NY. p. 125-139.



149. Ishikawa, K.-I., R. Nonaka, and W. Akamatsu, *Differentiation of Midbrain Dopaminergic Neurons from Human iPS Cells*, in *Experimental Models of Parkinson's Disease*, Y. Imai, Editor. 2021, Springer US: New York, NY. p. 73-80.
150. Koch, P.J., et al., *Differentiation of Human Induced Pluripotent Stem Cells into Keratinocytes*. *Current Protocols*, 2022. **2**(4): p. e408.
151. Genova, E., et al., *Biomarkers and Precision Therapy for Primary Immunodeficiencies: An In Vitro Study Based on Induced Pluripotent Stem Cells From Patients*. *Clinical Pharmacology & Therapeutics*, 2020. **108**(2): p. 358-367.
152. Hanna, J., et al., *Treatment of Sickle Cell Anemia Mouse Model with iPS Cells Generated from Autologous Skin*. *Science*, 2007. **318**(5858): p. 1920-1923.
153. Xu, D., et al., *Phenotypic correction of murine hemophilia A using an iPS cell-based therapy*. *Proceedings of the National Academy of Sciences*, 2009. **106**(3): p. 808-813.
154. Dimos, J.T., et al., *Induced Pluripotent Stem Cells Generated from Patients with ALS Can Be Differentiated into Motor Neurons*. *Science*, 2008. **321**(5893): p. 1218-1221.
155. Takahashi, J., *iPS cell-based therapy for Parkinson's disease: A Kyoto trial*. *Regenerative Therapy*, 2020. **13**: p. 18-22.
156. Thomas, C.A., et al., *Modeling of TREX1-Dependent Autoimmune Disease using Human Stem Cells Highlights L1 Accumulation as a Source of Neuroinflammation*. *Cell Stem Cell*, 2017. **21**(3): p. 319-331.e8.
157. Gray, E.E., et al., *Cutting Edge: cGAS Is Required for Lethal Autoimmune Disease in the Trex1-Deficient Mouse Model of Aicardi-Goutières Syndrome*. *The Journal of Immunology*, 2015. **195**(5): p. 1939.
158. Prince, H.E., *Biomarkers for diagnosing and monitoring autoimmune diseases*. *Biomarkers*, 2005. **10**(sup1): p. 44-49.
159. Casnellie, J.E. and E.G. Krebs, *The use of synthetic peptides for defining the specificity of tyrosine protein kinases*. *Advances in Enzyme Regulation*, 1984. **22**: p. 501-515.
160. Diks, S.H., et al., *Kinome Profiling for Studying Lipopolysaccharide Signal Transduction in Human Peripheral Blood Mononuclear Cells*. *Journal of Biological Chemistry*, 2004. **279**(47): p. 49206-49213.
161. Davis, M.I., D.S. Auld, and J. Inglese, *Bioluminescence Methods for Assaying Kinases in Quantitative High-Throughput Screening (qHTS) Format Applied to Yes1 Tyrosine Kinase, Glucokinase, and PI5P4K $\alpha$  Lipid Kinase*. *Methods in molecular biology (Clifton, N.J.)*, 2016. **1360**: p. 47-58.
162. González-Vera, J.A., *Probing the kinome in real time with fluorescent peptides*. *Chemical Society Reviews*, 2012. **41**(5): p. 1652-1664.
163. Cann, M.L., et al., *Measuring Kinase Activity—A Global Challenge*. *Journal of Cellular Biochemistry*, 2017. **118**(11): p. 3595-3606.
164. Liu, Q., J. Wang, and B.J. Boyd, *Peptide-based biosensors*. *Talanta*, 2015. **136**: p. 114-27.
165. Karimzadeh, A., et al., *Peptide based biosensors*. *TrAC Trends in Analytical Chemistry*, 2018. **107**: p. 1-20.
166. Wu, D., et al., *Peptide reporters of kinase activity in whole cell lysates*. *Biopolymers*, 2010. **94**(4): p. 475-86.

167. Placzek, E.A., et al., *A peptide biosensor for detecting intracellular Abl kinase activity using matrix-assisted laser desorption/ionization time-of-flight mass spectrometry*. *Anal Biochem*, 2010. **397**(1): p. 73-8.
168. Lipchik, A.M., et al., *KINATEST-ID: a pipeline to develop phosphorylation-dependent terbium sensitizing kinase assays*. *J Am Chem Soc*, 2015. **137**(7): p. 2484-94.
169. Sanz, A., et al., *Analysis of Jak2 Catalytic Function by Peptide Microarrays: The Role of the JH2 Domain and V617F Mutation*. *PLOS ONE*, 2011. **6**(4): p. e18522.
170. Ferraro, R.M., et al., *Generation of three iPSC lines from fibroblasts of a patient with Aicardi Goutières Syndrome mutated in TREX1*. *Stem Cell Research*, 2019. **41**: p. 101580.
171. Ferraro, R.M., et al., *Establishment of three iPSC lines from fibroblasts of a patient with Aicardi Goutières syndrome mutated in RNaseH2B*. *Stem Cell Research*, 2019. **41**: p. 101620.
172. Masneri, S., et al., *Generation of three isogenic induced Pluripotent Stem Cell lines (iPSCs) from fibroblasts of a patient with Aicardi Goutières Syndrome carrying a c.2471G>A dominant mutation in IFIH1 gene*. *Stem Cell Research*, 2019. **41**: p. 101623.
173. Russell, L.J., et al., *Deregulated expression of cytokine receptor gene, CRLF2, is involved in lymphoid transformation in B-cell precursor acute lymphoblastic leukemia*. *Blood*, 2009. **114**(13): p. 2688-2698.
174. Quentmeier, H., et al., *DNMT3A R882H mutation in acute myeloid leukemia cell line SET-2*. *Leukemia Research*, 2020. **88**: p. 106270.
175. Anteneh, H., J. Fang, and J. Song, *Structural basis for impairment of DNA methylation by the DNMT3A R882H mutation*. *Nature Communications*, 2020. **11**(1): p. 2294.
176. Pamies, D., et al., *Good Cell Culture Practice for stem cells and stem-cell-derived models*. *ALTEX - Alternatives to animal experimentation*, 2017. **34**(1): p. 95-132.
177. Young, L., et al., *Detection of Mycoplasma in cell cultures*. *Nature Protocols*, 2010. **5**(5): p. 929-934.
178. Montecchini, O., et al., *A Novel ELISA-Based Peptide Biosensor Assay for Screening ABL1 Activity in vitro: A Challenge for Precision Therapy in BCR-ABL1 and BCR-ABL1 Like Leukemias*. *Frontiers in Pharmacology*, 2021. **12**.
179. Laštovička, J., M. Rataj, and J. Bartůňková, *Assessment of lymphocyte proliferation for diagnostic purpose: Comparison of CFSE staining, Ki-67 expression and 3H-thymidine incorporation*. *Human Immunology*, 2016. **77**(12): p. 1215-1222.
180. Quah, B. and C. Parish, *The Use of Carboxyfluorescein Diacetate Succinimidyl Ester (CFSE) to Monitor Lymphocyte Proliferation*. *Journal of visualized experiments : JoVE*, 2010.
181. Bartsch, K., et al., *RNase H2 Loss in Murine Astrocytes Results in Cellular Defects Reminiscent of Nucleic Acid-Mediated Autoinflammation*. *Frontiers in immunology*, 2018. **9**: p. 587-587.
182. Morita, M., et al., *Gene-targeted mice lacking the Trex1 (DNase III) 3'-->5' DNA exonuclease develop inflammatory myocarditis*. *Molecular and cellular biology*, 2004. **24**(15): p. 6719-6727.
183. Reijns, M.A.M., et al., *Enzymatic removal of ribonucleotides from DNA is essential for mammalian genome integrity and development*. *Cell*, 2012. **149**(5): p. 1008-1022.
184. Lee, S.-H., et al., *Dynamic methylation and expression of Oct4 in early neural stem cells*. *Journal of Anatomy*, 2010. **217**(3): p. 203-213.

185. Ellis, P., et al., *SOX2, a Persistent Marker for Multipotential Neural Stem Cells Derived from Embryonic Stem Cells, the Embryo or the Adult*. *Developmental Neuroscience*, 2004. **26**(2-4): p. 148-165.
186. Yan, Y., et al., *Efficient and Rapid Derivation of Primitive Neural Stem Cells and Generation of Brain Subtype Neurons From Human Pluripotent Stem Cells*. *Stem Cells Translational Medicine*, 2013. **2**(12): p. 1022-1022.
187. Hiller, B., et al., *Mammalian RNase H2 removes ribonucleotides from DNA to maintain genome integrity*. *The Journal of experimental medicine*, 2012. **209**(8): p. 1419-1426.
188. Cerritelli, S.M. and R.J. Crouch, *Ribonuclease H: the enzymes in eukaryotes*. *The FEBS journal*, 2009. **276**(6): p. 1494-1505.
189. Lockhart, A., et al., *RNase H1 and H2 Are Differentially Regulated to Process RNA-DNA Hybrids*. *Cell Reports*, 2019. **29**(9): p. 2890-2900.e5.
190. Bulati, M., et al., *The Immunomodulatory Properties of the Human Amnion-Derived Mesenchymal Stromal/Stem Cells Are Induced by INF- $\gamma$  Produced by Activated Lymphomonocytes and Are Mediated by Cell-To-Cell Contact and Soluble Factors*. *Frontiers in Immunology*, 2020. **11**.
191. Göritz, C. and J. Frisén, *Neural Stem Cells and Neurogenesis in the Adult*. *Cell Stem Cell*, 2012. **10**(6): p. 657-659.
192. Garza, J.C., et al., *Leptin Increases Adult Hippocampal Neurogenesis in Vivo and in Vitro\**. *Journal of Biological Chemistry*, 2008. **283**(26): p. 18238-18247.
193. Kim, Y.H., et al., *Differential Regulation of Proliferation and Differentiation in Neural Precursor Cells by the Jak Pathway*. *Stem Cells*, 2010. **28**(10): p. 1816-1828.
194. Nicolas, C.S., et al., *The role of JAK-STAT signaling within the CNS*. *JAK-STAT*, 2013. **2**(1): p. e22925-e22925.
195. Bonni, A., et al., *Regulation of Gliogenesis in the Central Nervous System by the JAK-STAT Signaling Pathway*. *Science*, 1997. **278**(5337): p. 477-483.
196. Nakanishi, M., et al., *Microglia-derived interleukin-6 and leukaemia inhibitory factor promote astrocytic differentiation of neural stem/progenitor cells*. *European Journal of Neuroscience*, 2007. **25**(3): p. 649-658.
197. Nicolas, C.S., et al., *The Jak/STAT pathway is involved in synaptic plasticity*. *Neuron*, 2012. **73**(2): p. 374-390.
198. Yasuda, M., et al., *An activity-dependent determinant of synapse elimination in the mammalian brain*. *Neuron*, 2021. **109**(8): p. 1333-1349.e6.
199. Cuadrado, E., et al., *Chronic exposure of astrocytes to interferon- $\alpha$  reveals molecular changes related to Aicardi–Goutières syndrome*. *Brain*, 2013. **136**(1): p. 245-258.
200. Van Heteren, J.T., et al., *Astrocytes produce interferon-alpha and CXCL10, but not IL-6 or CXCL8, in aicardi-Goutières syndrome*. *Glia*, 2008. **56**(5): p. 568-578.
201. Sase, S., et al., *Astrocytes, an active player in Aicardi-Goutières syndrome*. *Brain pathology (Zurich, Switzerland)*, 2018. **28**(3): p. 399-407.
202. Dragoni, F., et al. *Characterization of Mitochondrial Alterations in Aicardi–Goutières Patients Mutated in RNASEH2A and RNASEH2B Genes*. *International Journal of Molecular Sciences*, 2022. **23**.

203. van Horssen, J., P. van Schaik, and M. Witte, *Inflammation and mitochondrial dysfunction: A vicious circle in neurodegenerative disorders?* Neuroscience Letters, 2019. **710**: p. 132931.
204. Fang, C., X. Wei, and Y. Wei, *Mitochondrial DNA in the regulation of innate immune responses.* Protein & cell, 2016. **7**(1): p. 11-16.
205. Gambardella, S., et al., *ccf-mtDNA as a Potential Link Between the Brain and Immune System in Neuro-Immunological Disorders.* Frontiers in Immunology, 2019. **10**.
206. Barrera, M.-J., et al., *Dysfunctional mitochondria as critical players in the inflammation of autoimmune diseases: Potential role in Sjögren's syndrome.* Autoimmunity Reviews, 2021. **20**(8): p. 102867.
207. McGarry, T., et al., *JAK/STAT Blockade Alters Synovial Bioenergetics, Mitochondrial Function, and Proinflammatory Mediators in Rheumatoid Arthritis.* Arthritis & Rheumatology, 2018. **70**(12): p. 1959-1970.
208. Lin, C.M., F.A. Cooles, and J.D. Isaacs, *Basic Mechanisms of JAK Inhibition.* Mediterranean journal of rheumatology, 2020. **31**(Suppl 1): p. 100-104.
209. Verstovsek, S. and R.S. Komrokji, *A comprehensive review of pacritinib in myelofibrosis.* Future Oncology, 2015. **11**(20): p. 2819-2830.
210. Jones, R.J. and N. Bischofberger, *Minireview: nucleotide prodrugs.* Antiviral Research, 1995. **27**(1): p. 1-17.
211. Furman, P.A., et al., *Phosphorylation of 3'-azido-3'-deoxythymidine and selective interaction of the 5'-triphosphate with human immunodeficiency virus reverse transcriptase.* Proceedings of the National Academy of Sciences, 1986. **83**(21): p. 8333-8337.
212. Sommadossi, J.P., R. Carlisle, and Z. Zhou, *Cellular pharmacology of 3'-azido-3'-deoxythymidine with evidence of incorporation into DNA of human bone marrow cells.* Molecular Pharmacology, 1989. **36**(1): p. 9.
213. Liu, L., et al., *The cell cycle in stem cell proliferation, pluripotency and differentiation.* Nature Cell Biology, 2019. **21**(9): p. 1060-1067.
214. Ceccatelli, S., et al., *Neural stem cells and cell death.* Toxicology Letters, 2004. **149**(1): p. 59-66.
215. Abe, T., Y. Marutani, and I. Shoji, *Cytosolic DNA-sensing immune response and viral infection.* Microbiology and immunology, 2019. **63**(2): p. 51-64.
216. Sanchez, G.A.M., et al., *JAK1/2 inhibition with baricitinib in the treatment of autoinflammatory interferonopathies.* The Journal of Clinical Investigation, 2018. **128**(7): p. 3041-3052.
217. Dolmetsch, R. and D.H. Geschwind, *The human brain in a dish: the promise of iPSC-derived neurons.* Cell, 2011. **145**(6): p. 831-834.
218. Yoshihara, M., Y. Hayashizaki, and Y. Murakawa, *Genomic Instability of iPSCs: Challenges Towards Their Clinical Applications.* Stem cell reviews and reports, 2017. **13**(1): p. 7-16.
219. Liang, G. and Y. Zhang, *Genetic and epigenetic variations in iPSCs: potential causes and implications for application.* Cell stem cell, 2013. **13**(2): p. 149-159.
220. Quentmeier, H., et al., *JAK2 V617F tyrosine kinase mutation in cell lines derived from myeloproliferative disorders.* Leukemia, 2006. **20**(3): p. 471-476.
221. Tasian, S.K. and M.L. Loh, *Understanding the biology of CRLF2-overexpressing acute lymphoblastic leukemia.* Critical reviews in oncogenesis, 2011. **16**(1-2): p. 13-24.

222. Zhong, J., et al., *TSLP signaling pathway map: a platform for analysis of TSLP-mediated signaling*. Database, 2014. **2014**.
223. Martinez-Anaya, D., et al., *t(X;14)(p22;q32) or t(Y;14)(p11;q32) IGH/CRLF2*. Atlas of Genetics and Cytogenetics in Oncology and Haematology, 2019.
224. Oku, S., et al., *JAK2 V617F uses distinct signalling pathways to induce cell proliferation and neutrophil activation*. British Journal of Haematology, 2010. **150**(3): p. 334-344.
225. Rubert, J., et al., *Bim and Mcl-1 exert key roles in regulating JAK2V617F cell survival*. BMC cancer, 2011. **11**: p. 24-24.
226. Gozgit, J.M., et al., *Effects of the JAK2 Inhibitor, AZ960, on Pim/BAD/BCL-xL Survival Signaling in the Human JAK2 V617F Cell Line SET-2*. Journal of Biological Chemistry, 2008. **283**(47): p. 32334-32343.
227. Tognon, R., et al., *Deregulation of apoptosis-related genes is associated with PRV1 overexpression and JAK2 V617F allele burden in Essential Thrombocythemia and Myelofibrosis*. Journal of hematology & oncology, 2012. **5**: p. 2-2.
228. Muller, R., *JAK inhibitors in 2019, synthetic review in 10 points*. European Journal of Internal Medicine, 2019. **66**: p. 9-17.
229. Cleary, M.M., et al., *Pacritinib, a Dual FLT3/JAK2 Inhibitor, Reduces Irak-1 Signaling in Acute Myeloid Leukemia*. Blood, 2015. **126**(23): p. 570-570.
230. Gilliland, D.G. and J.D. Griffin, *The roles of FLT3 in hematopoiesis and leukemia*. Blood, 2002. **100**(5): p. 1532-1542.
231. Armstrong, S.A., et al., *FLT3 mutations in childhood acute lymphoblastic leukemia*. Blood, 2004. **103**(9): p. 3544-3546.
232. Brown, P., et al., *FLT3 inhibition selectively kills childhood acute lymphoblastic leukemia cells with high levels of FLT3 expression*. Blood, 2005. **105**(2): p. 812-820.
233. Crisino, R.M., et al., *Matrix effect in ligand-binding assay: the importance of evaluating emerging technologies*. Bioanalysis, 2014. **6**(8): p. 1033-1036.
234. Di Battista, V., et al., *Genetics and Pathogenetic Role of Inflammasomes in Philadelphia Negative Chronic Myeloproliferative Neoplasms: A Narrative Review*. International Journal of Molecular Sciences, 2021. **22**(2).
235. Baccarani, M., et al., *Definition and treatment of resistance to tyrosine kinase inhibitors in chronic myeloid leukemia*. Expert Review of Hematology, 2014. **7**(3): p. 397-406.
236. Springuel, L., et al., *Cooperating JAK1 and JAK3 mutants increase resistance to JAK inhibitors*. Blood, 2014. **124**(26): p. 3924-3931.
237. Meyer, S.C. and R.L. Levine, *Molecular Pathways: Molecular Basis for Sensitivity and Resistance to JAK Kinase Inhibitors*. Clinical Cancer Research, 2014. **20**(8): p. 2051-2059.
238. Tasian, S.K., et al., *Aberrant STAT5 and PI3K/mTOR pathway signaling occurs in human CRLF2-rearranged B-precursor acute lymphoblastic leukemia*. Blood, 2012. **120**(4): p. 833-842.
239. Boni, C., et al., *Successful Preservation of Native BCR::ABL1 in Chronic Myeloid Leukemia Primary Leukocytes Reveals a Reduced Kinase Activity*. Frontiers in Oncology, 2022. **12**.